Grains and Grain Boundaries in Lamellar Styrene - Butadiene Block Copolymers

by

Randall T. Myers

Bachelor of Science, Chemical Engineering
University of Massachusetts, Amherst, Massachusetts, 1994

Masters of Science, Chemical Engineering Practice
Massachusetts Institute of Technology, Cambridge, Massachusetts, 1996

Submitted to the Department of Chemical Engineering
in partial fulfillment of the requirements for the degree of

DOCTOR OF PHILOSOPHY IN CHEMICAL ENGINEERING
AT THE
MASSACHUSETTS INSTITUTE OF TECHNOLOGY

JUNE 1999

© Massachusetts Institute of Technology, 1999. All rights reserved.

Signature of Author:_____
Department of Chemical Engineering
April 12, 1999

Certified by:_____
Robert E. Cohen
Department of Chemical Engineering
Thesis Supervisor

Accepted by:_____
Robert E. Cohen
St. Laurent Professor of Chemical Engineering
Chairman, Committee for Graduate Students

Science

MIT Libraries
Document Services

Room 14-0551
77 Massachusetts Avenue
Cambridge, MA 02139
Ph: 617.253.2800
Email: docs@mit.edu
http://libraries.mit.edu/docs

DISCLAIMER OF QUALITY

Due to the condition of the original material, there are unavoidable flaws in this reproduction. We have made every effort possible to provide you with the best copy available. If you are dissatisfied with this product and find it unusable, please contact Document Services as soon as possible.

Thank you.

Some pages in the original document contain pictures, graphics, or text that is illegible.

Pages 140-142

Grains and Grain Boundaries in Lamellar Styrene - Butadiene Block Copolymers

by

Randall T. Myers

Submitted to the Department of Chemical Engineering on April 12, 1999,
in partial fulfillment of the requirements for the degree of
Doctor of Philosophy in Chemical Engineering

ABSTRACT

Simultaneous determination of the lamellar morphological length scale and the grain size of several low molecular weight heterogeneous styrene - butadiene block copolymers was accomplished through the use of ultra small angle x-ray scattering measurements. NIST's X23A3 Ultra SAXS beamline in the Brookhaven National Laboratory provided a scattering vector, q, from 0.0004 to 0.1 $Å^{-1}$. Most of the block copolymer specimens display a clearly resolvable peak in the Ultra SAXS region, and grain size was determined using the spherical form factor. Determination of Porod's law constant and the value of the scattering invariant provided a verification of the scattering mechanism by solving for the contrast factor and the volume fraction of the grain boundaries in these specimens. Grain size in a given polymer was a function of annealing temperature and time. For the case of a block copolymer swollen with varying amounts of cumene, both the lamellar repeat distance, d, and the grain size, D, increased with the cube root of the volume fraction of solvent over the concentration range examined. Transmission Electron Microscopy validated Ultra SAXS grain size measurements for one of the block copolymer's solvent casting and annealed series.

Grain size can be altered in commercial styrene - butadiene block copolymers through the use of evaporation solvent and temperature. The styrene rich polymers can be altered from about 0.3 to 3.5 μm and from about 3.5 to 6.5 μm for the butadiene rich polymers. The solvents caused the same relative grain size for all polymers studied, from smallest to largest: chloroform, toluene, methylene chloride, tetrahydrofuran, ethyl acetate, cumene, and methyl ethyl ketone.

The mechanical properties of the commercial block copolymers were examined as a function of grain structure. In contrast to polycrystalline materials, the yield strength increases with increasing grain size for the two styrene rich block copolymers. The Ultra SAXS results suggest that the grain boundaries contain an enrichment of styrene which increases as the grains grow larger . Edge-view SAXS patterns, modulus measurements, and comparison with the mechanical properties of a highly oriented, grain-free specimen all indicate that the observed trends in mechanical yield are not dominated by variations of lamellar orientation with grain size. The changing composition and thickness of the grain boundary appears to be the cause of the increase of yield stress with grain size for these two block copolymers. For the two butadiene rich block copolymers, the trend is reversed, smaller grains have a higher yield strength. This is probably due to the enrichment of butadiene at the grain boundaries, which does not yield and acts as a sliding surface for the grains, as witnessed in semicrystalline polymers.

Thesis Supervisor: Robert E. Cohen, Professor of Chemical Engineering

Acknowledgments

I swore that I wasn't going to over acknowledge, and for the first couple of drafts of this thesis, the acknowledgments page simply read, "I would like to thank all the little people who helped make this possible." However, it became apparant that I did need at some point to fill in this page. I will apologize in advance to anyone whom I forget to mention here.

I want to thank my advisor, Bob Cohen, whose constant exuberance about this research topic and upbeat attitude even when things were rough were the main reasons I was able to finish this project. He was always receptive and welcomed changes in the project's direction and thrust, and I think the final product is satisfying, though probably nothing like he envisioned 5 years ago. Professor Cohen not only taught me a lot about polymer science, but about managing and treatment of people and leadership in general, and I know that if I can take advantage, this knowledge will benefit me at least as much as all of my Chemical Engineering learnings, wherever the next stop in my life is.

I want to thank Dr. Anuj Bellare. He was the person who showed me how to used just about every piece of equipment in 66-353 and 357 as well as around the MIT campus. Anuj was also the lucky soul who accompanied me down to Brookhaven for the 3-5 day long excursions where one of us had to work the over night shift. Anuj also ran all of the SANS experiments which are displayed in this thesis.

I would like to thank Dr. Alexander Karbach of Bayer A.G. who oversaw the generation of all the TEM and SEM images shown in this thesis. I would also like to thank Professor Thomas Russell of UMass and Professor Richard Register of Princeton who provided much insight into this project.

I would like to acknowledge the 5 years of Cohen group members with whom I have coexisted. I would especially like to acknowledge Alice Man who taught me how to run the NMR apparatus, Leslie Loo who helped me with the intricacies of the Instron apparatus, and Tom Wang who made sure the computers were always running in the Cohen lab.

I acknowledge NSF/MRSEC for partially funding this project. I also acknowledge NIST and namely Gabrielle Long and Zugen Fu for use of their Ultra SAXS machine and for helpful insight into data analysis. I would like to that Mike Frongillo, Joe Adario, Tim McClure, and Libby Shaw of the CMSE for working with me on how to use the TEM, SAXS, DMA, and AFM machines, respectively. I would like to thank Tony Caola for being the person I contacted when I had computer issues. Whether it be scanning images, importing and deciphering difficult files or even fixing my email accout, Tony was the man.

Table of Contents

List of Figures

List of Tables

1. Introduction

1.1 Motivation

The use of polymeric materials is increasing every year. Polymers are becoming primary materials of construction for products ranging from cups to automobiles to synthetic joints. One high growth area in the field of plastics is the use of block copolymers, namely those composed of styrene and butadiene. These block copolymers have excellent clarity, toughness and rigidity.[1] Applications for styrene - butadiene block copolymers include medical devices, toys, and food packaging.[2,3] These block copolymers are also used as a plastic modifier to polystyrene when making drinking cups and lids; because of the presence of styrene as a component block, styrene - butadiene block copolymers are compatable with general purpose polystyrene (GPPS). Addition of styrene - butadiene block copolymers removes the brittleness of general purpose polystyrene as well as improving the gloss.[4] Because styrene - butadiene block copolymers, a type of thermoplastic elastomer because of their functionality, don't undergo vulcanization after processing, they are completely reusable and recyclable,[5] giving rise to even more potential applications.

These block copolymers have current and potential applications. With each new application, different physical properties are needed. Every time a potential application arises with new physical property requirements, the traditional solution has been either synthesis of a novel polymer or blending two or more currently available polymers. This is a time-consuming and expensive process with sometimes varied results. It is therefore desirable to see if processing conditions can produce the same polymer with different physical properties. Therefore, knowledge of styrene - butadiene block copolymers at every important length scale and the effect features at this length scale have on the physical properties of the polymer is essential for continued expansion of the role of thermoplastic elastomers.

Many length scales exist and are important when examining block copolymers: atomic, molecular, mophological, and super-morphological. The atomic, molecular and morphological features of a block copolymer have been extensively studied and will be explained in later sections. The largest length scale is that supermorphological grains and is on the order of microns. Grains and grain boundaries have recently been the focus of investigation and are the subject of this thesis. The aim of this project was two-fold: to see if the grain size of an industrially available block copolymer could be controlled, and to see how this grain size affected the physical properties. Variables investigated in the formation of grain size include solvent choice, evaporation temperature, and annealing temperature and time. The investigated physical property was tensile deformation behavior, with yield stress and modulus being measurable quantities of this process.

1.2 Styrene - Butadiene Block Copolymers

Atatic polystyrene is an amorphous polymer with a density ranging between 1.04 and 1.065.[6] It consists of a phenyl group attached to the polymer backbone. Because its glass transition temperature, T_g, is about 100 °C, it is glassy, solid and brittle at room temperature.[6] Polybutadiene exists in two isomers. !,4-polybutadiene contains a double bond in the backbone of the polymer, while 1,2-polybutadiene contains a double bond as a side chain.[7] When polybutadiene is synthesized, both are present, but depending on reaction conditions, one or the other may be present in greater quantities. The chemical structures of both polystyrene and 1,4 and 1,2-polybutadiene are shown in Figure 1-1. The density of polybutadiene varies from 0.97 and 0.96 for 1,4 and 1,2 polybutadiene respectively to 0.89 for a homogenous combination of both isomeric repeat units.[6] The glass transition temperature, T_g, is around -90 °C for 1,4-polybutadiene and around -15 °C for 1,2-polybutadiene, meaning that polybutadiene is a rubber at room temperature, no matter how much of each isomer is present.[6]

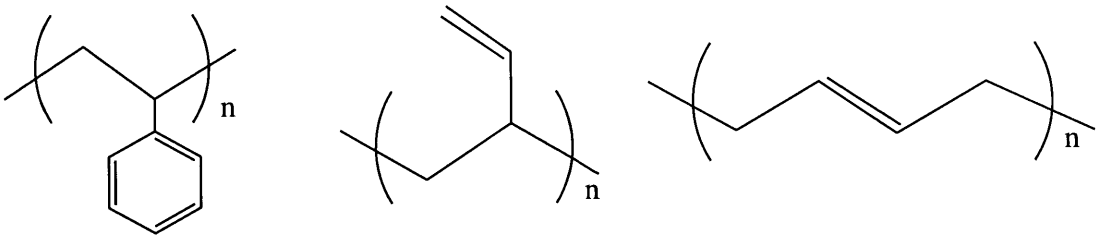

polystyrene 1,2-polybutadiene 1,4-polybutadiene

Figure 1-1: Molecular structures of of the repeat units of polystyrene, 1,2-polybutadiene and 1,4 polybutadiene

A styrene - butadiene copolymer may be organized in one of three ways. An alternating copolymer contains alternating styrene and butadiene repeat units. In a random copolymer, there is no greater order in the organization of styrene and butadiene repeat units. Because of the way the repeat units are bonded together, both alternating and random copolymers form a homogenous mixture and no greater morphology is witnessed.[8] A block copolymer contains a long chains of styrene repeat units bonded to long chains of butadiene repeat units. Because of the molecular ordering in block copolymers, if the blocks are not miscible, as is often the case with styrene and butadiene, microphase separation may occur, which will be discussed in greater detain in the next section. Examples of alternating, random, and block styrene - butadiene copolymers are shown in Figure 1-2. Repeat units of styrene are represented by the letter "S," and butadiene repeat units are "B."

alternating: ...-S-B-S-B-S-B-S-B-S-B-...
random: ...-S-S-S-B-S-B-B-S-S-B-...
block: ...-S-S-S-S-S-B-B-B-B-B-...

Figure 1-2: Examples of alternating , random, and block copolymers containing styrene (S) and butadiene (B)

From this point on, all copolymers discussed will be block copolymers. A long chain of polystyrene bonded to a long chain of polybutadiene is called a diblock copolymer. A block segment of styrene monomer units bonded to a block segment of butadiene monomer units bonded to another block segment of styrene units is called a triblock copolymer. Other types of block copolymers include three - armed and radial. Figure 1-3 illustrates all these types of block copolymers. Block copolymers with all of these types of molecular configurations are explored in this thesis.

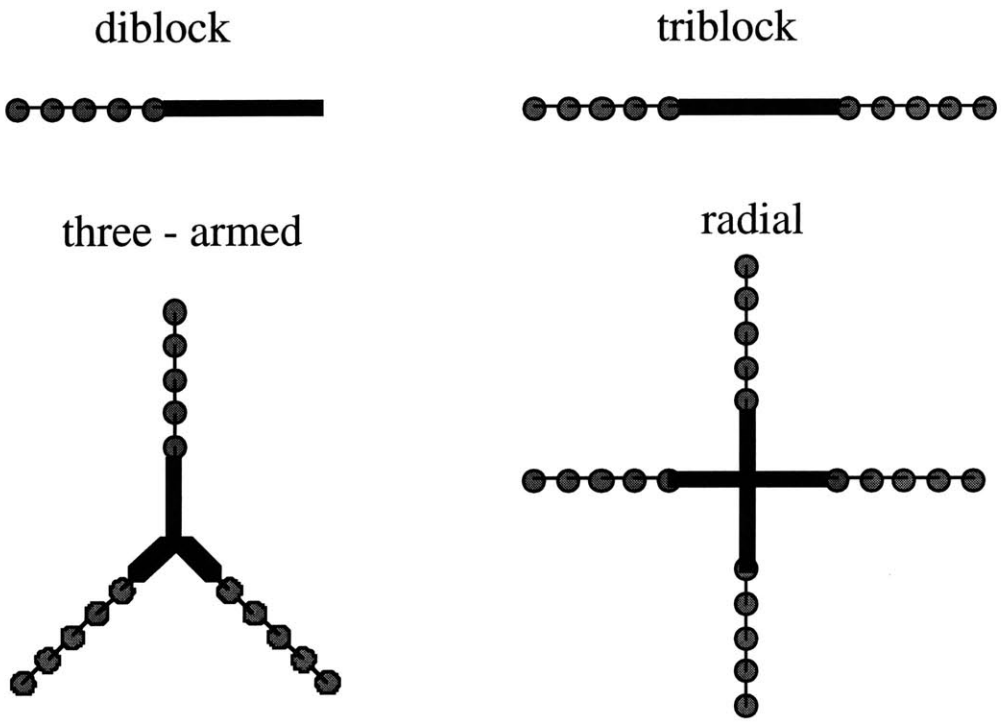

Figure 1-3: Examples of diblock, triblock, three-armed and radial colpolymers. The circles represent polystyryrene blocks and the solid lines represent butadiene blocks.

1.3 Microphase Separation

For a given block copolymer, there is only a narrow range of miscibility, where the block copolymer forms a homogenous phase. This can best be understood by exploring the thermodynamics of the macromolecular system. The Gibbs free energy of mixing, ΔG_{mix}, must be negative for miscibility to occur.[9] From classic thermodynamics:

$$\Delta G_{mix} = \Delta H_{mix} - T\Delta S_{mix} \tag{1-1}$$

From the Flory-Huggins theory for polymers, the enthalpy of mixing, ΔH_{mix}, can be expressed as:[10]

$$\Delta H_{mix} = \chi_{AB} n_A \phi_B kT \tag{1-2}$$

where χ_{AB} is the Flory - Huggins interaction parameter, and is defined as:

$$\chi_{AB} = \frac{z\Delta w_{AB} x_A}{kT} \tag{1-3}$$

and

n_i is the number of molecules of polymer *i*

ϕ_i is the volume fraction of polymer *i*

k is the Boltzman constant

T is the absolute temperature

z is the number of contacts between a repeat unit and its neighbors

Δw_{AB} is the change in energy of formation for an AB contact pair

x_i is the number of repeat units in polymer *i*

It can be seen that the enthalpy of mixing, ΔH_{mix}, will be both small and posititive for macromolecules as it is for traditional small molecules, since the large number of repeat units, x_i, is offset by the small number of molecules, n_i.. If we look at the entropy of mixing, ΔS_{mix} for polymers,[9]

$$\Delta S_{mix} = -kT(n_A \ln \phi_A + n_B \ln \phi_B) \quad (1\text{-}4)$$

we see that the entropy of the system increases very little when two polymers are mixed due to the relatively few molecules present. Therefore, the entropy of mixing, ΔS_{mix}, is usually too small to overcome the enthalpy of mixing, ΔH_{mix}, at room temperature causing the Gibbs free energy of mixing to be positive and leading to phase separation.

Looking at the Gibbs phase rule for two components:[11]

$$F = n + 2 - \pi \quad (1\text{-}5)$$

where: F is the number of degrees of freedom

n is the number of components

π is the number of phases

we see that with two components and two immiscible phases, we have two degrees of freedom, temperature and pressure. With a block copolymer, we still have temperature and pressure as the degrees of freedom, but now we only have one component. Therefore, by Gibbs phase rule, we can have just one phase, even though the component blocks want to phase separate. Because the component blocks are bonded together in a block copolymer, phase separation cannot occur in the traditional sense, resulting in one inhomogenous phase from the phenomena known as "microphase separation."[12] A good heuristic is that microphase separation will occur in a block copolymer when χN is greater than or equal to 10, where N is the number of moles of both A and B.

1.4 Equilibrium Morphologies

Because of the bond between component blocks in styrene butadiene block copolymers, true phase separation cannot happen and microphase separation occurs, with distinct domains of styrene and butadiene on the order of hundreds of angstroms. How

these domains are arranged on the nanometer length scale is called the morphology, and in general, the morphology tends to minimize the free energy and surface to volume ratios of the domains.[13,14]

Many different morphologies have been predicted theoretically and observed experimentally.[15-20] The most common morphologies include alternating lamellae of styrene and butadiene, cylinders of styrene or butadiene in a matrix of the other block, and spheres of styrene or butadiene in a matrix of the other block. These three most common morphologies are illustratred in Figure 1-4. Other morphologies, such as a continuous tetrapod network and ordered bicontinuous double diamond, have been observed in some polymers but are less prevalent.[19,20] Which of these morphologies is witnessed depends on the molecular weight of the polymer, the fraction of each block, the temperature, as well as the chemical structure of each block. In this research, all block copolymers were chosen with a lamellar morphology, and this morphology was observed with either transmission electron microscopy (TEM) or small angle x-ray scattering (SAXS).

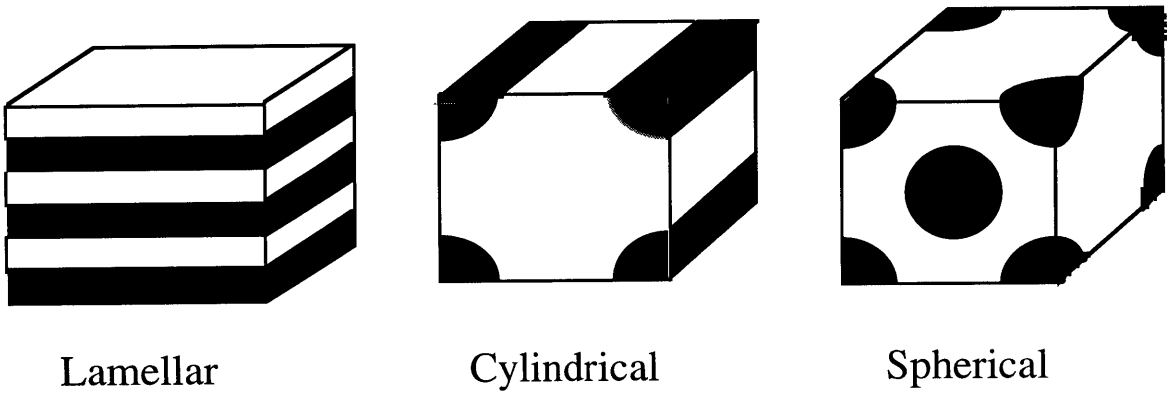

Figure 1-4: Examples of the most commonly observed equilibrium morphologies: lamellar, cylindrical, and spherical

1.5 Grains and Grain Boundaries

It is known that appropriate processing techniques can produce essentially perfectly ordered block copolymer morphologies with a single texture extending throughout the macroscopic dimensions of a specimen.[21] Methods for creating perfectly ordered block copolymers range from common techniques like extruding and shear to exotic methods like roll casting.[22-24] The characteristic repeating length scale, d, of these morphologies is dictated by the molecular weights of the constituent block sequences, on the order of 100 Å, and discussed in the previous section. In the absence of extraordinary processing procedures like roll casting, a second important length scale appears in the block copolymer. The perfection of the morphology is broken up into grains, each of which contains the ordered morphology of length scale d but with essentially random orientation relative to the specimen boundaries. These grains are local areas of orientation in a macroscopically disoriented polymer. Grains typically exhibit a characteristic size, D, which is one or more orders of magnitude larger than the morphological length scale, d, meaning that they are usually on the order of microns in size. Examples of globally ordered and grainy lamellar morphologies are illustrated in Figure 1-5.[25]

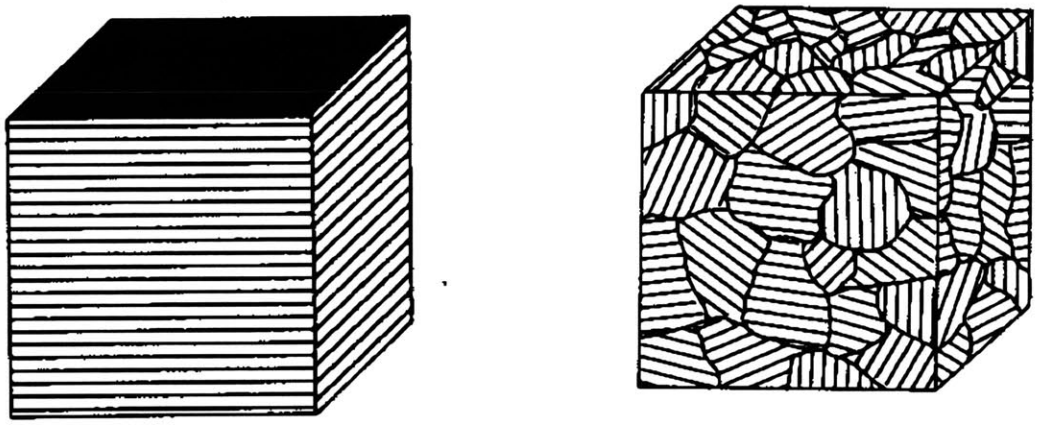

Figure 1-5: Examples of globally ordered (left) and grainy lamellar morphologies (right)

Since polystyrene and polybutadiene have widely different physical properties, it is easy to see how a block copolymer oriented with one of the aforementioned techniques would have different physical properties in one direction than the other, meaning that it is isotropic. Since we are looking at physical properties in this study, it is very important that the material be isotropic, so that the physical property not be a function of orientation. Any chance of orientation from shearing must be eliminated. A way to check for anisotropy is by 2 dimensional Small Angle X-Ray Scattering (SAXS). Examples of SAXS patterns are illustrated in Figure 1-6 for KK31, a styrene - butadiene triblock copolymer studied previously and further examined in this work.[26-28] The pattern on the left is from the original extruded material, which is oriented and the pattern on the right is from the same material dissolved in toluene and static cast, causing the material to be grainy and isotropic. As can be seen from the SAXS patterns, the oriented material does not have a complete ring, while the grainy KK31 has a complete ring meaning that there is no preferred orientation. Any amount of orientation will result in a darkening or lightening of the ring of the SAXS pattern for that material. All polymers processed in this thesis were tested for preferred orienation by this method.

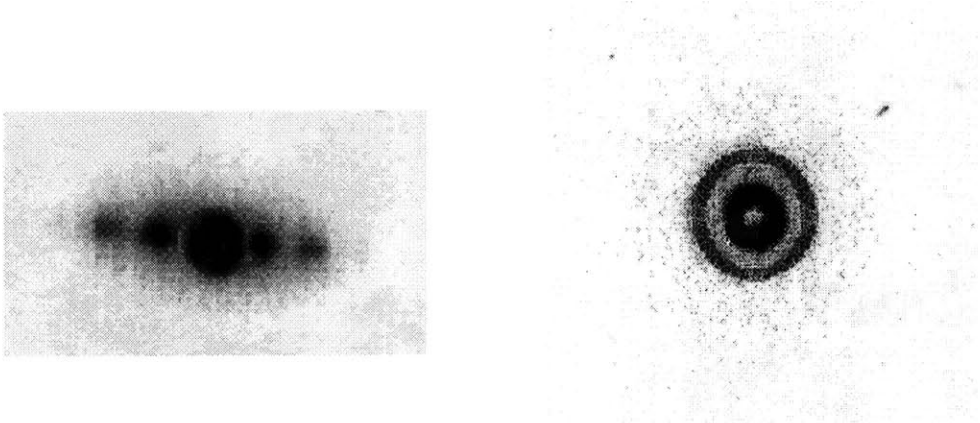

Figure 1-6: 2 Dimensional Small Angle X-Ray Scattering (SAXS) profiles of KK31. The pattern on the left is from an extruded sample, thus oriented and anisotropic, while the polymer corresponding to the pattern on the right was dissolved with toluene and static cast, thus isotropic and possessing grains.

Traditionally, Transmission Electron Microscopy (TEM) has been the preferred method for probing grains and proving they exist.[29] A TEM micrograph of KR03 with a grainy supermorphology is shown in Figure 1-7. KR03 is a three - armed block copolymer that has also been studied elsewhere and is further studied in this work.[30-33] Advantages of Transmission Electron Microscopy as a tool for grain size measurement include the fact that both the lamellae and the grains can be seen, so no errors in interpretation can occur. However, producing the appropriately uniform, large area, ultramicrotomed and stained sections required to obtain a meaningful and statistically significant grain size measurement, is a long, time consuming process with sometimes mixed results. With the number of samples which we wanted to measure the grain sizes of, this was deemed to be a nonviable option, which is why Ultra Small Angle X-Ray Scattering (Ultra SAXS) was decided as the measurement tool of choice, though results from this method were compared to measurements from TEM micrographs as a final test of this method's viability.

We know that the presence of grains can affect physical properties. Csernica et al. examined gas transport in a grainy, lamellar styrene - butadiene triblock copolymer.[26-28] They found that for all gasses studied, transport was significantly different from that observed in specimens specifically processed for series or parallel permeation or what the results from the oriented samples would have predicted. What hinted that the grain boundaries might have an effect on material proerties was when the results were compared to simlar results obtained by Sax and Ottino.[34] Sax and Ottino looked at polymer blends that exhibited the same small scale order and large scale disorder on the same length scale as block copolymers. Csernica found diffusivity results compared poorly with results from Sax and Ottino. This poor comparison in results lended to the belief that the existence of grain boundaries and material contained therein may actually affect physical properties.

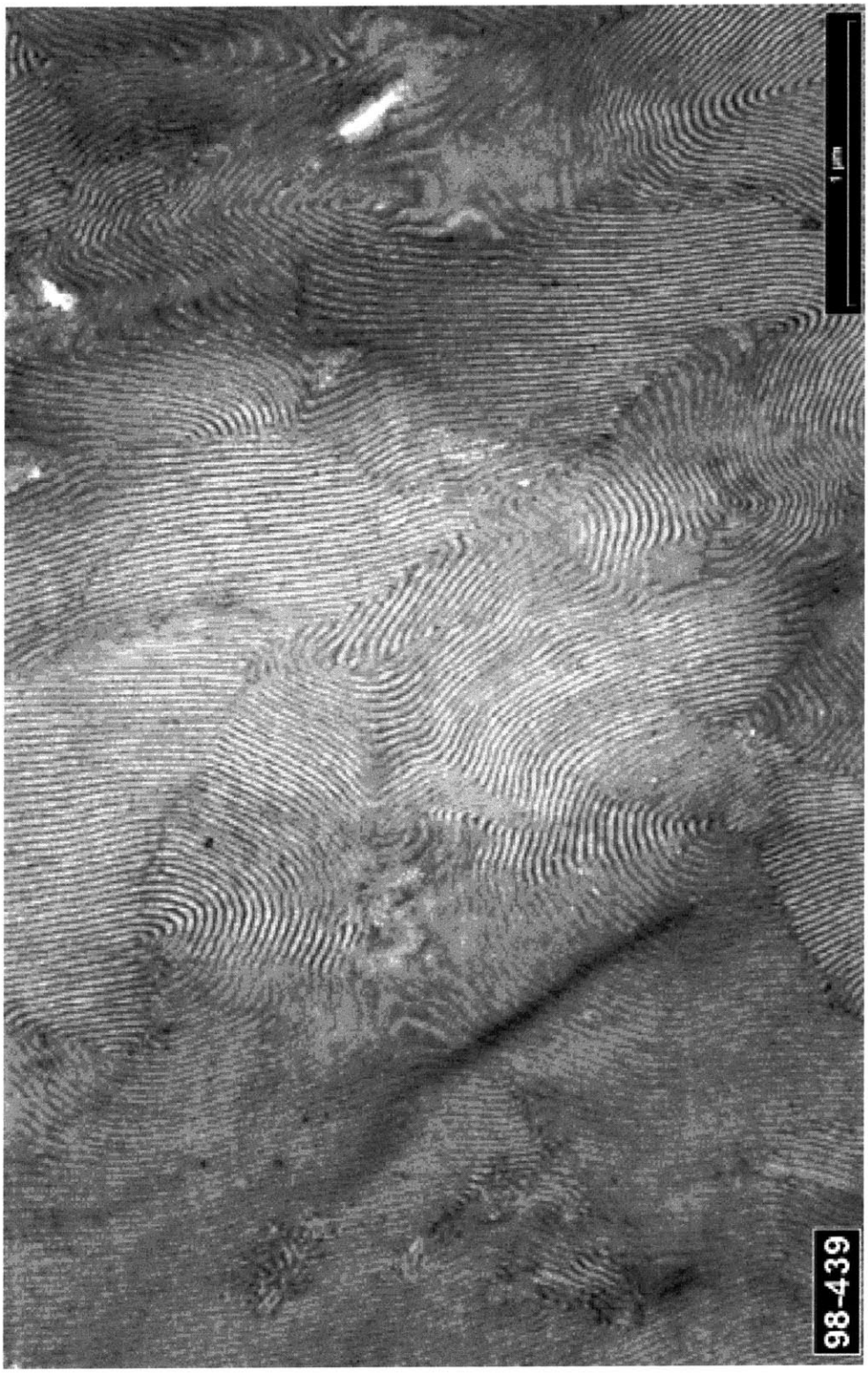

Figure 1-7: Transmission Electron Micrograph of KR03 polymer. Both the lamellar morphology and the grainy super morphology can be seen on this length scale. Micrograph courtesy of Dr. A. Karbach, Bayer A.G.

However, Csernica only used one set of processing conditions, leading to only one grain size, so the effect different grain sizes had on gas permeability was not explored.

Recently, grains and grain boundaries have been the subject of studies. The kinetics of grain growth in block copolymers has been examined extensively by Balsara et al.[35-39] Balsara worked with low molecular weight styrene - isoprene diblock copolymers; block lengths were typically on the order of 10,000. Typically, the polymers were heated above the order - disorder temperature, T_{ODT}, which presumably destroyed not only the lamellar morphology, but the grainy supermorphology. The polymer was then quenched below the order - disorder temperature, T_{ODT}, but above the glass transition temperature, T_g. Grain size was then measured as a function of time, as the grains nucleate and grow quickly in this temmperature range. Depolarized light scattering was the primary tool for measuring a correlation length, which was linked with TEM pictures and called the grain size.

Other recent studies have centered around studying the actual morphology of the grain boundaries as probed by TEM.[29,40-44] They agree that grain boundary defects are a result of a non-equilibrium origin; they constitute local disturbances in the long - range ordered lamellar microstructure. Several types of grain boundaries morphologies have been identified including but not limited to chevron, hellicoid, and omega; these have been grouped into two categories of grain boundaries: tilt and twist. What is not agreed upon is why certain grains boundaries are formed, the kinetics of grain growth, and whether certain aspects like an order - order transitition affect the grain size.[45] While it is certainly possible that different types of grain boundaries may affect the material properties differently, this was not a variable pursued in this thesis.

1.6 Similar Systems

Grains and grain boundaries in block copolymer systems have become an area of intense scrutiny in recent years. However, no deformation studies have been performed on

styrene - butadiene block copolymers with grain size as an independent variable. Two different systems will be examined and used as starting points in an attempt to understand the mechanical stress - strain behavior of styrene - butadiene block copolymers containing grains. The first is the grains and grain boundaries in metals and the second is semicrystalline polymers. Potential similarities and differences will be probed as well as deformation behavior for both of these systems.

1.6.1 Grains and Grain Boundaries in Metals

In material science, a grain boundary is defined as the interface separating two small grains or crystals having different crystallographic orientations in polycrystalline materials, i.e. metals.[46] The length scale of a typical grain in a metal is many orders of magnitude smaller than typical grains in block copolymers, as metal grains are on the order of angstroms, and metal grains are on the order of microns. Grains can also occur in homogeneuous metals, which is not the case for amorphous polymers, which must be block copolymers to witness the presence of grains. A metal with no grains is isotropic, but a block copolymer possessing no grains is anisotropic.

Despite these differences, grains and grain boundaries in metals may tell us something. As with block copolymers, the presence of grains is the result of the material not being in thermodynamic equilibrium. Also, an increase in temperature yields to a phenomenon known as "grain growth," as it does with block copolymers, though the temperature required for grain growth in block copolymers is much lower than for metals.

It appears that a metal with relatively small grains is stronger and less brittle than the same metal with large grains. A correlation has been developed between the size of grains in metals and the yield strength:

$$\sigma_y = \sigma_0 + k_y D^{-\frac{1}{2}} \qquad (1\text{-}6)$$

where: σ_y is the yield strength

σ_0 and k_y are material specific constants

D is the average grain diameter

The inverse relation between grain diameter and yield strength is because smaller grains posssess more grain boundary per unit volume, which in turn helps to impede dislocation.[46]

1.6.2 Semicrystalline Polymers

Another type of polycrystalline material from which comparisons can be drawn are semicrystalline polymers. Up until now, all polymers discussed have been amorphous, meaning that the polymer chains do not arrange themselves in any preferred orientation relative to the rest of the chain or other chains. Certain polymers, like nylon or polyethylene, possess regular enough chain structures that the polymer chains pack into an ordered, regular, three - dimensional crystal lattice.[47] In theory, if a polymer was regular enough and had enough hydrogen bonding, it could be completely crystalline. However, most polymers can't come close complete crystallinity; in fact, the highest degree of crystallinity achieved for a polymer to date is 98%.[47] Hence all crystalline polymers are in essence semicrystalline. The semicrystalline polymers tend to organize in packets of crystallinity, call spherulites, in an amorphous matrix.

Many investigations have delved into the effect of polymer morphology on yield stress in polycrystalline materials.[48-51] Starkweather and Brooks showed that yield stress of nylon 66 increased as the spherulite size was reduced.[51] Impinged spherulites look similar morphologically to amorphous grains and may provide a useful starting point for mechanical deformation studies. An analogy between impinged spherulites and grains may prove to be a better model than the essentially single crystals that the grains in metals possess.

However, degree of crystallinity becomes important for polycrystalline polymers, which is not an issue for amorphous block copolymers.[50] Also, depending on the polymer

and the processing conditions, the crystalline spherulites may not be impinged, which would have a significant impact on the deformation behavior.[52]

More recent theory has been presented to account for the grain boundary effects in deformation behavior in polycrystalline materials.[53-55] However, the proposed mechanism assumes that the grain boundary is a point where quasi-spherical grains can slide past one another. This means that the weakest part of the material is at the grain boundaries. This is accurate in metals, where the grain boundary is essentially a lack of material. It is also accurate for semicrystalline materials where the amorphous region between two spherulites is significantly more ductile than the more ordered crystals. It is believed that this theory may be accurate for diblock copolymers, as they would possess little or no molecular connectivity across grain boundaries. It is less certain if this theory will also hold for triblock, three - armed and radial block copolymers, as these materials have a great deal more molecular connectivity across grain boundaries, therefore not allowing grains to slide past one another. It is also not known if the grain boundary is actually the weakest point in the block copolymer, as it is in semicrystalline materials and metals. If the grain boundaries aren't the weakest point, grains wouldn't slide past one another and the grain boundaries may actually yield.

1.7 References

(1) Rader, C.P "Thermoplastic Elastomers" in *Modern Plastics Enclopedia*, W.L. Kaplen, ed. McGraw-Hill Co., New York, 1995.

(2) Phillips 66. *K-Resin Technical Service Memorandum 288: Food Packageability - K-Resin SB Copolymers*, 1991.

(3) Phillips 66. *K-Resin Technical Service Memorandum 292: Medical Applications of K-Resin Polymers*, 1990.

(4) Firestone. *Stereon Block Copolymers: Stereon 840A for Plastic Modification*, 1993.

(5) Inoue, T. *Block Polymers*. S. Aggarwal, ed. Plenum Press, New York, 1970.

(6) Brandup, J.; Immergut, E.H. *Polymer Handbook* Third Edition. John Wiley & Sons, New York, 1989.

(7) *CRC of Chemistry and Physics* 76th Edition. D.R. Lide, ed. CRC Press, Boca Raton, 1995.

(8) Young, R.J.; Lovell, P.A. *Introduction to Polymers*. Chapman & Hall, London, 1991.

(9) Smith, J.M. Van Ness, H.C. *Introduction to Chemical Engineering Thermodynamics* Fourth Edition. McGraw - Hill, New York, 1987

(10) Flory, P.J. *Principles of Polymer Chemistry*. Cornell Press, Ithica, NY, 1953.

(11) Model, M.; Reid, R.C. *Thermodynamics and Its Applications* Second Edition. PTR Prentice Hall, Englewood Cliffs, NJ, 1983.

(12) Sperling, L.H. *Introduction to Physical Polymer Science*. Wiley - Intersciences, New York, 1986.

(13) Helfand, E. *J. Chem. Phys.* **1975**, *62*, 999.

(14) Helfand, E.; Sapse, A.M. *J. Chem. Phys.* **1975**, *62*, 1327.

(15) Argon, A.S.; Cohen, R.E.; Jang, B.Z.; VanderSande, J.B. *Polym. Sci. Polym. Phys. Ed.* **1981**, *19*, 253.

(16) Bates, F.S.; Fredrickson, G.H. *Annu. Rev. Phys. Chem.* **1990**, *41*, 525.

(17) Liebler, L. *Macromolecules* **1980**, *13*, 1607.

(18) Hashimoto, T.; Tanake, H.; Hasegawa, H. *Macromolecules* **1985**, *18*, 1864.

(19) Thomas, E.L.; Alward, D.B.; Kinning, D.J.; Martin, D.C.; Handlin, P.L.; Fetters, L.J. *Macromolecules* **1986**, *19*, 2197.

(20) Hasegawa, H.; Tanaka, H.; Yamasaki, K.; Hashimoto, T. *Macromolecules* **1987**, *20*, 1651.

(21) Keller, A.; Pedemonte, E.; Willmouth, F.M. *Nature* **1970**, *225*, 538.

(22) Morrison, F.A.; Winter, H.H.; Gronski, W.; Barnes, J.D. *Macromolecules* **1990**, *23*, 4200.

(23) Albalak, R.J.; Thomas, E.L. *Journal of Polymer Science Part B: Polymer Physics* **1994**, *32*, 341.

(24) Albalak, R.J.; Thomas, E.L.; Capel, M.S. *Polymer* **1997**, *38*, 3819.

(25) Stankovic, R.I.; Lenz, R.W.; Karasz, F.E. *Eur. Polym. J.* **1990**, *26*, 359.

(26) Csernica, J.; Baddour, R.F.; Cohen, R.E. *Macromolecules* **1987**, *20*, 2468.

(27) Csernica, J.; Baddour, R.F.; Cohen, R.E. *Macromolecules* **1989**, *22*, 1493.

(28) Csernica. J *Gas Permeation in Block Copolymer Films*, PhD Thesis, M.I.T., 1989.

(29) Gido, S.P.; Gunther, T.; Thomas, E.L.; Hoffman, D. *Macromolecules* **1993**, *26*, 4506.

(30) Fodor, L.M.; Kitchen, A.G.; Baird, C.C. *ACS Organ. Coat. and Plast. Chem. Prepr.* **1974**, *34*, 130.

(31) Gebizlioglu, O.S.; Argon, A.S.; Cohen, R.E. *Polymer* **1985**, *26*, 519.

(32) Gebizlioglu, O.S.; Argon, A.S.; Cohen, R.E. *Polymer* **1985**, ***26***, 529.

(33) Argon, A.S.; Cohen, R.E.; Jang, B.Z.; Vandersande, J.B. *J. Poly. Sci.: Poly. Phys.* **1981**, *19*, 253.

(34) Sax, J.; Ottino, J.M. *Polym. Eng. Sci.* **1983**, *23*, 165.

(35) Garetz, B.A.; Balsara, N.P.; Dai, H.J.; Wang, Z.; Newstein, M.C. *Macromolecules* **1996**, 29, 4675.

(36) Balsara, N.P.; Dai, H.J.; Watanabe, H.; Sato, T.; Osaki, K. *Macromolecules* **1996**, *29*, 3507.

(37) Balsara, N.P.; Dai, H.J.; Kesani, P.K.; Garetz, B.A.; Hammouda, B. *Macromolecules* **1994**, *27*, 7406.

(38) Garetz, B.A.; Newstein, M.C.; Dai, H.J.; Jonnalagadda, S.V.; Balsara, N.P. *Macromolecules* **1993**, *26*, 3151.

(39) Balsara, N.P.; Garetz, B.A.; Dai, H.J. *Macromolecules* **1992**, *25*, 6072.

(40) Nishikawa, Y.; Kawada, H.; Hasegawa, H.; Hashimoto, T. *Acta Polymer.* **1993**, *44*, 247.

(41) Gido, S.P.; Thomas, E.L. *Macromolecules* **1994**, *27*, 849.

(42) Gido, S.P.; Thomas, E.L. *Macromolecules* **1994**, *27*, 6137.

(43) Gido, S.P.; Thomas, E.L. *Macromolecules* **1997**, *30*, 3739.

(44) Carvalho, B.L.; Lescanec, R.L.; Thomas, E.L. *Macromol. Symp.* **1995**, *98*, 1131.

(45) Kimishima, K.; Koga, T.; Kanazawa, Y.; Hashimoto, T. *Fall Proceedings of the ACS, PMSE Division* **1998**, *79*, 371.

(46) Callister Jr., W.D. *Material Science and Engineering: An Introduction* Second Edition. John Wiley & Sons, New York, 1991.

(47) Rosen, S.L. *Fundamental Principles of Polymeric Materials* Second Edition. John Wiley & Sons, New York, 1993.

(48) Halpin, J.C.; Kardos, J.L. *J. Appl. Phys.* **1972**, *43*, 2235.

(49) Andrews, E.H. *Pure and Appl. Chem.* **1972**, *31*, 91.

(50) Bassett, D.C.; Carder, D.R. *Phil Mag.* **1973**, *28*, 535.

(51) Starkweather, H.W.; Brooks, R.E. *J. Appl. Polymer Sci.* **1959**, *1*, 236.

(52) Stein, R.S.; Rhodes, M.B. *J Appl Physics* **1960**, *31*, 1873.

(53) Chen, R.W.; Argon, A.S. *Acta Metallurgica* **1979**, *27*, 749.

(54) Chen, R.W.; Argon, A.S. *Acta Metallurgica* **1979**, *27*, 785.

(55) Bao, G., Hutchinson, J.W.; McMeeking, R.M. *Acta Metallurgica* **1991**, *39*, 1871.

2. Use of Ultra Small Angle X-Ray Scattering to Measure Grain Size in Styrene - Butadiene Block Copolymers

2.1 Introduction

As has been mentioned previously, it is imperative to have a fast and accurate way to absolutely measure grain size in order to link grain size to material properties. The primary method to date has been using transmission electron microscopy to look at both the lamellar and grain size length scales.[1] The advantages is that both the lamellar morphology and grainy super morphology can be seen directly. Transmission electron microscopy (TEM) is a time - consuming process, and is not optimal for measuring the grain size of the numerous samples required for grain size measurement in this thesis. Also, though it is relatively elementary to verify the existence of grains and grain boundaries with TEM, producing appropriately uniform, large-area ultramicrotomed sections required to obtain a meaningful and statistically significant measurement of grain size is a much more difficult proposition. Later in this chapter, through collaborative work, we will compare grain sizes found by Ultra SAXS with results from TEM micrographs.

Conventional small angle x-ray scattering (SAXS) techniques have been employed for decades to characterize block copolymers at the morphological length scale d[2,3]. Recently Ultra SAXS beamlines have been constructed to probe significantly larger morphological features.[4] The direct and non-destructive examination of grains in bulk, three-dimensional specimens via Ultra SAXS is advantageous in our ongoing effort to connect mechanical behavior with grain structure in block copolymers.

Ultra SAXS, like SAXS requires an electron density difference in order to observe morphological differences. It is easy to see how the styrene and butadiene lamellae have a difference in electron density, and thus contrast in scattering, as electron density is defined as:

$$\rho_e = \frac{\rho_m e N_A}{m} \qquad (2\text{-}1)$$

where: ρ_e is the electron density in electrons per unit volume

ρ_m is the mass density per unit volume

e is the number of electrons per monomer unit

N_A is Avogadro's number

m is the molecular weight of the monomer unit

It is less clear to see the how there may be a difference in the electron density of the grain boundary and the mean electron density of the grain. Figure 2-1 shows a transmission electron micrograph of a grain boundary in the S12B10 styrene - butadiene diblock copolymer (9900/9700) studied later in this chapter.

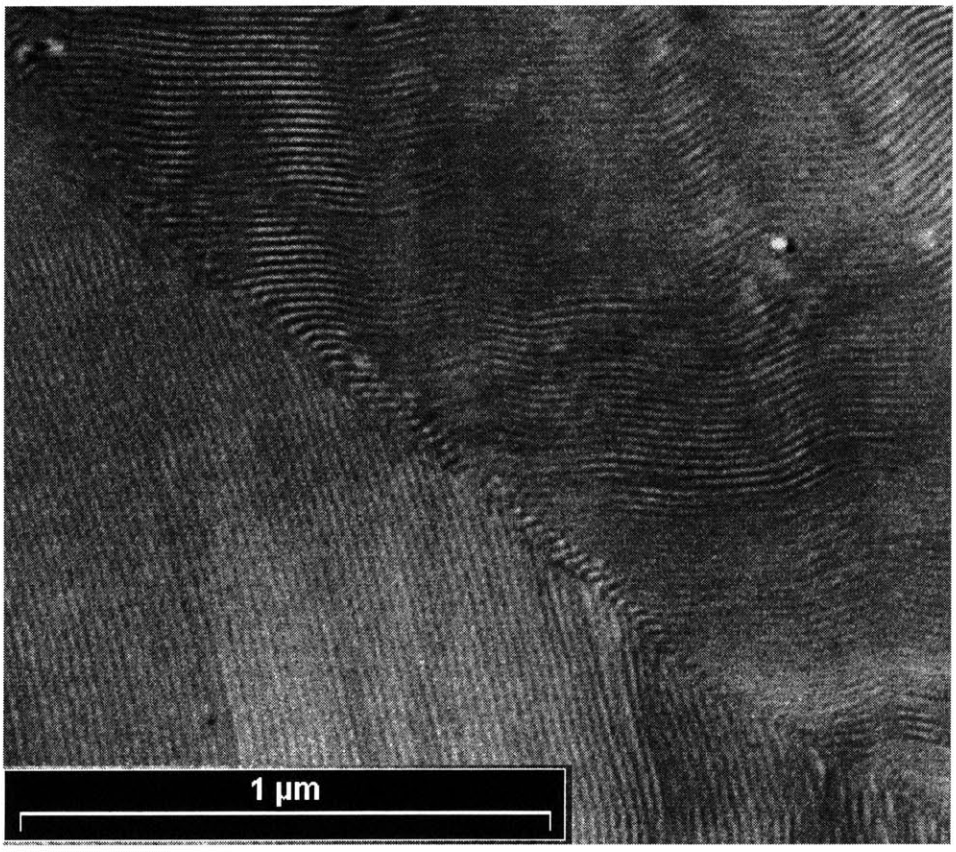

Figure 2-1: Transmission Electron Micrograph of a grain boundary in the S12B10 (9900/9700) styrene - butadiene diblock copolymer.

Looking at the TEM micrograph of Figure 2-1, it is not only possible but probable that the electron density of the grain boundary is different from the mean electron density of the grain, ρ_{GB}. It is believed that the presence of a coating or shell of grain boundary material with a local electron density, $\rho_{GB} \neq \rho_m$, will provide a source of scattering contrast in a manner not unlike the scattering of radiation in foams,[5-7] and thus allow for an absolute measurement of grain size to be made.

In this chapter, we will develop a mechanism for scattering that will allow for a measurement of grain size when a peak is present. We will calculate results for several polymers and validate these results with features of the tail of the scattering curve that has been attributed to the presence of grains. We will then compare our results to those from other viable mechanisms to show that there is little difference in the tabulated values. TEM micrographs from which a grain size can be determined will be compared to the results obtained from Ultra SAXS scattering. We will show how to estimate a grain size when no peak is present from Porod's Law and the invariant. To dispel any misconceptions that the scattering is due to the presence of voids, we will swell the polymer in a solvent to show that not only is the scattering still present, but that the grain size computed scales with volume fraction polymer.

2.2 Experimental

2.2.1 Polymers Used

In general, lower molecular weight polymers tend to produce a smaller lamellar spacing, d. Because of this, it was believed that lower molecular weight polymers would lead to smaller grains, everything else equal. Because of this, the four polymers chosen to test and validate Ultra SAXS as a grain measurement tool were styrene - butadiene block copolymers all had molecular weights less than 30,000 to minimize the chance that the grain sizes would exceed the limits of the Ultra SAXS machine. All four diblock

copolymers were synthesized and sold by Polymer Source, Inc.[8] Important molecular, morphological, and physical property data are summarized in Table 2.1

Polymer	M_S	M_B	*p*	*d (Å)*
SB5	5400	5350	1.03	100
SB9	9400	9000	1.03	290
SB15	14800	14100	1.02	230
S12B10	9900	9700	1.02	170

Table 2.1: Molecular weights of the styrene and butadiene blocks, M_S and M_B respectively, values of the polydispersity, p, and the lamellar spacing, d, for the low molecular weight polymers studied.

The values of the lamellar spacing, d, were determined by conventional, two - dimensional x-ray scattering (SAXS), and the existence of peaks in the characteristic ratio of 1, 2, 3,... verifies that all block copolymers studied microphase segregate into a lamellar morphology. It is not known why the lower molecular weight SB9 polymer has a larger d-value than the SB15 polymer. The presence of solid, uninterrupted rings for four polymers indicate that the material is isotropic and thus grainy. Two dimensional SAXS data and the corresponding one dimensional integration of intensity versus scattering vector, q, have been collected for all polymers in this thesis and are included in Appendix A.

The first three polymers listed in the table above: SB5, SB9 and SB15 contain about 90% 1,4 butadiene in the rubber block while the final entry, S12B10 conversely contains about 90% 1,2 butadiene in the rubber block. This is found from NMR spectroscopy, and by a analytical method presented elsewhere.[9] Sample NMR spectra of the polymers studied in this thesis are displayed in Appendix B.

2.2.2 Polymer Processing

As has been stated earlier, any processing of the polymer must not impart any shear, or the polymer might orient. Any orientation, however slight will skew both the 1 dimensional Ultra SAXS measurements and the deformation experiments that are presented later. Static casting and annealing are the chosen methods for processing, because no shear is imparted, thus no orientation.

2.2.2.1 Solvent Casting

For these experiments, the polymers were first dissolved to less than 10 wt% in a solution of either chloroform or methylene chloride. It has been shown by SAXS, at this value of polymer in solution, any pre-existing morphology is destroyed. Chloroform and methylene chloride were chosen as solvents because they have high relative volatilities at room temperature, and would therefore evaporate quickly, presumably creating very small grains.

This 10 wt% solution was poured into a casting boat constructed from Teflon - coated aluminum foil pressed to a glass microscope slide. The casting boat was then placed in a large glass dish and covered with another large glass dish, such that there was about 1 cm of clearance around the entire circumference. After the bulk of the solvent had evaporated, the resultant film was placed under vacuum for at least 48 hours or until there was no weight change with time to remove any trace amounts of solvent.

2.2.2.2 Annealing

Annealing at elevated temperatures leads to growth of grains.[10] For the polymers seen here, it was desirable to see a systematic growth of grains, so this was the next processing undergone after static casting.

The films were cut into 1 cm × 1 cm squares and were then annealed at an elevated temperature for consecutively longer times: 5 minutes, 1 hour, 2 hours, and 4 hours. One sample of each polymer wasn't annealed. It was important to pick a temperature that would lead to grain growth in the time frames selected, but not too high as to degrade the

polymers. For the SB9, SB15 and S12B10 polymers, the temperature selected was 75°C and for the lower molecular weight SB5, the temperature selected was 50°C.

2.2.2.3 Polymer Swelling

To avoid the inevitable criticism that x-ray scattering at very low angles is dominated by the presence of voids in rigid undiluted polymers, a second set of experiments involved swelling a styrene-butadiene block copolymer with solvent. The results are presented in Section 2.9. Phillips KR03 Resin, a styrene-butadiene block copolymer was used for these experiments. It contains 23 wt% butadiene units and has a molecular weight of 217,000 g/mole. More details of the molecular architecture and TEM characterization of the lamellar morphology appear elsewhere.[11,12] These K-resin pellets (ca. 2 mm diameter spheres) were mixed with various amounts of cumene. Polymer volume fractions of 0.66, 0.57, 0.45 and 0.29 were used. The samples were prepared by adding the selected amount of cumene to the KR03 resin in a closed container; the components were allowed to mix with occasional gentle agitation over a period of weeks until a uniform, pourable, transparent material was obtained. Immediately prior to x-ray measurements the mixtures were loaded into specially prepared specimen cells with Kapton windows. Essentially no solvent evaporation occurred during the processing and x-ray examination of the specimens. Based on the methodologies used for specimen preparation, it was anticipated that whatever pre-existing grain structure was present in the K-resin pellets would remain intact in the final specimens, albeit swollen by the cumene solvent. For comparative purposes, Ultra SAXS scattering of a pure KR03 pellet, the form which KR03 is sold, was also measured.

2.2.3 Ultra SAXS

2.2.3.1 The Beamline

The Ultra SAXS experiments were performed at the National Synchotron Light Source in the Brookhaven National Laboratory , Long Island, NY. The X23A3 beamline

operated by the National Institute of Standards and Technology is tuned for one dimensional Ultra SAXS results. The available range of scattering vector, $q = (4\pi/\lambda)\sin\theta$, was 0.1 $Å^{-1}$ to 0.0004 $Å^{-1}$, where θ is one half the scattering angle and $\lambda = 1.299$ Å is the x-ray wavelength.[13] The x-ray source was collimated using two orthogonal pairs of slits to produce a beam with a square cross section of 0.2 mm x 0.2 mm. Both the x-ray beam and the detector (scintillation counter) with a 5 mm x 5 mm window contributed to smearing effects.

2.2.3.2 Desmearing

The scattering data were desmeared to account for the geometry of the X23A3 beamline using software provided by Dr. Gabrielle Long of the National Institute of Standards and Technology and designed for this specific beamline. The program incorporated the methodology of Lake.[14] Although desmearing altered to a small extent the shapes, locations and magnitudes of the peaks in the scattering curves as is presumed, there was no case in which desmearing caused a peak to appear when none was present in the smeared data.

2.3 Mechanism of Scattering

Figure 2-2 is a set of double logarithmic plots of absolute intensity, I, vs scattering vector, q, for sample S12B10 (9900/9700). More curves will be displayed in the results sections; this was just presented to show the existence of scattering in the Ultra SAXS region. This scattering is at inverse lengths associated with grains and necessitates a mechanism. Two peaks are observed in the scattering curves. The peak at higher q appears in the conventional SAXS regime and corresponds to the periodic lamellar morphology of the SB diblock copolymer. The lamellar spacing $d = \frac{2\pi}{q_{MAX}} = 170$ Å is essentially unchanged by the annealing protocol described in the figure and agrees with the value of d obtained by traditional SAXS and displayed in Appendix A. The position of the peak at the left varies with annealing time, spanning a range corresponding to a spacing of

about 1 μm. As discussed in detail below, we associate this low-q peak with the presence of grains in the materials. We also note that continued annealing shifts the peak to lower values of q, corresponding to a larger material length scale; this phenomenon of grain growth is verified elsewhere.[15]

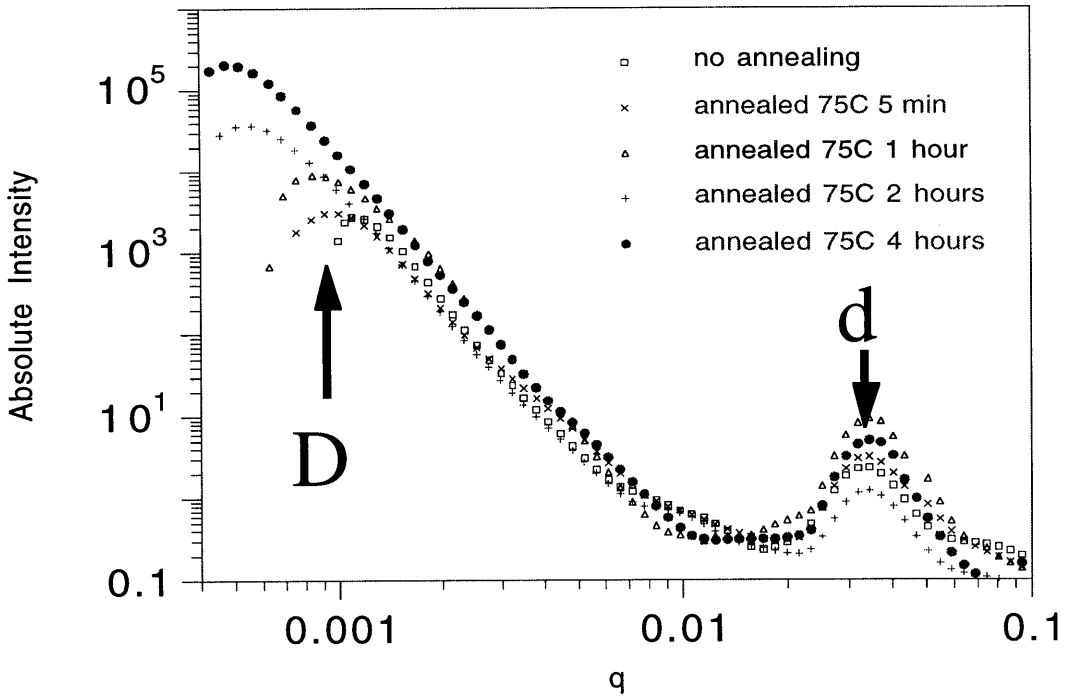

Figure 2-2: Logarithm of absolute intensity vs log q at various annealing times for the 9900/9700 styrene - 1,2 butadiene block copolymer (S12B10) cast from methylene chloride. The right peaks correspond to the interlamellar spacing, d, and the left peaks refer to the grain spacing, D.

As has been stated in the introduction, there have been studies focused on the detailed structure of grain boundary morphologies in styrene - butadiene block copolymers.[16-19] In these detailed microscopic observations there are clear suggestions that the local composition in the grain boundaries is different from the overall mean composition of the material, as witnessed in Figure 2-1. It is also known that a free surface leads to an

altered local composition in block copolymers[20] and we make the assumption that similar, although perhaps smaller, composition fluctuations arise at the grain boundaries. A schematic of this scattering mechanism is shown in Figure 2-3, where the scattering contrast seen in the Ultra SAXS region is shown by the bold line and the contrast from the styrene - butadiene lamellar spacing is ghosted in.

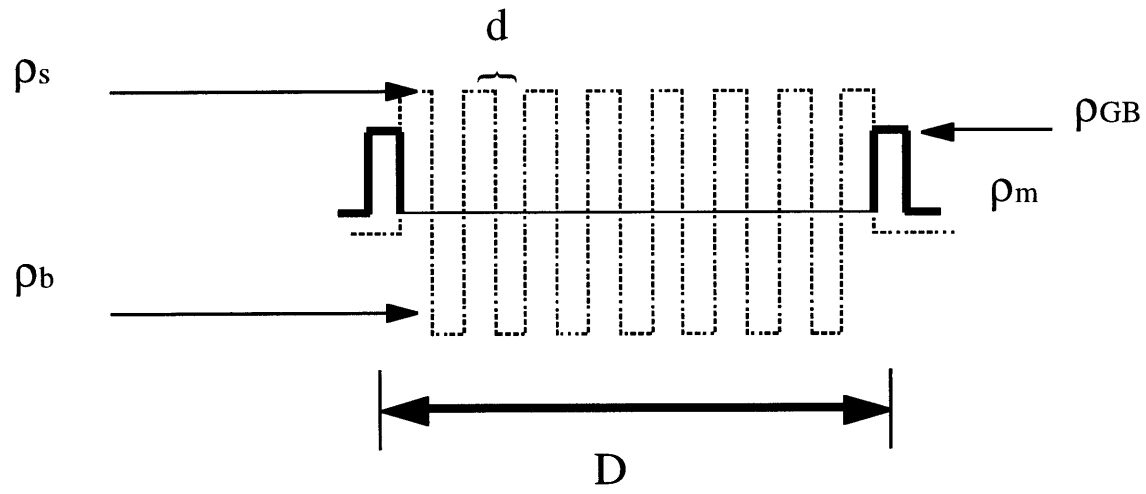

Figure 2-3: Schematic representation of the proposed mechanism. The dark lines represent the electron density differences represented in the Ultra SAXS region corresponding to the grain size. The electron density differences relating to interlamellar spacing are ghosted in.

In Figure 2-3, D and d correspond to the grain size and the lamellar spacing respectively and all of the densities, ρ, correspond to electron densities. The subscripts "s" and "b" on ρ correspond to the electron densities of styrene and butadiene respectively, "m" refers to the mean density of the grain and "GB" is the electron density of the grain boundary, which can either be closer to styrene, as depicted, or closer to butadiene. We will test the internal consistency of this assumption later in the analysis, recognizing that the assumed contrast factor, $(\rho_{GB} - \rho_m)^2$, must always lie between zero and either $(\rho_s - \rho_m)^2$ or $(\rho_b - \rho_m)^2$ in order for this analysis to be accurate.

2.3.1 Spherical Form Factor

In the very low-q range (below about 0.005), the x-rays are oblivious of the short-range lamellar structure of the length scale, d, and are influenced by the mean grain density, ρ_m, over the entire volume of the grain. The presence of a coating or shell of grain boundary material with a local density, $\rho_{GB} \neq \rho_m$, provides a source of scattering contrast. We proceed with a quantitative analysis of our scattering data along the lines of the mechanism outlined in Figure 2-3, and we employ the spherical form factor proposed in the 1960's by Stein et al to determine the size of spherulites in low angle light scattering experiments.[21,22]

Two other mechanisms quickly come to mind when attempting to analyze the data: Bragg - like scattering, and the use of correlation functions. These are both viable explanations, and numerical comparisons of the results obtained by all three methods are compared in Section 2.7 of this thesis. The reason that spherical form factor was applied was because among discussions with other research group, it was realized that there is a readily recognized morphological, even if not mechanistic, analogy between our impinged grains and Stein's spherulite analysis. Because it meshed well with the mechanistic ideas that we lay out, we have de-emphasized the other methods of accounting for the Ultra SAXS peaks.

The spherical form factor is defined as:

$$U = \left(\frac{4\pi}{\lambda}\sin\frac{\theta}{2}\right)R = qR \qquad (2\text{-}2)$$

and exhibits a peak at a value U=4.0.[22] For each scattering curve which exhibits a peak in the Ultra SAXS region, we can use this to obtain the grain size from the relation

$$D = \frac{8}{q_{MAX}} \qquad (2\text{-}3)$$

which in fact differs only slightly from a simple quasi-Bragg analysis.

2.3.2 Contrast Factor and Grain Boundary Volume Fraction

There are features in the Ultra SAXS data which enable us to make certain internal consistency checks to support the proposed mechanism of scattering. In particular, the cartoon of Figure 2-3 indicates that $\Delta\rho^2$ should have an upper bound of $(\rho_s - \rho_m)^2$ or $(\rho_b - \rho_m)^2$, either of which to a good approximation for our morphologically linear diblock copolymers is equal to $\left(\frac{\rho_s - \rho_b}{2}\right)^2$. In other words, the difference in electron density between the grain boundary and the mean density of the grain cannot be larger than the difference between either styrene or butadiene and the average of styrene and butadiene. If the difference is greater, the grain boundary is essentially denser than styrene or less dense than butadiene, invalidating the mechanism. Extracting the contrast factor, $(\Delta\rho)^2$, from our data would therefore provide one method to support or discredit the scattering mechanism. Also, both Figure 2-3 and transmission electron micrographs of grainy styrene - butadiene block copolymers like Figure 2-1, suggest that the volume fraction of the grain boundary is small compared to the volume of material in the grain with mean density, ρ_m. If the analysis of the data indicates otherwise, the mechanism suggested in Figure 2-3 is in doubt. We use Porod's Law and the scattering invariant, both of which are readily accessible characteristics of the scattering curves in the Ultra SAXS region, to test our mechanism. Porod's Law constant, C_1, is obtained from the region to the right of the low-q scattering peak where intensities decrease with a q^{-4} dependence.

$$C_1 \equiv \frac{1}{2\pi} \lim_{q \to \infty} \left(q^4 i\right) = (S/V)(\rho_{GB} - \rho_m)^2 \qquad (2\text{-}4)$$

where: i is the absolute desmeared intensity

(S/V) is the surface to volume ratio

If we assume that a grain is essentially a sphere, the surface to volume ratio is equal to 6/D. The invariant in this case is defined as the total area under the iq^2 vs q plot associated with grain scattering, and can be expressed as follows:

$$C_2 \equiv \frac{1}{2\pi^2}\int_0^\infty i(q)q^2dq = \phi(1-\phi)(\rho_{GB}-\rho_m)^2 \qquad (2\text{-}5)$$

where: ϕ is the volume fraction of grain boundary material.

This grain invariant is constructed from the left peak of Figure 2-2. In the portion of the scattering curve where the tail of the grain peak overlaps the start of the lamellar peak, the intensity is assumed to follow a Porod - like q^{-4} dependence. Combining equations (2-4) and (2-5) eliminates the contrast factor $(\Delta\rho)^2$ and yields:

$$D = 6(V/S) = \frac{6C_2}{C_1\phi(1-\phi)} \qquad (2\text{-}6)$$

This equation can be solved for ϕ because the grain size D has been determined from the Spherical Form Factor and the Ultra SAXS peak locations.

2.4 Verifying Porod's Law

2.4.1 Porod Constant

In order to use the contrast factor, $(\Delta\rho)^2$, and the grain boundary volume fraction, ϕ, as methods to validate the mechanism that the scattering is caused by grain boundaries scattering against the grains, it is important that the scattering in the tail of the peak in the Ultra SAXS region obey Porod's Law. If we look at equation 2-4, we see that in the Porod region, iq^4 is a constant. If we plot iq^4 versus q in this region, we should get a

horizontally flat line. Figure 2-4 replots the data from Figure 2-2 in this fashion, and we can see the flat horizontal lines in the Porod region. Values of the Porod constant, vary from about 2×10^{-9} to 8×10^{-9} from the scattering of these block copolymers.

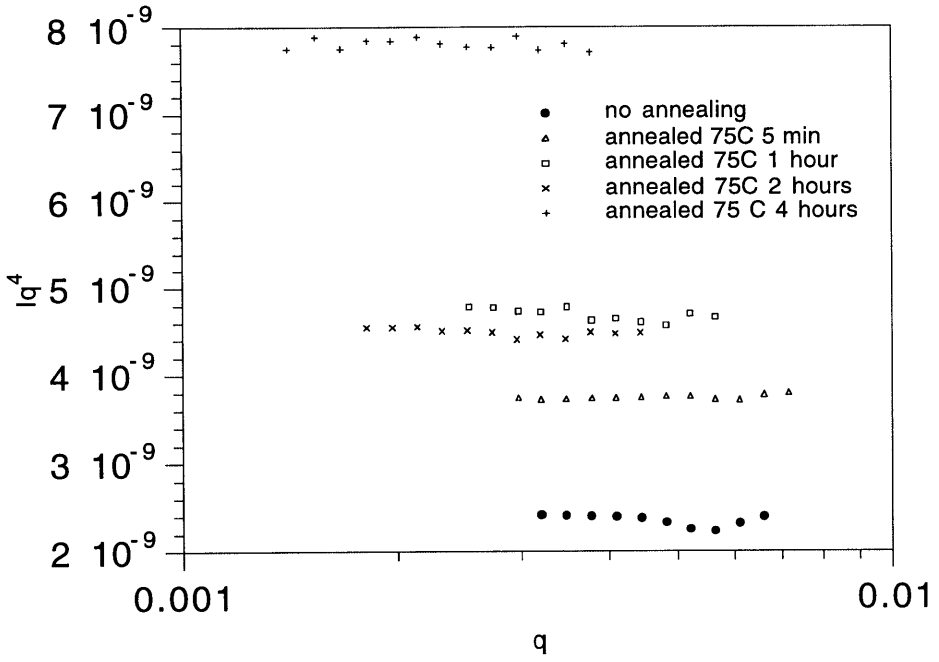

Figure 2-4: Iq^4 vs log q in the Porod Region at various annealing times for the 9900/9700 styrene - 1,2 butadiene block copolymer (S12B10) cast from methylene chloride. The flat horizontal lines indicate Porod's Law is obeyed.

2.4.2 Interference Function

It is believed by some that plots of Iq^4 vs q are insufficient for determining that Porod's Law is observed. Instead, it is necessary to look at the Interference function , C_1-Iq^4. Any systematic deviations in the Interference function may manifest in estimates of the grain boundary volume fraction ,ϕ. Figures 2-5, 2-6, 2-7, 2-8, and 2-9 show the values of the Interference function versus scattering vector, q, at various annealing times for S12B10 for the Porod region plots shown in Figure 2-4.

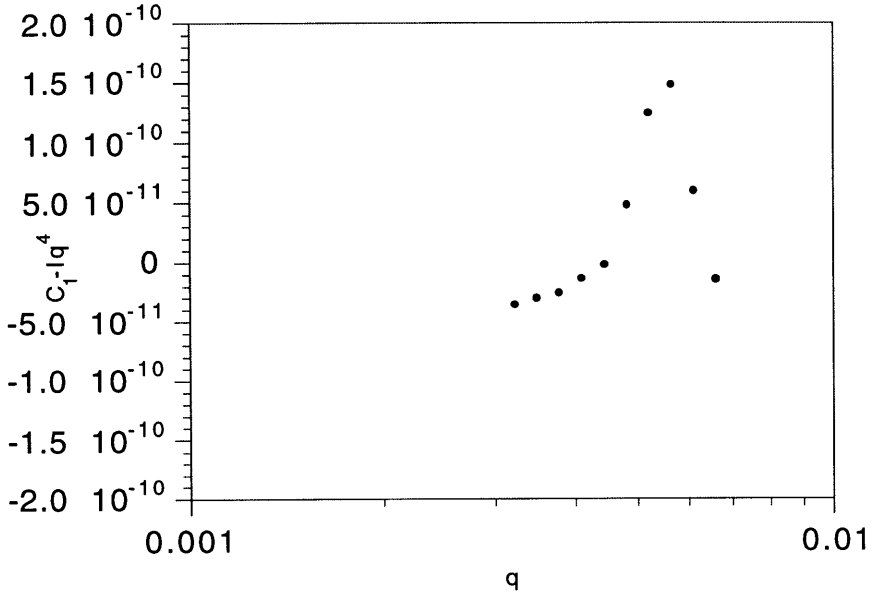

Figure 2-5: Interference Function, C_1-Iq^4, versus log q for the S12B10 polymer cast from methylene chloride, no annealing.

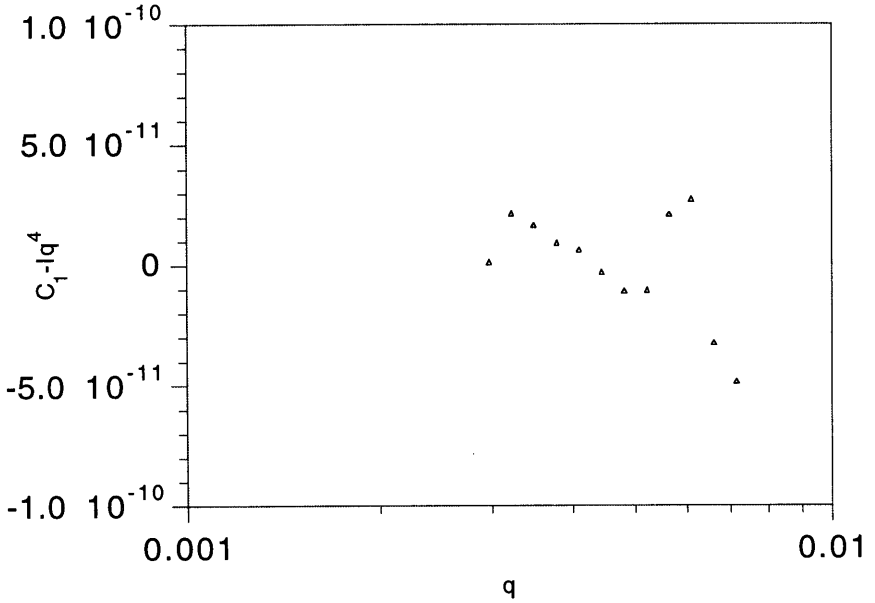

Figure 2-6: Interference Function, C_1-Iq^4, versus log q for the S12B10 polymer cast from methylene chloride, annealed at 75°C for 5 minutes.

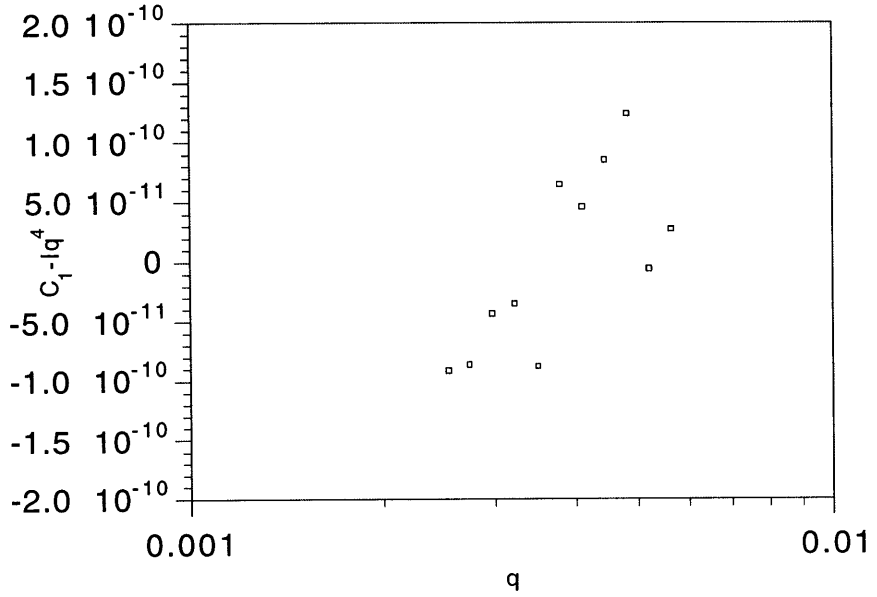

Figure 2-7: Interference Function, C_1-Iq^4, versus log q for the S12B10 polymer cast from methylene chloride, annealed at 75°C for 1 hour.

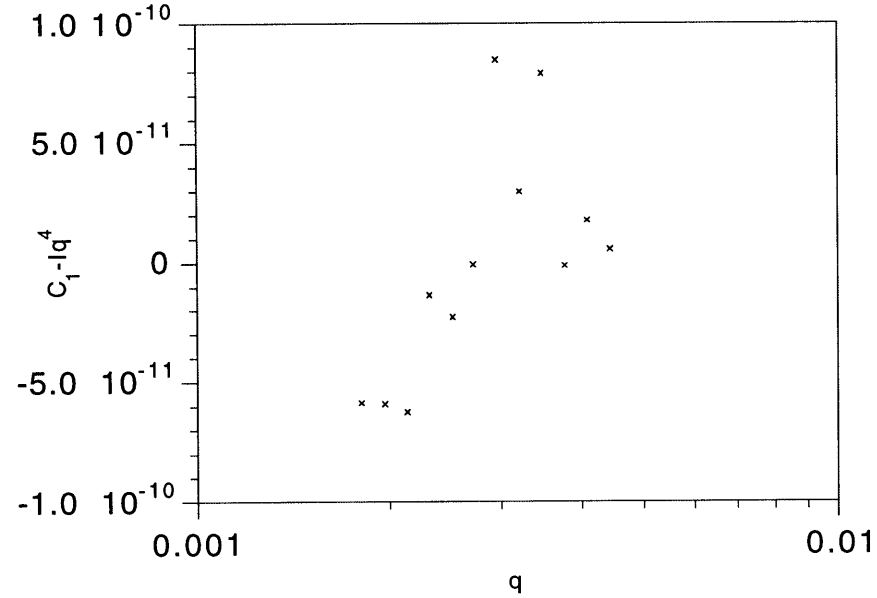

Figure 2-8: Interference Function, C_1-Iq^4, versus log q for the S12B10 polymer cast from methylene chloride, annealed at 75°C for 2 hours.

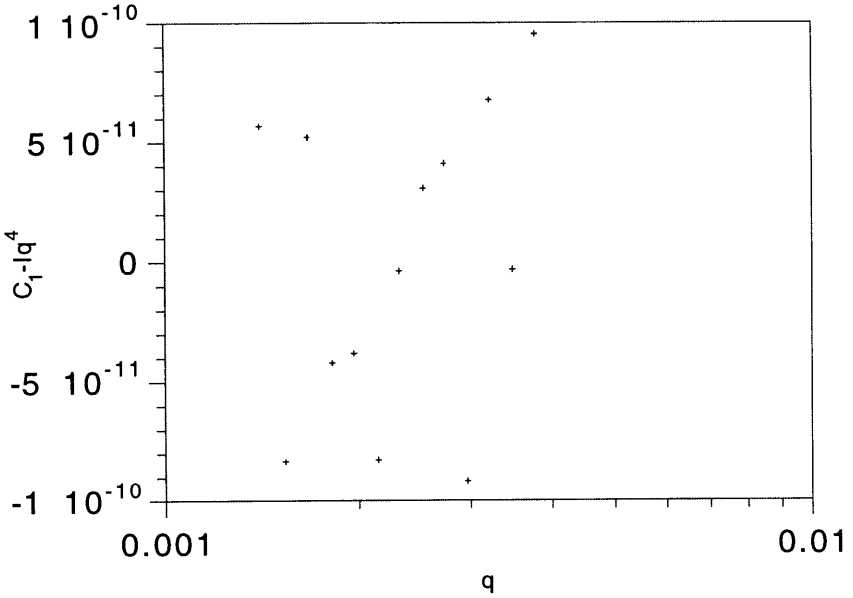

Figure 2-9: Interference Function, C_1-Iq^4, versus log q for the S12B10 polymer cast from methylene chloride, annealed at 75°C for 4 hours.

It is possible that systematic errors, if any, in the Interference function will manifest in the estimates of the grain boundary thickness, ϕ. We should look for any trends in the interference function as well as the relative magnitude of the Interference function compared to the Porod constant, C_1. As can be seen from the previous 5 graphs, no value of the interference function is greater than 2×10^{-10}, and most are on the order of 10^{-11} and less, compared to the values of Iq^4 that had been reported in section 2.4.1 which range between 2×10^{-9} and 8×10^{-9}. Also, there is no systematic error or trend witnessed in the Interference function which would manifest itself as an error in the Porod Constant and thus the estimate of ϕ. This analysis has been performed on all data presented in this thesis, but its inclusion would be redundant and unnecessary. From this analysis, we can conclude that Porod's Law is observed in the tail of the peak of the Ultra SAXS scattering

curve, and that subsequent analysis can be used to validate the mechanism of grain scattering. Similar analytical techniques to those presented in the last two sections have recently been employed on scattering data of semicrystalline polymers by Murthy and colleagues as well as Donald et al.[23-25] They also have analyzed the tails of scattering curves to extract important information.

2.5 Grain Size Results from Scattering Curves with a Clearly Discernible Peak

2.5.1 S12B10 (9900/9700)

The scattering curves for S12B10 (9900/9700) cast from methylene chloride and annealed for various times at 75°C has already been shown in Figure 2-2. This data is replotted as Iq^2 vs q in Figure 2-10. As can be seen, all curves have a clearly discernible peak. Because of this, the spherical form factor can be used to calculate grain size, D.

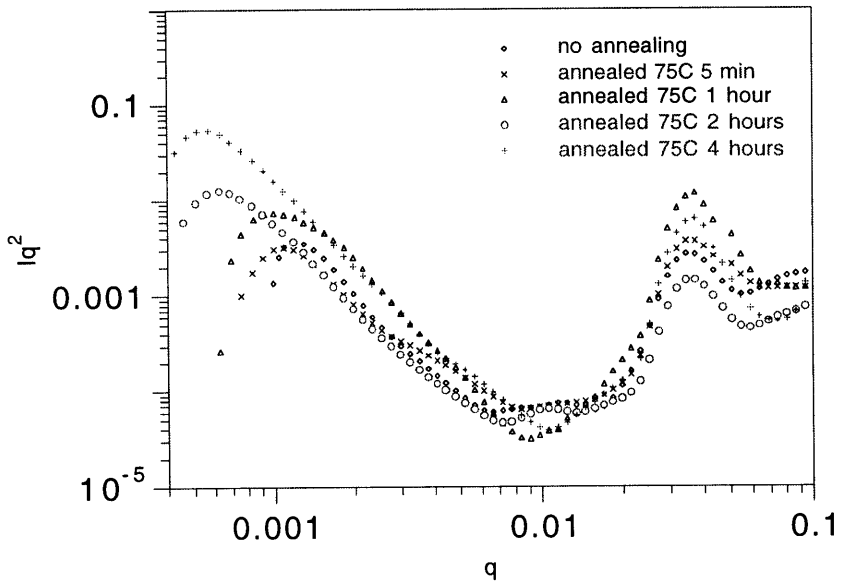

Figure 2-10: Log Iq^2 vs log q for the S12B10 (9900/9700) cast from methylene chloride annealing at 75°C for various amounts of time.

After the spherical form factor has been used to calculate D, Porod's Law and the invariant can be used to calculate the contrast factor, $(\Delta\rho)^2$ and the volume fraction taken by the grain boundary, ϕ. These results as well as the number of lamellae per grain, D/d. are summarized in Table 2.2.

Annealing Time at 75 °C	*D (μm)*	$(\Delta\rho)^2$	ϕ	*D/d*
none	0.67	3.70E-6	0.106	39
5 minutes	0.74	3.84E-6	0.104	44
1 hour	0.80	6.90E-6	0.108	47
2 hours	1.28	8.80E-6	0.108	75
4 hours	1.40	9.98E-6	0.102	82

Table 2.2: Values of Grain Size, D; Phase Fraction, ϕ; and Electron Density Differences, $(\Delta\rho)^2=(\rho_{GB}-\rho_m)^2$, and the number of lamellae per grain, D/d, as a Function of Annealing Time at 75°C for 9900/9700 Styrene 1,2 Butadiene (S12B10)

The grain size increases by a factor or 2 due to annealing, from 0.67 μm to 1.40 μm. What should also be noted is that the volume fraction of grain boundary is roughly constant at a value of $\phi \cong 0.1$. The contrast factor, $(\Delta\rho)^2$, apparently increases monotonically, up almost to a value of 10^{-5}, but this is still far away from the upper limit of $\left(\frac{\rho_s - \rho_b}{2}\right)^2 = 4.0 \times 10^{-4}$ that is proposed by this mechanism. These results will be discussed further at the end of this section.

2.5.2 SB15 (14800/14100)

Figure 2-11 presents results for the case of sample SB15 (14800/14100). This polymer was dissolved and static cast from chloroform. Again the lamellar spacing (d=230Å for this polymer) remains essentially unchanged with time while the low-q peak shifts with annealing by an amount which corresponds to about a factor of 3 in morphological length scale. The data at the lowest values of q in Figure 2-11 fall off in the direction of zero intensity; this trend, coupled with the exceedingly low value of q at the low end of the Ultra SAXS resolution facilitates calculation of the Ultra SAXS invariant, with insignificant low-q truncation error.

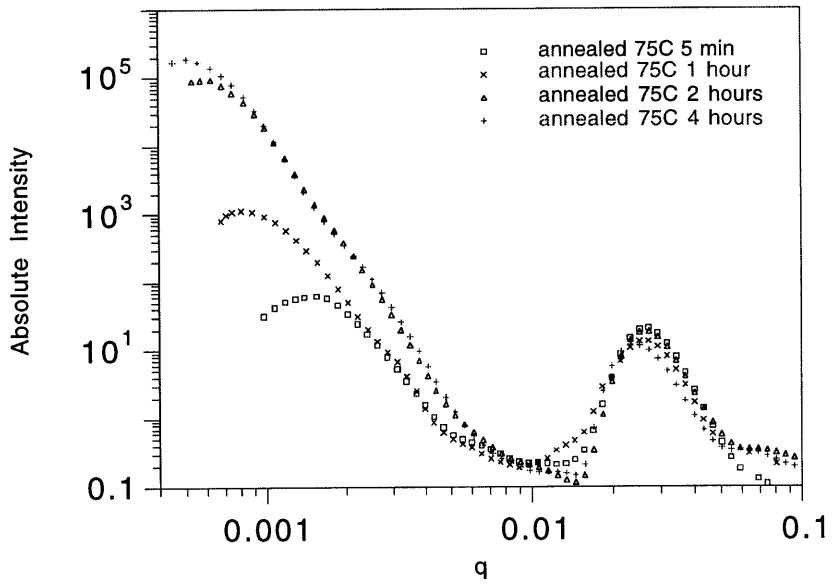

Figure 2-11: Logarithm of the absolute intensity vs log q at various annealing times for the 14800/14100 styrene - 1,4 butadiene block copolymer (SB15) cast from chloroform.

Figure 2-12 redisplays the log-log plots in the familiar format of Iq^2 vs q. As with the S12B10 results, all curves display a clearly resolvable peak, and thus, the spherical form factor can be used to determine the grain size, D. Porod's Law and the invariant can be

used to calculate the contrast factor, $(\Delta\rho)^2$, and the volume fraction of the grain boundary, ϕ. These results as well as the number of lamellae per grain, D/d. are summarized in Table 2.3.

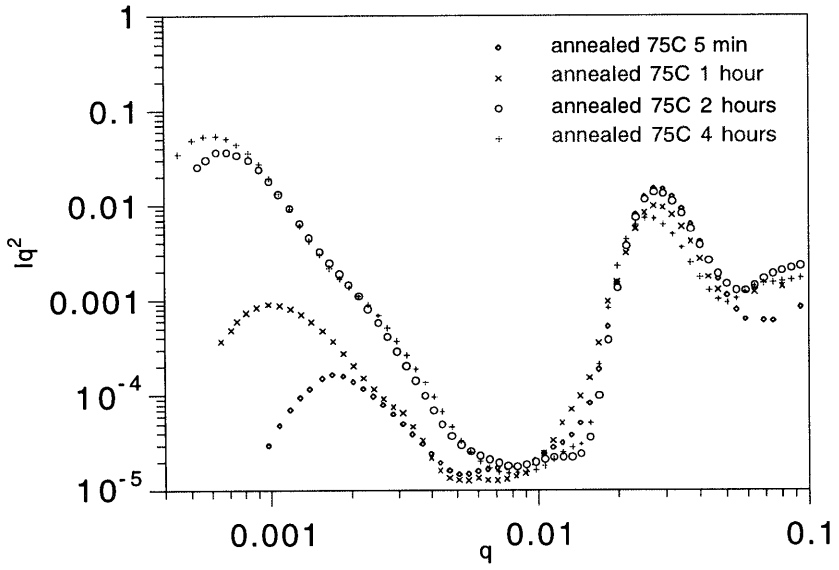

Figure 2-12: Logarithm of Iq^2 vs log q at various annealing times for the 14800/14100 styrene - 1,4 butadiene block copolymer (SB15) cast from chloroform.

The grain sizes vary between about 0.5 and 1.3 μm for these processing conditions. As with the S12B10 polymer, the grain boundary volume fraction hovers around a value of $\phi \cong 0.1$. The contrast factor also increases monotonically, as with the S12B10 polymer, and still falls short of the limit proposed by the mechanism.

Annealing Time at 75 °C	*D (μm)*	$(\Delta\rho)^2$	ϕ	*D/d*
5 minutes	0.47	3.75E-7	0.093	20
1 hour	0.81	1.27E-6	0.092	35
2 hours	1.17	2.33E-5	0.101	51
4 hours	1.29	3.27E-5	0.103	56

Table 2.3: Values of Grain Size, D; Phase Fraction, ϕ; Electron Density Differences, $(\Delta\rho)^2=(\rho_{GB}-\rho_m)^2$, and the number of lamellae per grain, D/d, as a Function of Annealing Time at 75°C for 14800/14100 Styrene 1,4 Butadiene (SB15)

2.5.3 SB5 (5400/5350)

Figure 2-13 presents absolute intensity versus scattering vector, q, results for the sample SB5 (5400/5350) cast from chloroform. As with the previous two sets of data, the lamellar spacing (d=100Å for this polymer) remains essentially unchanged with time while the low-q peak shifts with annealing by an amount which corresponds to about a factor of 2 in morphological length scale. Again, data at the lowest values of q in both Figure 2-13 fall off in the direction of zero intensity; this trend, coupled with the exceedingly low value of q at the low end of the Ultra SAXS resolution facilitates calculation of the invariant.

The SB5 polymer is a very low molecular weight block copolymer and it was worried that annealing at 75°C, as all of the other polymers have been, would possibly degrade the polymer, and definitely grow the grains at a rate which would test the limit of the machine. Therefore, this polymer was annealed at 50°C, which, is reflected in the legend of Figure 2-13. As can be seen from the figure, annealing at this temperature allowed all scattering curves to have clearly resolvable peaks in the Ultra SAXS region. Figure 2-14 redisplays the log-log plot in the familiar format of Iq^2 vs q.

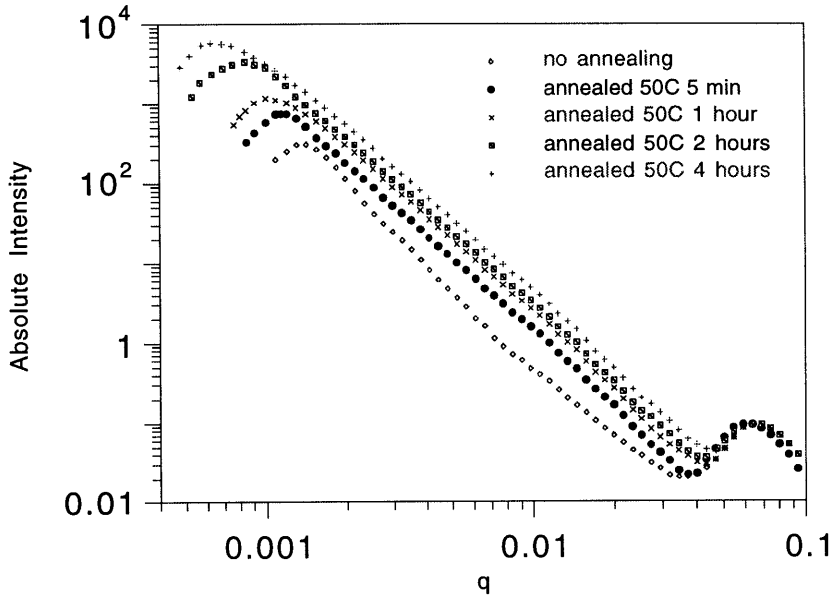

Figure 2-13: Logarithm of absolute intensity vs log q at various annealing times for the 5400/5350 styrene - 1,4 butadiene block copolymer (SB5) cast from chloroform.

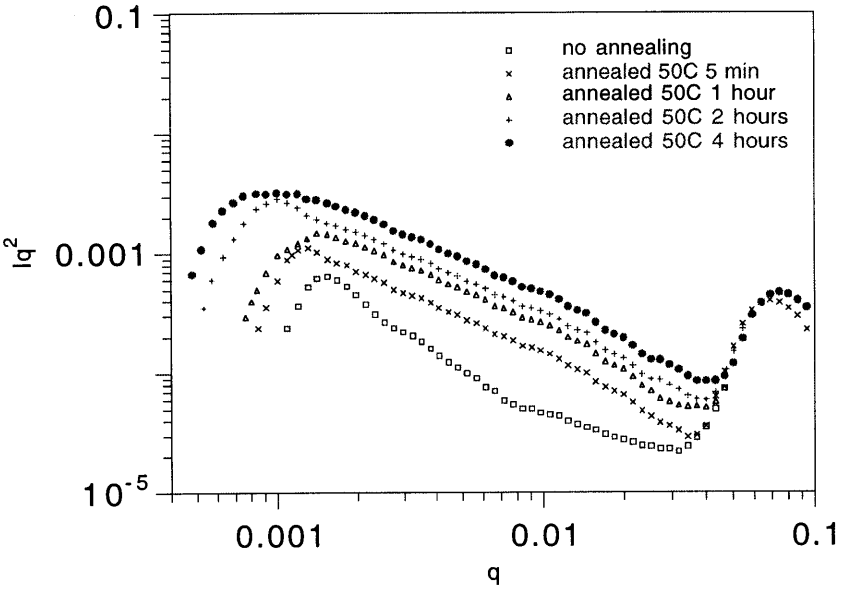

Figure 2-14: Log Iq^2 vs log q at various annealing times for the 5400/5350 styrene - 1,4 butadiene block copolymer (SB5) cast from chloroform.

Since all curves display a clearly resolvable peak, the spherical form factor can be used to determine the grain size, D, and the invariant and Porod's Law can be used to determine the contrast factor, $(\Delta\rho)^2$, and the grain boundary volume fraction, ϕ. All of these results are summarized in Table 2.4.

Annealing Time at 75 °C	*D (μm)*	*$(\Delta\rho)^2$*	*ϕ*	*D/d*
none	0.52	1.48E-6	0.0975	52
5 minutes	0.61	1.73E-6	0.0991	61
1 hour	0.75	2.29E-6	0.1057	75
2 hours	0.87	2.51E-5	0.0994	87
4 hours	0.95	3.36E-5	0.1000	95

Table 2.4: Values of Grain Size, D; Phase Fraction, ϕ; Electron Density Differences, $(\Delta\rho)^2=(\rho_{GB}-\rho_m)^2$, and the number of lamellae per grain, D/d as a Function of Annealing Time at 50°C for 5400/5350 Styrene 1,4 Butadiene (SB5)

The grain sizes vary by a factor of three for this polymer and these processing conditions. As with the S12B10 polymer, the grain boundary volume fraction hovers around a value of $\phi \cong 0.1$. The contrast factor also increases monotonically, as with the S12B10 polymer, and falls short of the limit proposed by the mechanism.

2.5.4 Discussion

From the three data series where all of the curves show a clearly resolvable peak, several observations can be made. Firstly, the grain boundary volume fraction, ϕ, remains

essentially constant at a value of 0.1 for all of the polymers studied. If we continue the previous assumption that the grain boundaries are a shell around spherical grains, the grain boundary thickness turns out to be approximately 1.7% of the grain diameter. In other words, for the SB15 (14800/14100) sample possessing a grain diameter of 0.81 the corresponding grain boundary thickness is about 140 Å, which is less than one repeat distance of the block copolymer lamellar morphology.

We can also note that the contrast factor increases with increasing grain size, such that it approaches the maximum allowed by the mechanism explained in this chapter. More simply, the grain boundaries are becoming richer in either styrene or butadiene as the grains grow. We see that we can control grain size by annealing by about a factor of three for all three polymers studied up to this point. Finally from the last column in Tables 2.2, 2.3 and 2.4, we can see the values of D/d for the three polymers. These values are not the same for similar processing conditions, so it can be said that the number of lamellae per grain is also a function of the polymer as well as the processing conditions.

2.6 Other Interpretations of Grain Size

In the previous analysis, an absolute grain size was found from the peak of the scattering data using the spherical form factor. As previously discussed, this method was chosen because there is a readily recognized morphological, even if not mechanistic, analogy between grains and Stein's spherulites. Because the spherical form factor gelled well with the proposed mechanism, this method has been stressed, and other methods of accounting for the Ultra SAXS peaks have been de-emphasized up until now. Two other ways of determining an absolute grain size from the Ultra SAXS peaks exist. The first method is to assume that the source of contrast is similar to the that of the lamellar spacing, and therefore the grain diameter can be found from Bragg's Law:

$$D_{Bragg} = \frac{2\pi}{q_{MAX}} \qquad (2\text{-}7)$$

It can be seen that this method of grain size determination leads to values that are always 22% less than those of the spherical form factor, as $D = 8/q_{MAX}$ for this method. Another method of grain size determination is to use the correlation function:[26]

$$D_{CF} = \frac{\pi \int_0^{\infty} I(q)qdq}{C_2} \qquad (2\text{-}8)$$

where: C_2 is the invariant mentioned previously

One advantage of the correlation function is that the geometry of the grains need not be known. However, as the peak position is not used in the calculations, there is no way to verify the mechanism. Grain sizes using all three methods were determined for the S12B10 polymer cast from methylene chloride, where the data was displayed in Figure 2-2 and again in Figure 2-10. Mechanistic results for these scattering curves were given in section 2.5.1. Table 2.5 displays the grain sizes found from Bragg's Law and the correlation function as well as the values found using the spherical form factor that has previously been used.

As can be seen from Table 2.5, the correlation function approach reveals the same trend for grain size with annealing as what is shown by the spherical form factor and Bragg's Law. The grain sizes calculated by the spherical form factor are consistently larger (by about a factor of 1.6 to 1.7) than those obtained by the correlation function. This is probably a result of a different weighting of the population distribution in these two methods.

Since the trends are the same for all three methods of grain size determination, the spherical form factor will continue to be the method used in the rest of this thesis because of the previously mentioned morphological similarities between impinged spherulites and grains. It is to be noted that the correlation function is another way to calculate an absolute

grain size, and choosing the spherical form factor approach in no way suggests that it is the only method to determine an absolute grain size from the Ultra SAXS scattering curves.

Annealing Time at 75 °C	D_{CF} (μm)	D_{Bragg} (μm)	D_{SFF} (μm)
none	0.40	0.53	0.67
5 min	0.46	0.58	0.74
1 hour	0.48	0.63	0.80
2 hours	0.74	1.01	1.28
4 hours	0.85	1.10	1.40

Table 2.5: Values of the Grain Diameter calculated from the correlation function (CF), Bragg's Law (Bragg) as well as the Spherical Form Factor (SFF), for the S12B10 sample cast from methylene chloride and annealed at 75°C for various amounts of time.

2.7 Comparison of Grain Size Obtained by Ultra SAXS and Transmission Electron Microscopy

Figure 2-15 is another set of double logarithmic plots of absolute intensity, I, vs scattering vector, q, for sample S12B10 (9900/9700). Though the samples are still reported as a function of annealing time at 75°C, this time the original casting solvent is chloroform instead of methylene chloride.

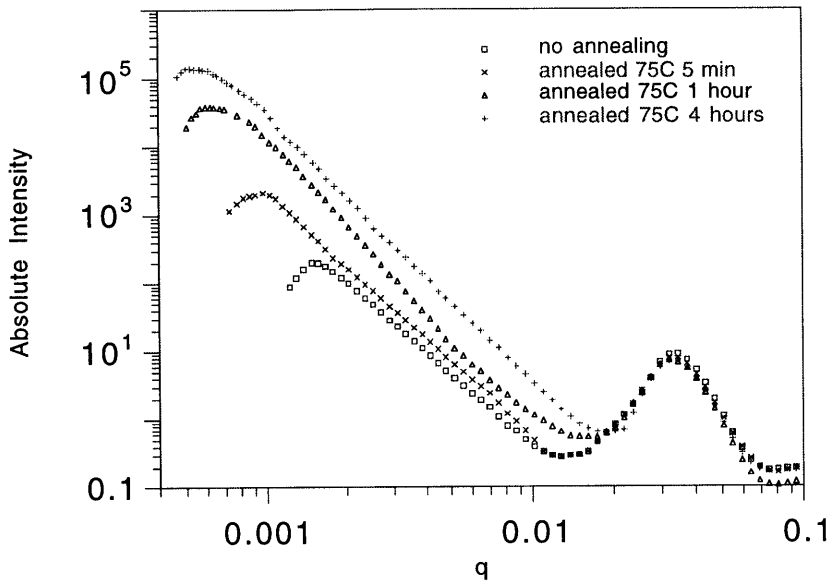

Figure 2-15: Logarithm of absolute intensity vs log q at various annealing times for the 9900/9700 styrene - 1,2 butadiene block copolymer (S12B10) cast from chloroform.

The lamellar spacing as determined by Bragg's Law, $d = \frac{2\pi}{q_{MAX}} = 170\,\text{Å}$, is unchanged by the annealing protocol of up to 4 hours at 75°C. It is also exactly the same spacing as when the sample was cast from methylene chloride and shown in Figures 2-2 and 2-10. A similar shift in the peak positions is witnessed in the left peak that is attributed to the grain diameter, though the positions are slightly different than those found when the polymer was static cast from methylene chloride. The data are replotted in the more familiar form of log Iq^2 vs. q and shown in Figure 2-16.

As has done before, since all scattering curves show a clearly discernible peak, we can use the spherical form factor to calculate D and Porod's Law and the invariant to

determine the contrast factor, $(\Delta\rho)^2$, and the grain boundary volume fraction, ϕ. These values are displayed in Table 2.6.

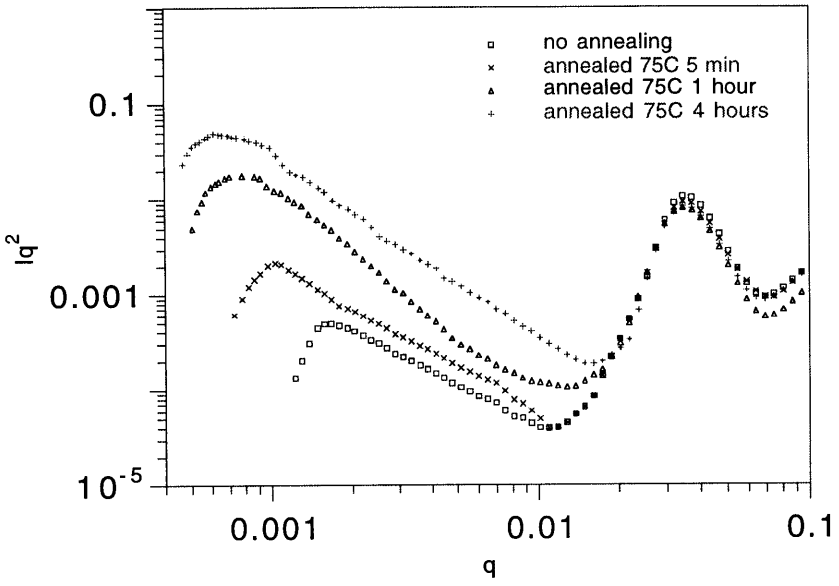

Figure 2-16: Log Iq^2 vs log q at various annealing times for the 9900/9700 styrene - 1,2 butadiene block copolymer (S12B10) cast from chloroform.

Annealing Time at 75 °C	*D (μm)*	*$(\Delta\rho)^2$*	*ϕ*	*D/d*
none	0.51	1.90E-6	0.0995	30
5 minutes	0.78	3.11E-6	0.0991	46
1 hour	1.03	1.36E-5	0.1038	61
4 hours	1.53	1.78E-5	0.0987	90

Table 2.6: Values of Grain Size, D; Phase Fraction, ϕ; Electron Density Differences, $(\Delta\rho)^2=(\rho_{GB}-\rho_m)^2$, and the number of lamellae per grain, D/d as a Function of Annealing Time at 75°C for 9900/9700 Styrene 1,2 Butadiene (S12B10)

Through a collaboration with Dr. Alexander Karbach of Bayer A.G. in Germany, we have been able to produce the appropriately uniform, large-area, stained with osmium tetroxide and ultramicrotomed sections required to produce a TEM micrograph with enough grains present to attempt to obtain a meaningful measurement of grain size. Figures 2-17, 2-18, and 2-19 show Transmission Electron Microscopy (TEM) micrographs for the first three S12B10 (9900/9700) samples tested using Ultra SAXS. These figures again demonstrate the existence of grains in the block copolymer samples.

Underwood proposes a method for determining sizes from micrographs for certain particle geometries taking into account the inherent stereology.[27] We can calculate a *mean intercept length*, which for an aggregate containing grains is the average diameter. The surface to volume ratio (S/V) is

$$S/V = 2\,P_L \tag{2-9}$$

where P_L is the number of grain boundaries per unit length.

From Underwood's analysis, the diameter, D, is

$$D = \frac{2}{(S/V)} \tag{2-10}$$

The reason the grain diameter is only twice the surface to volume ratio, and not six times as had been employed in all of our analysis up to this point has to do when trying to extract three dimensional lengths from a two dimensional image.[27] Employing this analysis on Figures 2-17, 2-18 and 2-19, we can get an average grain size. These grain sizes are summarized in Table 2-7 along with the diameters found by Ultra SAXS.

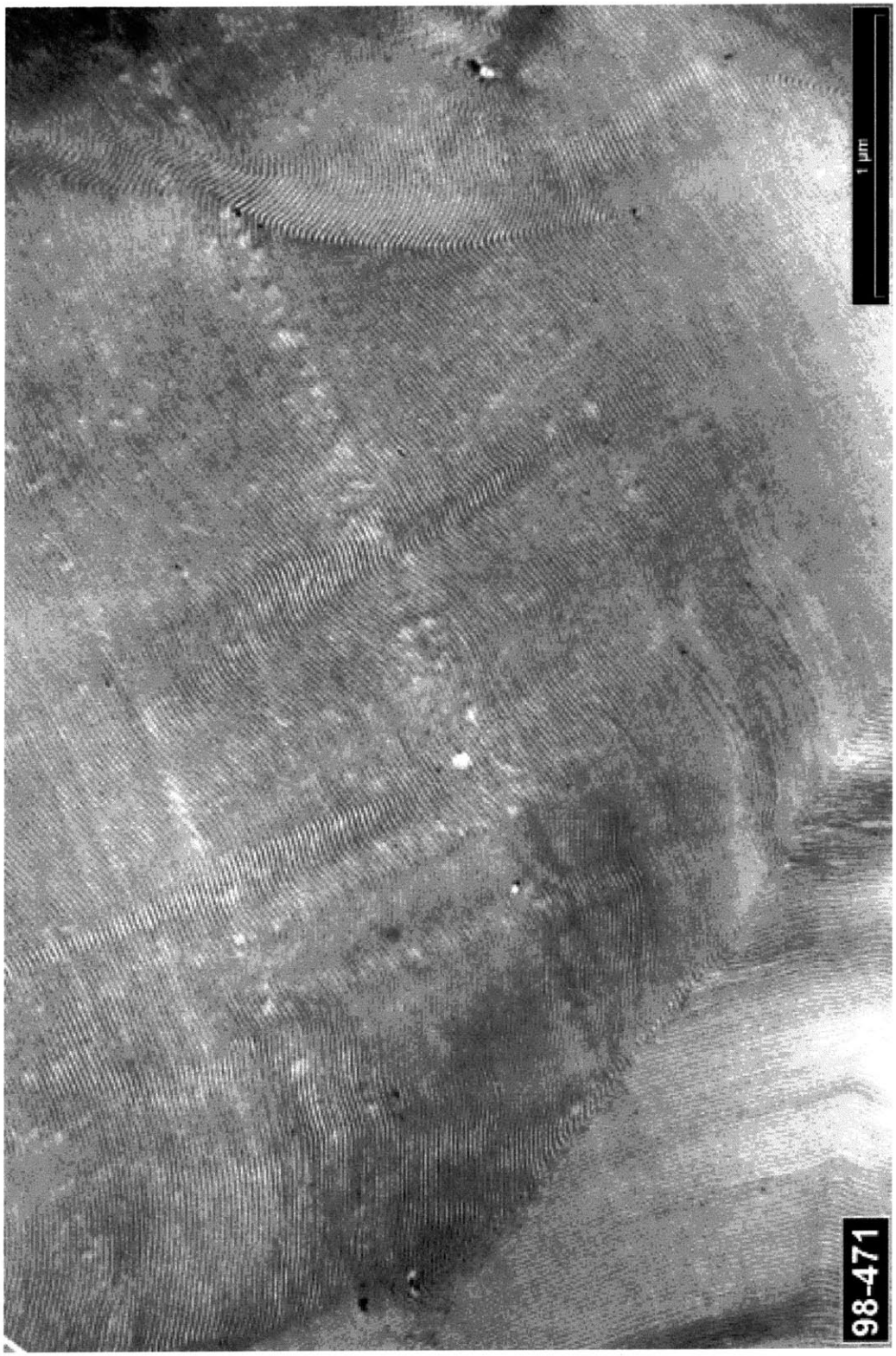

Figure 2-17: Transmission electron micrograph of the 9900/9700 styrene - 1,2 butadiene block copolymer (S12B10) cast from chloroform, unnanealed, ultramicrotomed and stained with OsO4. Micrograph courtesy of Dr. A. Karbach, Bayer A.G.

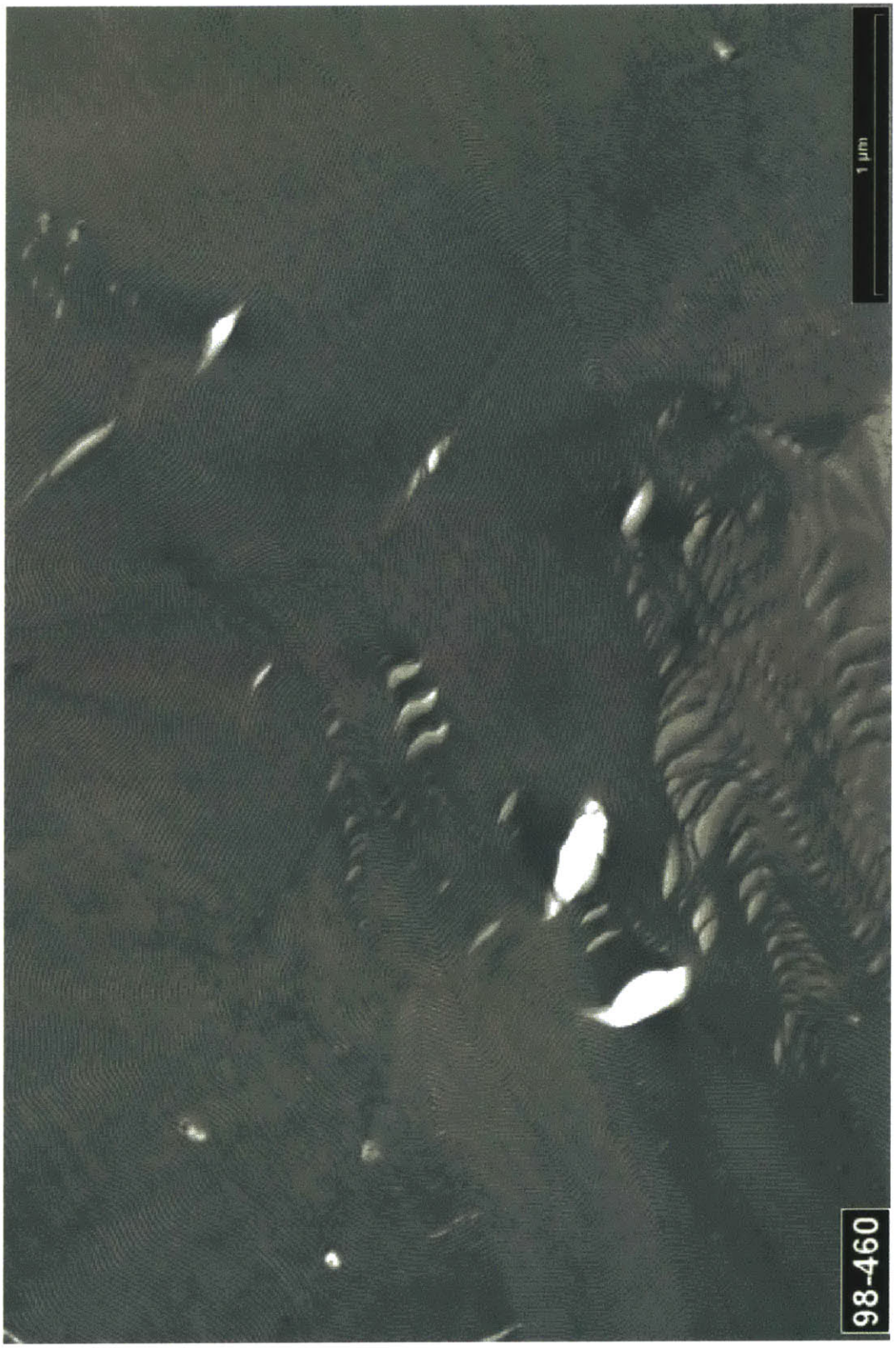

Figure 2-18: Transmission electron micrograph of the 9900/9700 styrene - 1,2 butadiene block copolymer (S12B10) cast from chloroform, annealed at 75°C for 5 minutes, ultramicrotomed and stained with OsO4. Micrograph courtesy of Dr. A. Karbach, Bayer A.G.

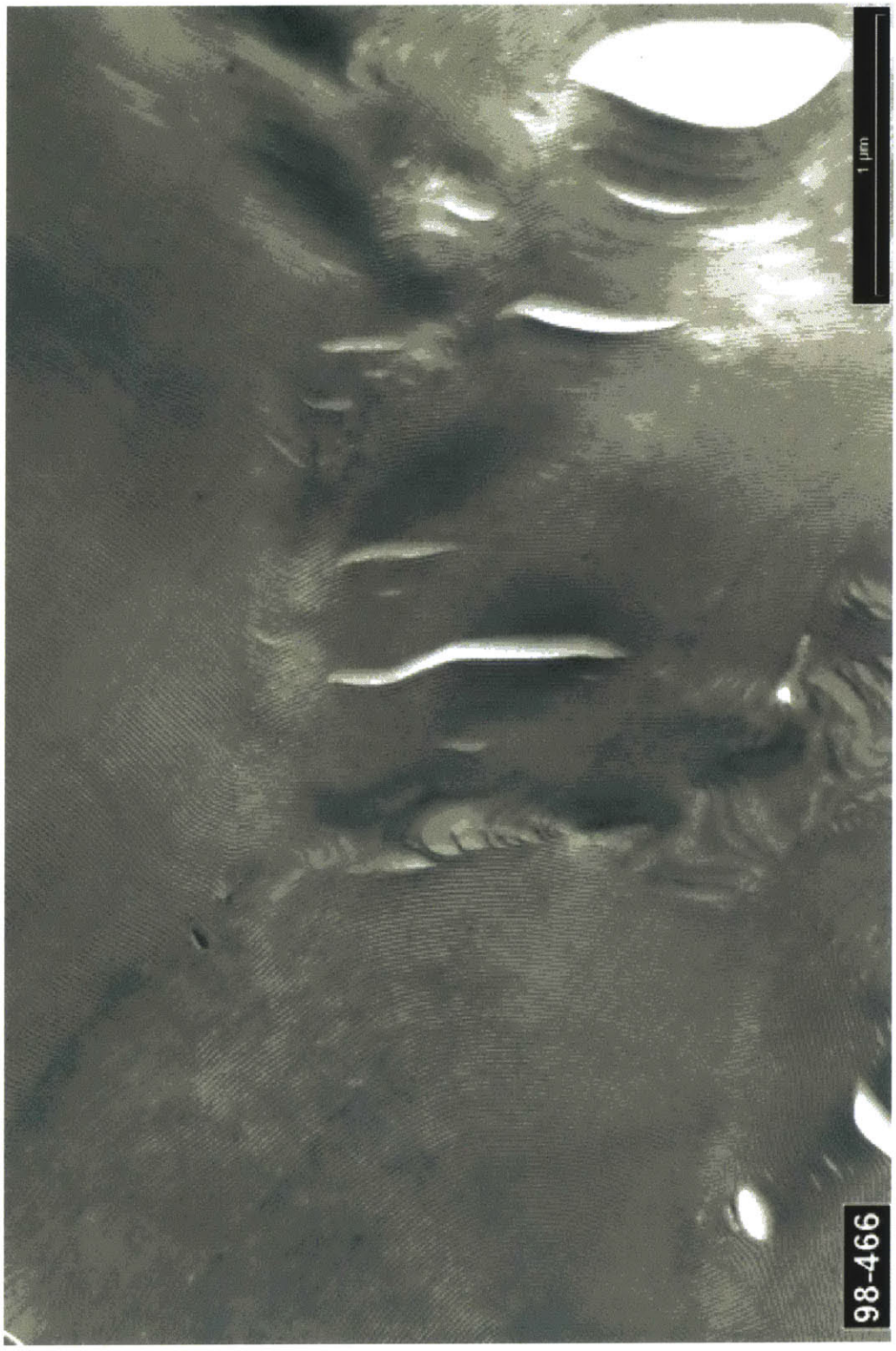

Figure 2-19: Transmission electron micrograph of the 9900/9700 styrene - 1,2 butadiene block copolymer (S12B10) cast from chloroform, annealed at 75°C for 1 hour, ultramicrotomed and stained with OsO4. Micrograph courtesy of Dr. A. Karbach, Bayer A.G.

Annealing Time at 75°C	D_U (μm)	D_{TEM} (μm)
none	0.51	0.45
5 minutes	0.78	0.55
1 hour	1.03	0.83

Table 2.7: Values of Grain Size found from Ultra SAXS, D_U and Grain Size from TEM micrographs, D_{TEM} as a Function of Annealing Time at 75°C for 9900/9700 Styrene 1,2 Butadiene (S12B10) cast from chloroform.

As can be seen, the grain sizes are closely correlated; the values obtained from the TEM data are between 71% and 82% of those obtained by Ultra SAXS. This analysis verifies visually that Ultra SAXS is a viable measurement tool for grain size in styrene - butadiene block copolymers.

2.8 Estimating Grain Size in the Absence of the low-q Peak

Figure 2-20 shows the scattering profiles for the 9400/9000 styrene – 1,4 butadiene block copolymer (SB9) cast from chloroform. The lamellar peak centers around a Bragg value of $d = \frac{2\pi}{q_{MAX}} = 290\,\text{Å}$. The grain peaks are readily seen in the Ultra SAXS region for four out of the five curves. The peak associated with grains shifts to the left with increasing annealing time and after annealing 4 hours, the low-q peak is no longer resolvable.

Sometimes a peak that is not clearly resolvable in the intensity versus q plots is found more easily from a Iq^2 vs. q plot. The data is Figure 2-20 is replotted as such and shown in Figure 2-21. No peak is still found for the scattering curve of the 4 hour annealed sample. Though grain size can still be found by using the spherical form factor for the first four curves, the lack of the peak makes this an impossibility for the last curve.

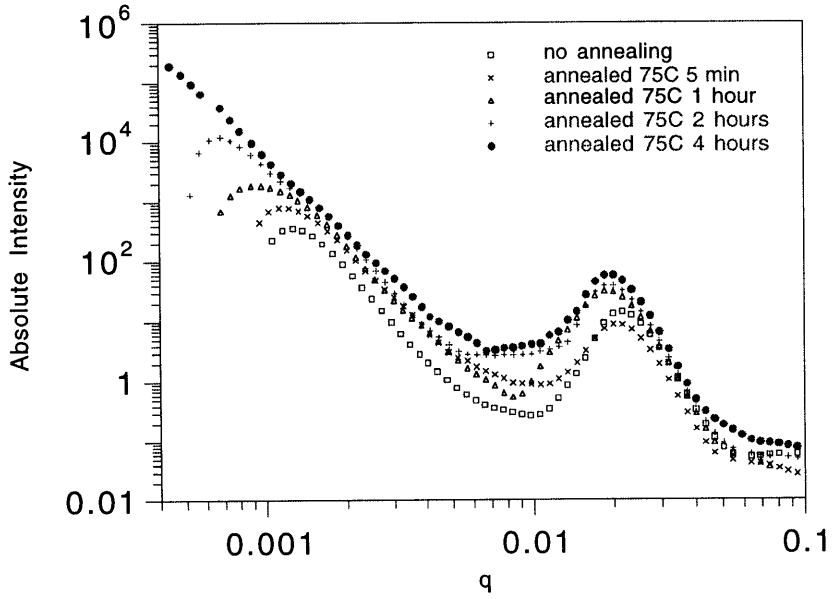

Figure 2-20: Logarithm of absolute intensity vs log q at various annealing times for the 9400/9000 styrene - 1,4 butadiene block copolymer (SB9) cast from chloroform.

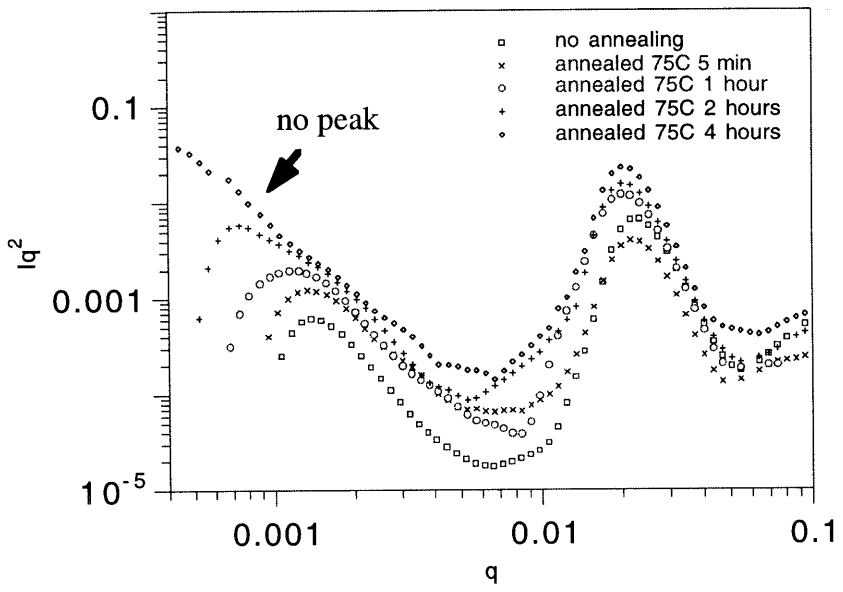

Figure 2-21: Log Iq^2 vs log q at various annealing times for the 9400/9000 styrene - 1,4 butadiene block copolymer (SB9) cast from chloroform.

The correlation length approach described in section 2.6 is a possible method for grain size determination, but the absolute number from this method would probably be different by a factor of 1.6 fo 1.7 because of the alternate weighting factor on the data as has been used for all of the other specimens. The trend of grain growth might thus not be witnesses for this final specimen.

It is possible, however, to estimate a grain size using Equation 2-6, which was a combination of Porod's Law and the invariant that eliminated all variables except the Porod Constant, C_1, the invariant, C_2, and the grain boundary volume fraction, ϕ. The data on the 4 hour annealed sample provide reliable values of C_1 and C_2 in the absence of the low-q peak. The required value of ϕ cannot be determined independently, but over the range of four polymers and numerous specimens examined and evaluated in this chapter, the grain boundary volume fraction, ϕ, remains essentially constant at a value of 0.1. Thus, assuming $\phi = 0.1$ and using the experimentally determined values of C_1 and C_2, equation 2-6 provides the desired value of D. Table 2.8 indicates that the grain size estimated in this way is consistent with the trends of the overall set of results on sample SB9, as well as all data presented to this point.

The grain size estimated for the last specimen is 2.09 Å, which is a feasible diameter, as this would correspond to a peak location at a value of q=0.000383. Since the limit of the machine is q=0.0004, it is reasonable that no peak is present. As with the scattering curves that display a peak, the contrast factor, $(\Delta\rho)^2$, is within the limit of 4×10^{-4} proposed by the mechanism. As with the other scattering data analyzed, the value

of the grain boundary volume fraction, ϕ, hovers around a value of 0.1, so making the assumption for the curve not displaying a clearly resolvable peak is deemed to be valid.

Annealing Time at 75 °C	*D (μm)*	*$(\Delta\rho)^2$*	*ϕ*	*D/d*
none	0.58	8.75E-7	0.098	20
5 minutes	0.66	2.20E-6	0.107	23
1 hour	0.70	2.63E-6	0.103	24
2 hours	1.08	7.40E-6	0.099	37
4 hours*	2.09	9.13E-6	0.1 assumed	72

* Peak falls outside range of Ultra SAXS machine. D is found with Equation 2-6, and ϕ=0.1

Table 2.8: Values of Grain Size, D; Phase Fraction, ϕ; Electron Density Differences, $(\Delta\rho)^2=(\rho_{GB}-\rho_m)^2$, and the number of lamellae per grain, D/d, as a Function of Annealing Time at 75°C for 9400/9000 Styrene 1,4 Butadiene (SB9)

2.9 Results from Swelling in a Non - Volatile Solvent

Figure 2-22 presents absolute intensity, i, versus scattering vector, q, results for the cumene swollen samples of the KR03 resin; the procedure for this was outlined in section 2.2.2.3. In this case there is a clear and systematic shift of the lamellar, d, peak to lower values of q as the amount of cumene increases from 0 to 61 volume percent. There is a corresponding decrease in the level of scattered x-ray intensity over the entire range of q owing to the reduction of the contrast factor which accompanies the addition of cumene solvent. The unswollen and lightly swollen specimens reveal a peak in the Ultra SAXS region while for the more highly swollen specimens, this peak appears to be shifted to the left, beyond the lower limit of q for the instrument. The q^{-4} dependence of the intensity is

preserved in the region of q to the right of the low-q peak for all of the specimens of Figure 2-22.

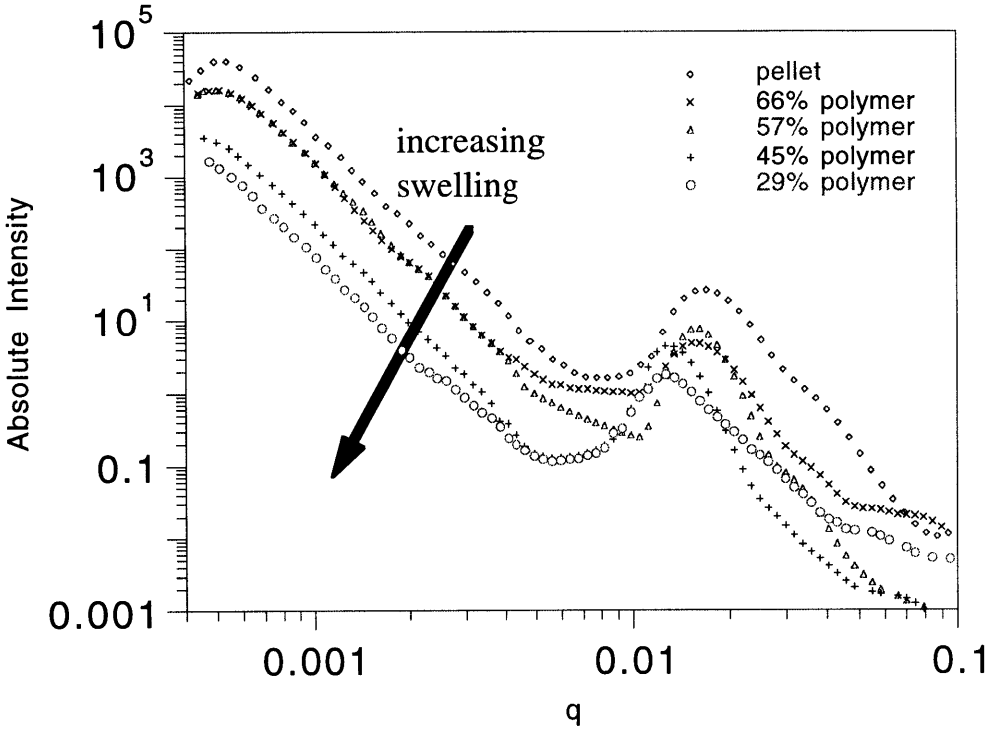

Figure 2-22: Logarithm of absolute intensity as a function of log q for KR03 resin diluted with various amounts of cumene.

Pellets of KR03 resin were swelled with various amounts of cumene, with processing conditions designed not to alter grain size. The first thing to be noted is that even at 29% polymer and 61% cumene, there is scattering in the Ultra SAXS region, nullifying the theory that scattering in the Ultra SAXS region is dominated by voids. The scattering profiles of the pellet and two of the swollen samples show low-q peaks and can be analyzed using the spherical form factor. The two samples with the most cumene do not show peaks and are analyzed under the assumption $\phi_{GB} = 0.1$. Results are presented in Table 2.9. First we note that the lamellar repeat distance, d, increases as the block

copolymer is swollen with increasing amounts of cumene. The grain size D also increases with cumene swelling, and since the ratio of D/d is nearly constant, it is apparent that both length scales are increasing in the same fashion. That both length scales, d and D, are proportional to the inverse cube root of polymer volume fraction is apparent from the essentially constant value of the product $D_0 = D\phi_p^{1/3}$, shown in the final column of Table 2.9.

% Polymer (ϕ_p)	*d(Å)*	*D(μm)*	ϕ_{GB}	$D_0=D\phi_p^{1/3}$	*D/d*
1.00	318	1.35	0.104	1.35	42
0.66	343	1.56	0.102	1.36	45
0.57	389	1.59	0.095	1.32	41
0.44	440	1.85	0.1*	1.41	42
0.29	479	2.07	0.1*	1.37	43

* No peak in detectable range. D is found from Equation 2-6, assuming ϕ=0.1

Table 2.9: Summary of Results of KR03 Resin Swelled with Various Amounts of Cumene.

For this section of analysis, the grain boundary volume fraction, ϕ, has been given a subscript and is referred to ϕ_{GB} for purposes of clarity as the volume fraction of polymer in cumene solution is called ϕ_p. As can be seen, at polymer samples swollen all the way to 61% with cumene, the original grain structure is preserved. Both the lamellar spacing and the grain size scales with the cube root of the volume fraction. The assumption that the grain boundary volume fraction, ϕ_{GB} , is equal to 0.1 for grain boundary estimation when no peak is present in the Ultra SAXS region is still valid for this polymer and these conditions.

2.10 Grain Boundary Volume Fraction

This section explores the grain boundary volume fraction, ϕ. It tries to answer the question, "What is so magical about 0.1, anyway?" A constant value of ϕ requires that the grain boundary thickness, Δr, increases proportionally with the grain diameter, D. For a value of ϕ=0.1 and assuming that the grain boundary is a shell around a spherical grain, the grain boundary thickness will always be 1.73% of the grain diameter. Though kinetics of grain growth has been explored, the morphology of grain growth has not been explained. For semi - crystalline spherulites, the grains often grow at the expense of amorphous regions. This cannot account for the observed range of grain growth witnessed in these polymers, as TEM evidence shows small grain boundary thicknesses. Some other phenomena must occur to account for this grain growth. The formation of grains is a combination of nucleation and defects,[1,17-20] and it is possible that grain growth is the result of "combing out" of some of the smaller defects, thus leaving only the thicker and richer boundaries, accounting for this perceived enrichment from the scattering data. This is just a postulation, however, and not reinforced with any data.

Table 2.10 shows values of the grain boundary volume fraction, ϕ, the grain boundary thickness, Δr, and the grain boundary thickness to grain diameter ratio, $\Delta r/D$, over the range of observed directly measurable grain sizes, if the grain boundary is the fixed quantity 0.1.

On the other hand, one might like to assume that the grain boundary thickness is constant. Choosing the value of 173 Å for the grain boundary thickness at 1 μm leads to the varying volume fraction shown in Table 2.11.

A third way to look at the grain boundary is to assume that there is a constant volume of grain boundary material. In other words, the grain boundary is a skin around the grain, and as the grain grows, the skin is stretched thinner. Table 2.12 shows results from this assumption, again choosing the value of 173 Å for the grain boundary thickness at 1 μm.

D (μm)	*φ*	*Δr (Å)*	*Δr/D*
0.5	0.1	86	0.0173
0.75	0.1	129	0.0173
1	0.1	173	0.0173
1.5	0.1	259	0.0173
2	0.1	345	0.0173

Table 2.10: Geometric grain variation assuming a constant grain boundary volume fraction of 0.1 over the range of grain diameters from 0.5 to 2.0 μm

D (μm)	*φ*	*Δr (Å)*	*Δr/D*
0.5	0.19	173	0.0345
0.75	0.13	173	0.023
1	0.1	173	0.0173
1.5	0.067	173	0.0115
2	0.051	173	0.0086

Table 2.11: Variation in the volume fraction of grain boundary material if a constant grain boundary thickness is assumed.

As can be seen from Table 2.12, assuming a constant volume of the grain boundary causes implausible results in the values of the grain boundary volume fraction and the thickness. However, the results from the constant grain boundary thickness are consistent over the range of grain boundaries measured. So, it is possible that this is in fact what is happening, and that this phenomena is well represented over the limited range of grain sizes that are able to be measured.

D (μm)	ϕ	Δr (Å)	$\Delta r/D$
0.5	0.80	10400	0.208
0.75	0.24	324	0.0432
1	0.1	173	0.0173
1.5	0.03	75	0.005
2	0.013	42	0.0021

Table 2.12: Variation in the volume fraction of grain boundary material if a constant grain boundary volume is assumed.

Thus, while a sensibly constant value of the grain boundary thickness, ϕ, fits the data, we recognize that more data covering a wider range of grain sizes to understand just how persistent this observation may be. So, in conclusion, there is nothing particularly magical about the value of ϕ=0.1 except that an inspection of all the scattering curves and data presented in this chapter, the values do indeed congregate around this number. With this observation in hand, we used this value to obtain a grain size estimation in the few cases where the peak was not discernible. We also make no attempt to explain why in the swollen samples the cumene partitions itself in such a way that ϕ remains around 0.1 for those peaks maintaining a discernible peak.

2.11 References

(1) Gido, S.P.; Gunther, J.; Thomas, E.L.; Hoffman, D. *Macromolecules* **1993**, *26*, 4506.

(2) Hashimoto, T.; Nagatoshi, K.; Todo, A.; Hasegawa, H.; Kawai, H. *Macromolecules* **1974**, *7*, 364.

(3) Hashimoto, T.; Shibayama, M.; Kawai, H. *Macromolecules* **1980**, *13*, 1237.

(4) Long, G.G.; Jemian, J.R.; Weertman, J.R.; Black, D.R.; Burdette, H.E.; Spal, R. *J. Appl. Cryst.* **1991**, *24*, 30.

(5) Pine, D.J.; Weitz, D.A.; Zhu, J.X.; Herbolkzheimer, E. *J Phys France* **1990**, *51*, 2101.

(6) Durian, D.J.; Weitz, D.A.; Pine, D.J.; *J Phys: Condens Matter* **1990**, *2*, SA433.

(7) Zhu, J.X.; Pine, D.J.; Weitz, D.A. *Phys Review A* **1991**, *44*, 3948.

(8) *http://www.polymersource.com/*

(9) Senn Jr., W.L. *Anal. Chim. Acta* **1963**, *29*, 505.

(10) Garetz, B.A.; Balsara, N.P.; Dai, H.J.; Wang, Z.; Newstein, M.C. *Macromolecules* **1996**, 29, 4675.

(11) Fodor, L.M.; Kitchen, A.G.; Baird, C.C. *ACS Organ. Coat. and Plast. Chem. Prepr.* **1974**, *34*, 130.

(12) Gebizlioglu, O.S.; Argon, A.S.; Cohen, R.E. *Polymer* **1985**, *26*, 519.

(13) Long, G.G.; Jemian, J.R.; Weertman, J.R.; Black, D.R.; Burdette, H.E.; Spal, R. *J. Appl. Cryst.* **1991**, *24*, 30.

(14) Lake, J.A. *Acta Cryst.* **1967**, *23*, 191.

(15) Garetz, B.A.; Balsara, N.P.; Dai, H.J.; Wang, Z.; Newstein, M.C. *Macromolecules* **1996**, 29, 4675.

(16) Nishikawa, Y.; Kawada, H.; Hasegawa, H.; Hashimoto, T. *Acta Polymer.* **1993**, *44*, 247.

(17) Gido, S.P.; Thomas, E.L. *Macromolecules* **1994**, *27*, 849.

(18) Gido, S.P.; Thomas, E.L. *Macromolecules* **1994**, *27*, 6137.

(19) Gido, S.P.; Thomas, E.L. *Macromolecules* **1997**, *30*, 3739.

(20) Mayes, A.M.; Kumar, S.K. "Tailored Polymer Surfaces", *MRS Bulletin* **1997**, *22*, 43.

(21) Stein, R.S.; Rhodes, M.B. *J Appl Physics* **1960**, *31*, 1873.

(22) Clark, R.J.; Miller R.L.; Stein, R.S. *J Polymer Sci* **1960**, *42*, 275.

(23) Murthy, N.S.; Akkapeddi, M.K.; Otis, W.J.; *Macromolecules* **1998**, *31*, 142.

(24) Murthy, N.S.; Zero, K.; *Polymer* **1997**, *38*, 1021.

(25) Butler, M.F.; Donald, A.M.; *Macromolecules* **1998**, *31*, 6234.

(26) Porod, G. in *Small Angle X-Ray Scattering*, O. Glatter and O. Kratky eds. Academic Press, London, 1982. 25.

(27) Underwood, E.E. *Quantative Stereology*, Addison Wesley, Reading MA: **1970**. 80-95.

3. Controlling Grain Size in Industrial Polymers

3.1 Introduction

Now that a robust technique for absolute grain size measurement has been developed for low molecular weight specialty diblock copolymers, this knowledge can be used to answer the first question of the thesis, which is can grain size be controlled in commercial block copolymers? It known and has been shown in the previous chapter that annealing at elevated temperatures does lead to grain growth, but this is not the desirable method for changing the grain size for samples where mechanical studies are going to be performed for two reasons. Firstly, annealing at temperatures high enough to cause any significant grain growth in the high molecular weight commercial block copolymers would have to be at or above 100°C, and at this temperature and annealing times, degradation would occur in the styrene - butadiene block copolymers. This probably would mask any effect that the change in grain size would have on the deformation behavior. Secondly, it is known that thermal history of a bulk-crystallized polymer strongly affects the yield strength; the annealing of HDPE increases the yield stress, but if strongly annealed under pressure, the polymer becomes more brittle.[1,2] It is not desirable to have block copolymers undergo processing conditions that are known to alter physical properties in other polymers that don't form grains, as any material property changes would be difficult to attribute to grain size.

Instead, we have chosen to static cast the industrial block copolymers from a variety of solvents. It is believed that the different vapor pressures and solubility parameters will cause the block copolymers to organize into different grain sizes through a mechanism of different nucleation and grain growth rates. For one polymer, the polymers were static cast at different temperatures, which raised the vapor pressure without changing the solubility parameters.

3.2 Experimental

3.2.1 Polymers Used

For this study, four lamellar, industrial styrene - butadiene block copolymers were used. Two of the commercial block copolymers contained more styrene than butadiene and were supplied by Phillips Petroleum Co. as part of their K-Resin series. They are sold under the names KR03 and KK31. Both the KR03 block copolymer[3-6] and KK31 block copolymer[7,8] have been studied previously. The other two commercial block copolymers contain more butadiene than styrene, and are sold by DEXCO, a joint venture between the Dow Chemical Company and the Exxon Corporation, as part of their Vector grade of block copolymers. These two polymers are called 4461 and DPX-555, and have also been studied previously.[9,10] Table 3.1 shows some of the important information about these polymers. Unlike the specialty polymers studied in chapter 2, none of the commercially available polymers are diblocks, they are triblocks, 3-armed or radial block copolymers, which are explained in chapter 1. The molecular weight reported is M_N, the number average molecular weight and the polydispersity is M_N/M_W. The weight % styrene was determined by proton NMR studies, which are displayed in Appendix B.

Polymer	*Type*	*MW*	*polydispersity*	*wt% styrene*
styrene - rich				
KR03	3-arm	217,000	2.1	79 %
KK31	triblock	187,000	1.5	75 %
butadiene-rich				
4461	triblock	82,000	1.2	45 %
DPX-555	radial	164,000	1.2	45 %

Table 3.1: Industrial polymers studied and selected physical property data.

These same NMR studies also reveal that the polybutadiene portions of all four polymers consist of about 90% 1,4 segments.

3.2.2 Static Casting

All of the polymers were dissolved in various solvents at concentrations in the range of 10 weight % and static cast. This concentration has been shown by SAXS studies to destroy any predisposed super morphology (i.e. grains and grain boundaries) and allow formation of different grain sizes. The procedure for static casting was similar to the procedure for the samples processed in chapter 2. For samples where elevated temperature was required, heating tape was affixed to the static casting apparatus, which was then attached to a temperature controller. The static cast films generally emerged with a thickness of 0.4 to 0.7 mm. When visible evaporation was complete, the films were placed under vacuum for several days until no weight change with time was observed and then heated to 100°C to remove any residual solvent.

3.2.3 Evaporation Solvents

Table 3.2 shows all of the solvents used for static casting to create different grain sizes for the commercial block copolymers studied. The chemical structures are shown for all of the solvents in Figure 3-1. The vapor pressure at 25°C, P_V, is shown in the table.[11] The higher the vapor pressure is, the quicker the solvent will evaporate. Also, a higher vapor pressure generally corresponds to a lower boiling temperature, T_B, which is also displayed in Table 3.2.[11] The solvent evaporation rate in the form of the vapor pressure is one of the parameters that will be explored when looking at grain size; the other will be the solubility parameter, which is shown in the last column of Table 3.2.[12] The solubility parameter is a number used to determine if two materials are miscible, or if one material can dissolve another. Using the principle that "like dissolves like," it can be reasoned that the closer the solubility parameters are to one another, the more likely the materials are to be

miscible. For a point of reference, the solubility parameter of water has been measured at 48 $MPa^{1/2}$,[12] a significantly different value than any of the solvents here, which is why most polymers are water insoluble.

Solvent	P_V *(kPa) @25°C*	T_B *(°C)*	δ *(MPa)*$^{1/2}$
methylene chloride	58	40	19.8
chloroform	26	61	19
tetrahydrofuran	22	65	18.6
ethyl acetate	12.6	77	18.6
methyl ethyl ketone	12.6	80	19.0
toluene	3.8	111	18.2
cumene	0.61	152	17.6*

* No solubility parameter found. δ is estimated from the similar molecules, cymene, toluene, styrene, and xylene and using the group molar attraction constants

Table 3.2 Solvents used and their vapor pressures, boiling points, and solubility parameters

The solubility parameter, δ, of polybutadiene is between 17.2 and 17.6 $MPa^{1/2}$ and for polystyrene is between 18.6 and 19.0 $MPa^{1/2}$.[12] With the given solubility parameters, it can be seen that all the solvents dissolve the SB block copolymers. Toluene has a solubility parameter of 18.2 $MPa^{1/2}$ and is generally regarded as a "neutral solvent," meaning that the solvent is just as likely to dissolve the butadiene block as it is to dissolve the styrene block. Most of the solvents in Table 3.2 had solubility parameters higher than this value, meaning that they preferentially dissolve the polystyrene block to varying degrees. It is believed that the solubility parameter may have some effect on how the polymer acts when in solution. Therefore the solubility parameter should have an effect of

how a polymer reacts to solvent evaporation and thus the grain size, though to what means is not conjectured.

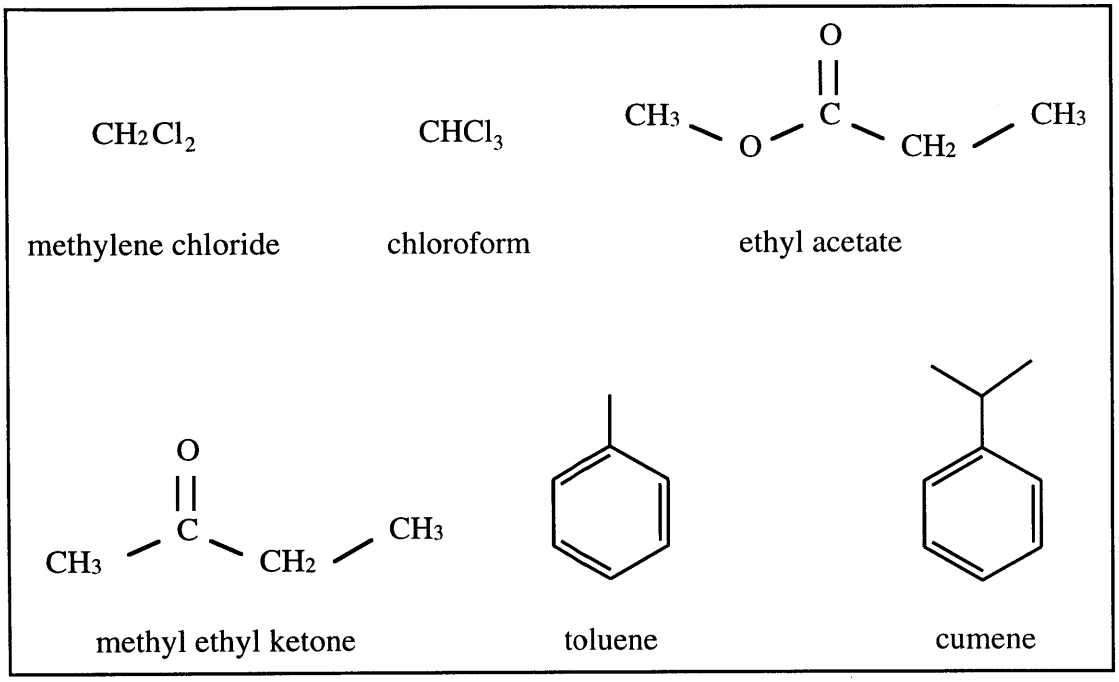

Figure 3-1 Chemical structures of the solvents used.

3.2.4 Ultra SAXS

Grain size was determined using Ultra Small Angle X-ray Scattering in a method described previously in the last chapter. As before, these experiments were performed on the X23A3 beamline operated by the National Institute of Standards and Technology at the National Synchrotron Light Source, a part of Brookhaven National Laboratory, Long Island, NY. The available range of scattering vector, $q = (4\pi/\lambda)\sin\theta$, was 0.1 $Å^{-1}$ to 0.0004 $Å^{-1}$, where θ is one half the scattering angle and $\lambda = 1.299$ Å is the x-ray wavelength.[13] The scattering data were desmeared to account for the geometry of the X23A3 beamline using software provided by Dr. Gabrielle Long of the National Institute of Standards and Technology and designed for this specific beamline. The program incorporated the methodology of Lake.[14]

3.3 Results

3.3.1 KR03

The specimens of KR03 processed for grain size measurement were cast from three solvents: cumene, methyl ethyl ketone, and ethyl acetate. The Ultra SAXS scattering patterns in the form of absolute intensity versus scattering vector, q, is shown for this polymer and these processing conditions in Figure 3-2. The legend shows both the solvent and the evaporation temperature for each scattering curve. As with the low molecular weight diblocks in the previous chapter, the lamellar spacing peak, d, is unaffected by the processing conditions and stays constant at a Bragg spacing value of $d = \frac{2\pi}{q_{MAX}} = 320\,\text{Å}$.

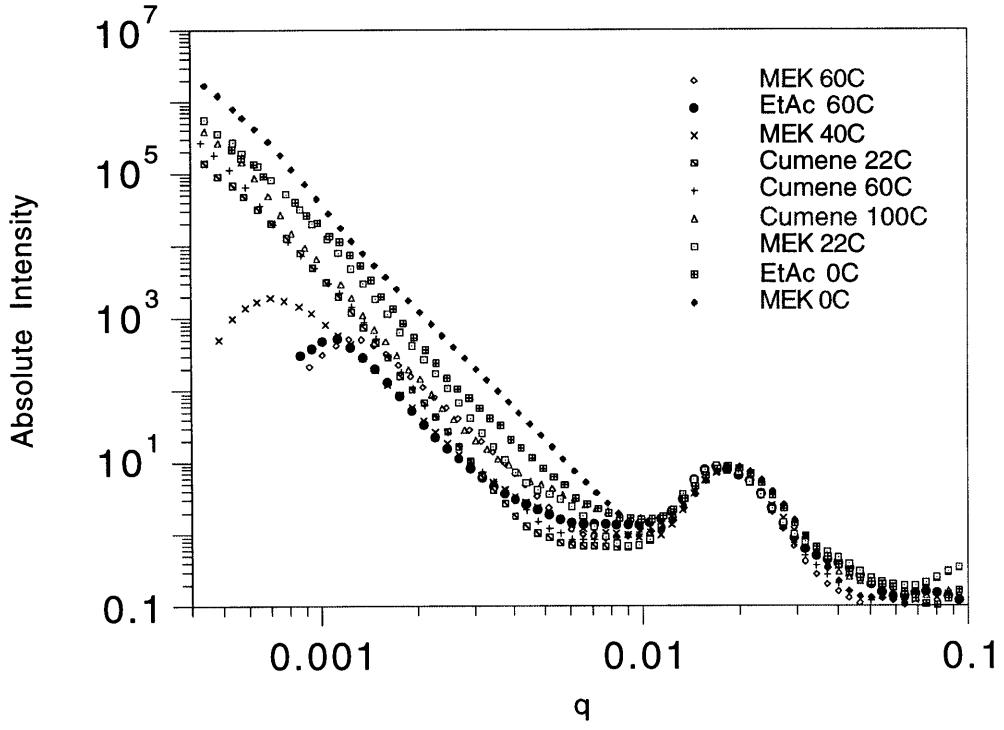

Figure 3-2: Logarithm of absolute intensity vs log q for the KR03 block copolymer cast from three solvents and at various temperatures .

Three of the curves display a clearly resolvable peak in the Ultra SAXS region, so the grain diameter, D, for those specimens can be directly calculated by the spherical form factor. For the other curves which do not have a clearly resolvable peak, Porod's Law and the invariant must be used in conjunction with the grain boundary volume fraction assumption, ϕ=0.1. The grain diameter as a function of both solvent and evaporation temperature is shown in Figure 3-3.

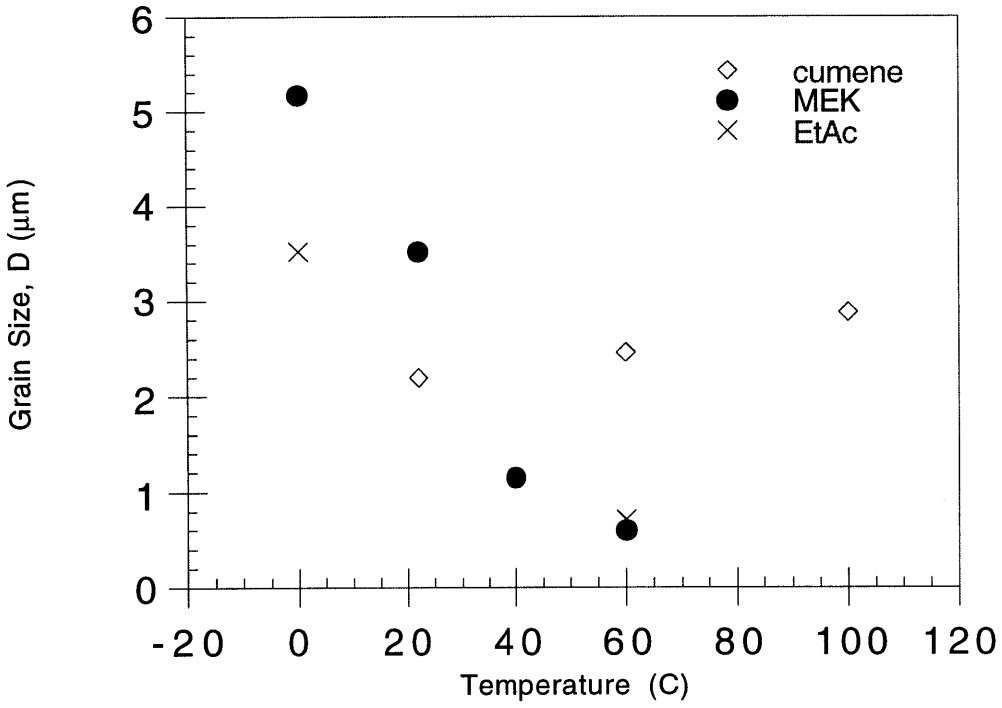

Figure 3-3: Grain size (μm) as a function of casting solvent and temperature for the KR03 block copolymer.

For both methyl ethyl ketone and ethyl acetate, an increase in the temperature equates to a smaller grain size. This is possibly because an elevated temperature means a higher vapor pressure, shorter evaporation times, and thus less time for large grains to form. However, for the cumene series, an elevation in temperature leads to a small increase in the grain size.

This may be that since cumene has such a low vapor pressure that the evaporation times are extremely long relative to the other solvents. Even though the temperature increase may lead to faster evaporation, the polymer may be undergoing a competing annealing-like phenomenon. The net result is a slight increase in the grain size with annealing temperature with this casing solvent.

Casting Solvent and Temperature	*D (μm)*	ϕ	$(\Delta\rho)^2$
methyl ethyl ketone 60°C	0.6	0.103	$3.31 \cdot 10^{-7}$
ethyl acetate 60°C	0.71	0.106	$1.03 \cdot 10^{-6}$
methyl ethyl ketone 40°C	0.93	0.094	$1.86 \cdot 10^{-6}$
cumene 23°C	2.2	0.1*	$2.37 \cdot 10^{-6}$
cumene 60°C	2.46	0.1*	$6.57 \cdot 10^{-6}$
cumene 100°C	2.88	0.1*	$1.04 \cdot 10^{-5}$
methyl ethyl ketone 23°C	3.52	0.1*	$1.88 \cdot 10^{-5}$
ethyl acetate 0°C	3.56	0.1*	$3.19 \cdot 10^{-5}$
methyl ethyl ketone 0°C	5.17	0.1*	$7.94 \cdot 10^{-5}$

* no peak in the Ultra SAXS region. D is found assuming ϕ=0.1.

Table 3.3: Values of grain size, D; grain boundary volume fraction, ϕ; and electron density differences, $(\Delta\rho)^2$, as a function of casting solvent and temperature for KR03.

It should be noted that the grain size can be altered by almost an order of magnitude by changing these process parameters, which should allow any grain size affects to be

witnessed when making deformation measurements. It should also be noted that in two cases, different processing conditions led to essentially the same grain size: MEK at room temperature and ethyl acetate at 0°C hovered around 3.5 μm, and MEK and ethyl acetate at 60°C produced roughly similar grain sizes. This is important, as it allows us to test to see if similar grain sizes produced by similar methods have similar mechanical properties; this will be addressed in the next chapter.

3.3.2 KK31

Figure 3-4 shows the Ultra SAXS scattering curves for the KK31 block copolymer. KK31 was evaporated from all of the solvents in Table 3.2 except cumene in an attempt to produce several different grain sizes; all specimens were evaporated at room temperature. The Bragg peak associated with the lamellar spacing is constant for all of the processing conditions, $d = \frac{2\pi}{q_{MAX}} = 350\,\text{Å}$.

Four of the six scattering curves have a clearly resolvable peak in the Ultra SAXS region, q less than 0.01 $Å^{-1}$. From the value of the scattering vector at the peak location, q_{MAX}, the grain size, D, can be directly measured by using the spherical form factor, as has been done with both the low molecular weight block copolymers shown in chapter 2 and the KR03 resin shown in both chapter 2 and the previous section. For the two that do not have a clearly resolvable peak, Porod's Law and the invariant coupled with the grain boundary volume fraction assumption, ϕ=0.1, provide a means to obtain a suitable estimate of grain size. The grain diameter, D, and the rest of the important scattering results for the KK31 block copolymer cast from the various solvents are summarized in Table 3.5.

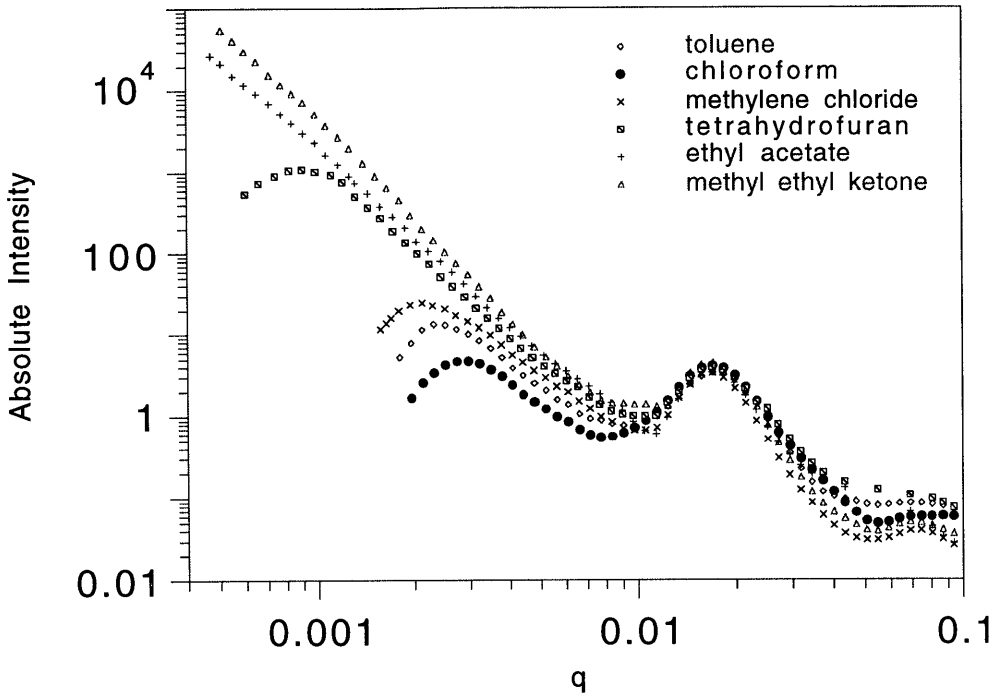

Figure 3-4: Logarithm of absolute intensity vs log q for the KK31 block copolymer cast from various solvents.

As was the case with the KR03 resin, it should be noted that grain size can be altered by about a factor of ten, from about 0.3 μm to over 3 μm. The grain boundary volume fraction also centered around ϕ=0.1 from the Ultra SAXS scattering curves of this polymer with these casting solvents; this was the case with the low molecular weight diblocks studied in chapter 2 validating the proposed mechanism and the KR03 resin studied in the previous section. The electron density difference, $(\Delta\rho)^2$, is also consistent with the previously obtained results and the validated mechanism stating that the contrast is due to the grains scattering against the mean density of the grains.

Casting Solvent	*D (μm)*	ϕ	$(\Delta\rho)^2$
chloroform	0.27	0.098	$2.43 \cdot 10^{-7}$
toluene	0.35	0.101	$5.95 \cdot 10^{-7}$
methylene chloride	0.38	0.101	$7.97 \cdot 10^{-7}$
tetrahydrofuran	0.89	0.099	$2.47 \cdot 10^{-6}$
ethyl acetate	2.33	0.1*	$1.02 \cdot 10^{-5}$
methyl ethyl ketone	3.31	0.1*	$2.29 \cdot 10^{-5}$

* no peak in the Ultra SAXS region. D is found assuming ϕ=0.1.

Table 3.4: Values of grain size, D; grain boundary volume fraction, ϕ; and electron density differences, $(\Delta\rho)^2$, as a function of casting solvent for KK31.

3.3.3 4461

Figure 3-5 shows the Ultra SAXS scattering curve of absolute intensity versus scattering vector, q, for the 4461 block copolymer as a function of the casting solvent. The legend contains an abbreviation of the solvent name: ***chl*** corresponds to chloroform, ***tol*** corresponds to toluene, ***mcl*** is methylene chloride, ***thf*** is tetrahydrofuran, ***eac*** is ethyl acetate, and ***cum*** is cumene. Though the polymer was soluble in methyl ethyl ketone, it was unable to be cast into a film, the end result of several static cast attempts was spider web-like agglomerations.

The lamellar spacing does not vary based on the solvent choice and remains constant at a value of $d = \frac{2\pi}{q_{MAX}} = 280\,\text{Å}$. The difference between this set of scattering curves and all of the other displayed previously in both this chapter and the previous one is

that none of the curves display a peak in the Ultra SAXS region. In fact, it seems that the curves are far from displaying a peak in the range of q less than 0.01 $Å^{-1}$, in other words D is a good deal larger than 2 μm. However, there is a difference in the location of the tails of these peaks, so it is possible to use Porod's Law, the invariant, and the grain boundary volume assumption, ϕ=0.1, to obtain an estimate of the grain size, which is displayed in Table 3.5 along with the electron density differences.

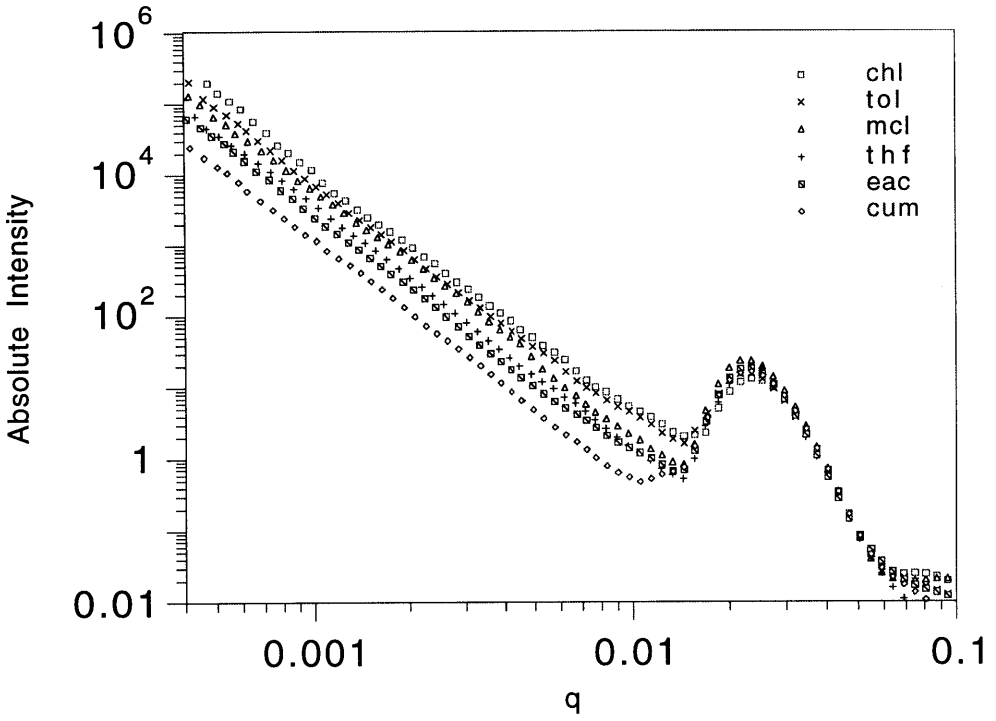

Figure 3-5: Logarithm of absolute intensity vs log q for the 4461 triblock copolymer cast from various solvents.

The grain sizes are, in fact, quite a bit larger than 2 μm. The values of the contrast factors, $(\Delta\rho)^2$, are also on the same order of magnitude as the values obtained for the other

polymers in both this chapter and chapter 2, and are consistent with the mechanism of scattering.

Casting Solvent	*D (μm)*	$(\Delta\rho)^2$
chloroform	3.72	9.65E-6
toluene	4.13	6.59E-6
methylene chloride	4.54	5.24E-6
tetrahydrofuran	4.88	3.04E-6
ethyl acetate	4.95	2.45E-6
cumene	5.80	1.30E-6

Table 3.5: Values of grain size, D, and electron density differences, $(\Delta\rho)^2$, as a function of casting solvent for 4461 with the constant grain boundary volume fraction assumption, ϕ=0.1.

3.3.4 DPX-555

Figure 3-6 shows the Ultra SAXS scattering curve of absolute intensity versus scattering vector, q, for the DPX-555 radial block copolymer as a function of the casting solvent. The legend contains an abbreviation of the solvent name, which are the same abbreviations that were used in the graph for the 4461 polymer and described in the previous section.

The lamellar spacing does not vary based on the solvent choice and remains constant at a value of $d = \frac{2\pi}{q_{MAX}} = 280\,\text{Å}$, which happens to be exactly the same distance as the lamellar spacing for the 4461 polymer. This is not surprising, as the DPX-555 polymer is essentially two 4461 triblock polymers bonded together at the middle of the butadiene blocks.

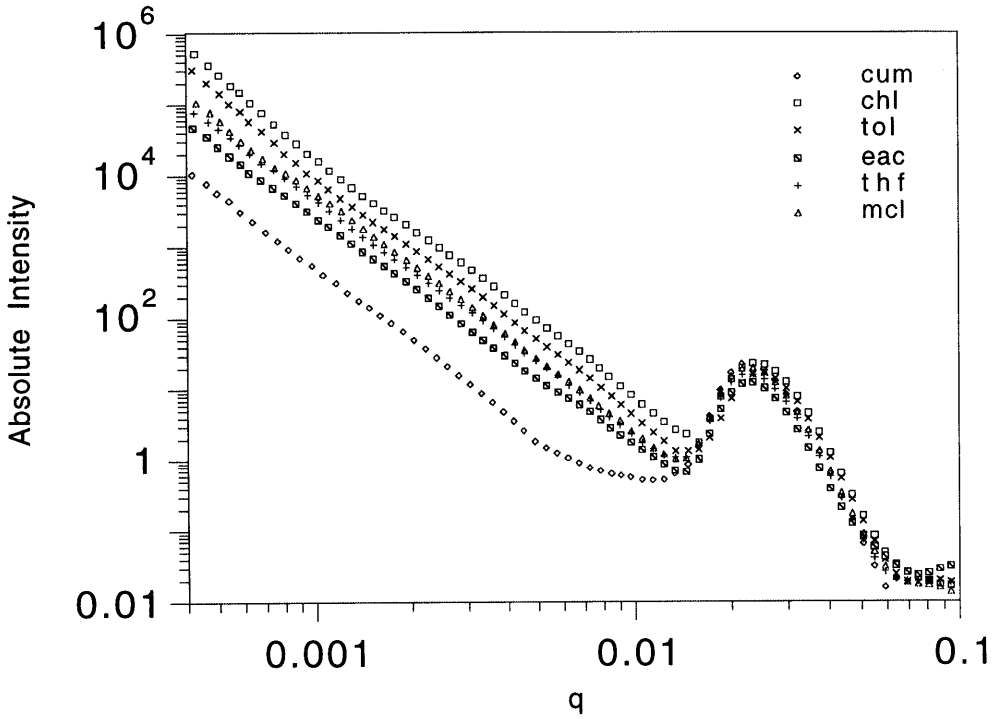

Figure 3-6: Logarithm of absolute intensity vs log q for the DPX-555 radial block copolymer cast from various solvents.

As with the 4461 polymer, none of the scattering curves show a grain peak in the range of q less than 0.01 $Å^{-1}$, meaning that all of the grains formed from these solvents are larger than 2 μm. We also can note from the scattering curves that the span of grain sizes for the DPX-555 polymer is greater as the tails of the grain peaks cover a wider range of intensity values; the same tails on the 4461 scattering curves tend to be more clustered. As with the 4461 polymer, we can estimate the grain sizes from these scattering curves using Porod's Law, the invariant, and the constant grain boundary volume fraction assumption, ϕ=0.1. These results are summarized in Table 3.6.

Casting Solvent	*D (μm)*	$(\Delta\rho)^2$
chloroform	3.59	1.64E-5
toluene	4.16	9.36E-6
methylene chloride	4.65	5.02E-6
tetrahydrofuran	5.04	3.96E-6
ethyl acetate	5.41	2.18E-6
cumene	6.44	5.97E-7

Table 3.6: Values of grain size, D, and electron density differences, $(\Delta\rho)^2$, as a function of casting solvent for DPX-555 with the constant grain boundary volume fraction assumption, ϕ=0.1.

It can be seen that the range of grain sizes obtained for this polymer is in fact greater than for the 4461 polymer; the DPX-555 grains vary by almost 3 μm in diameter compared to just over 2 μm for the 4461 polymer. As was the case for the 4461 polymer, the values of the contrast factors, $(\Delta\rho)^2$, are consistent with the values obtained for the other polymers earlier in this chapter and also in chapter 2, and are in concord with the mechanism of scattering.

3.4 Discussion

Grain size for commercially available block copolymers that have a molecular weight an order of magnitude more than the specialty block copolymers also organize into grains that can either be directly measured or estimated using Ultra SAXS. Grain size can be altered in these polymers without having to subject the polymers to annealing. The styrene rich polymers tended to form smaller grains than the butadiene rich polymers in the absence of extraordinary temperature conditions: the styrene rich polymers organized into

grains spanning sizes from 0.3 to 3.5 μm, compared to 3.5 to 6.5 μm for the butadiene block copolymers cast from the same solvents and having undergone the same processing. We did not foresee this difference, especially since the styrene rich polymers are both higher in molecular weight and microphase separate into a lamellar morphology with a longer length scale. One possible reason for the smaller grains in the styrene rich block copolymers may be that because these polymers contain more of the high glass temperature transition material, they are less mobile in solution and become "locked" in a grain size earlier in the solvent evaporation process; thus, the smaller grain sizes across the board.

Another important note is that by varying the temperature in the KR03 polymer as well as the solvent, we were able to twice produce similar grain sizes by different processing conditions. This will allow a consistency check to see if grains of the similar size produced by different means have correspondingly similar material properties, namely deformation behavior examined in the next chapter.

3.4.1 Effect of Evaporation Temperature on Grain Size

The only polymer for which evaporation temperature was explored was KR03. KR03 was evaporated from three solvents: methyl ethyl ketone, ethyl acetate, and cumene. Static cast temperatures ranged from 0°C to almost the boiling points of the solvent. For the two solvents with reasonably high vapor pressures at 25°C: methyl ethyl ketone and ethyl acetate, an increasing the casting temperature equates to the KR03 organizing into smaller grain. This is possibly because an elevated temperature means a higher vapor pressure, shorter evaporation times, and thus less time for large grains to form. In contrast, the casting from cumene, a solvent of extremely low volatility, an elevation in temperature does not lead to a decrease in the average grain diameter. The higher evaporation temperature actually leads to a very small increase in the grain size. This may be because cumene has such a low vapor pressure (0.61 kPa at room temperature), the evaporation times are extremely long relative to the other solvents. Even though the

temperature increase may lead to faster evaporation, the polymer may be undergoing a competing annealing-like phenomenon. The net result is a slight increase in the grain size with evaporation temperature with this casing solvent.

3.4.2 Effect of Casting Solvent on Grain Size

Casting solvent was the only variable in grain size formation for three of the commercial block copolymers studied in this thesis: the styrene rich KK31 and the two butadiene rich polymers, with the trade names 4461 and DPX-555. Though the butadiene rich polymers tended to form grains approximately 3 μm larger than the styrene rich KK31, the relative sizes formed from each of the casting solvents was exactly the same. From smallest to largest, the order of the solvents was chloroform, toluene, methylene chloride, tetrahydrofuran, ethyl acetate, methyl ethyl ketone (KK31) and cumene (4461 and DPX-555). Figure 3-7 shows a graph of grain size as a function of vapor pressure at 25°C for all three polymers. While it certainly seems that a higher vapor pressure, and thus a shorter evaporation time, seems to cause smaller grains to be formed, there also seems to be an effect of solvent type, and Figure 3-8 shows a graph of grain size as a function of solubility parameter for all three polymers.

It does seem that there is a trend for the evaporation rate, in the form of vapor pressure, and grain size, as predicted. However, casting from a neutral solvent such as toluene creates small grain sizes as well. What can be concluded is that for a given solubility parameter, a higher vapor pressure at 25°C, will cause smaller grains to be formed. For a given vapor pressure, a more neutral solvent will cause smaller grains to be formed. Finally, a given solvent affects grain formation in the same way relative to the other solvents for all polymers studied.

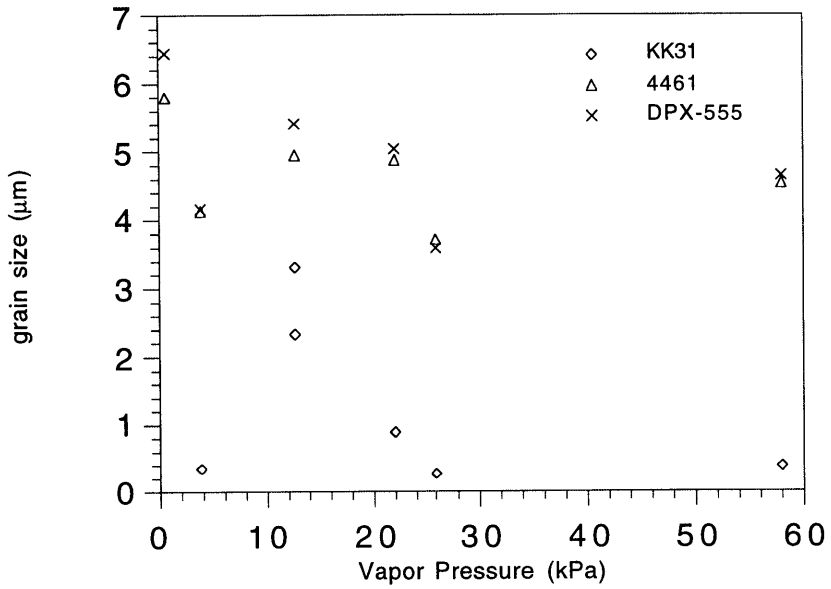

Figure 3-7: Grain size as a function of vapor pressure at 25°C for the KK31, 4461 and DPX-555 polymers.

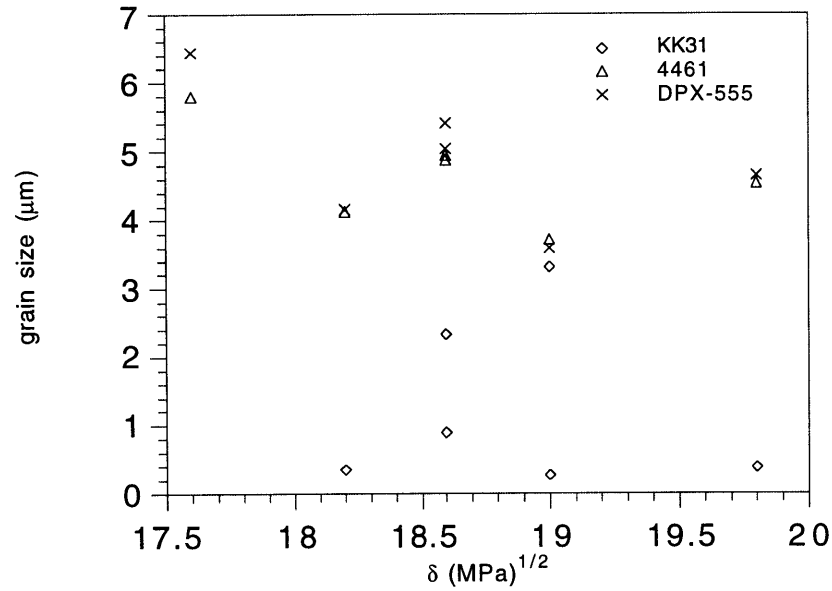

Figure 3-8: Grain size as a function of solubility parameters for the KK31, 4461 and DPX-555 polymers.

3.5 References

(1) Bowden, P.B.; Young, R.J. *J. Mater. Sci.* **1974**, *9*, 2034.

(2) Bassett, D.C.; Carder, D.R. *Phil. Mag.* **1973**, *28*, 535.

(3) Fodor, L.M.; Kitchen, A.G.; Baird, C.C. *ACS Organ. Coat. and Plast. Chem. Prepr.* **1974**, *34*, 130.

(4) Gebizlioglu, O.S.; Argon, A.S.; Cohen, R.E. *Polymer* **1985**, *26*, 519.

(5) Gebizlioglu, O.S.; Argon, A.S.; Cohen, R.E. *Polymer* **1985**, *26*, 529.

(6) Argon, A.S.; Cohen, R.E.; Jang, B.Z.; Vandersande, J.B. *J. Poly. Sci.: Poly. Phys.* **1981**, *19*, 253.

(7) Csernica, J.; Baddour, R.F.; Cohen, R.E. *Macromolecules* **1987**, *20*, 2468.

(8) Csernica, J.; Baddour, R.F.; Cohen, R.E. *Macromolecules* **1989**, *22*, 1493.

(9) Albalak, R.J.; Thomas, E.L. *Journal of Polymer Science Part B: Polymer Physics* **1994**, *32*, 341.

(10) Albalak, R.J.; Thomas, E.L.; Capel, M.S. *Polymer* **1997**, *38*, 3819.

(11) *CRC Handbook of Chemistry & Physics* 76th edition. Lide, D.R., ed. CRC Press, Boca Raton, FL, 1995.

(12) *Polymer Handbook* Third Edition. Brandup, J.; Immergut, E.H., eds. John Wiley & Sons, New York, 1989.

(13) Long, G.G.; Jemian, J.R.; Weertman, J.R.; Black, D.R.; Burdette, H.E.; Spal, R. *J. Appl. Cryst.* **1991**, *24*, 30.

(14) Lake, J.A. *Acta Cryst.* **1967**, *23*, 191.

4. Effect of Grain Structure on the Mechanical Properties

4.1 Introduction

In this chapter we have made use of our Ultra SAXS characterization methodologies developed in Chapter 2 and the grain measurements of the commercial block copolymers displayed in Chapter 3 to examine the influence of grain structure on the tensile stress - strain behavior of polystyrene/polybutadiene block copolymers. We note that many experimental studies of mechanical behavior have been carried out in the past on grainy block copolymers.[1-5] The most comprehensive studies by Kawai and coworkers on SB block copolymers with lamellar[1] and cylindrical[5] morphologies, combine the information from SAXS patterns and deformation/recovery experiments to suggest mechanisms of deformation in various regions of the stress and strain cycles. None of the prior studies, however, explicitly addresses the influence of grain size or grain boundary structure on the observed mechanical response. Because grain size of block copolymers known to change with solvent processing conditions as shown in Chapters 2 and 3, and grain boundary structure also appears to depend on these processing parameters, it is important to elucidate the degree to which processing-induced changes in grain structure alter the mechanical properties of these materials.

In this thesis, we have concentrated on tensile deformation behavior as the key mechanical property examined, some of the measurable quantities from these stress strain curves compared. Figure 4-1 shows a typical stress strain curve for a styrene butadiene block copolymer, with all of the key features labeled. The initial sharp increase in the stress strain curve is due to all of the applied load deforming the stronger polystyrene, and the slope of this part of the stress strain curve is called the modulus. At the end of the initial sharp increase in the slope is a small relaxation and the stress at the peak of this curve is called the yield strength. This corresponds to the point where the polystyrene is permanently deformed; even if no more load is applied, the material can't contract back to its original shape. After yield, the polystyrene breaks up and the material deforms like a

particle toughened rubber, until it breaks at the tensile strength and break strain. In this thesis, we are going to primarily look at the yield strength and the modulus of the grainy block copolymers. We believe this is where any grain boundary effects are going to principally manifest. Also, the breaking point is not a very reproducible result, so this should not be explored initially, but possibly in a secondary study.

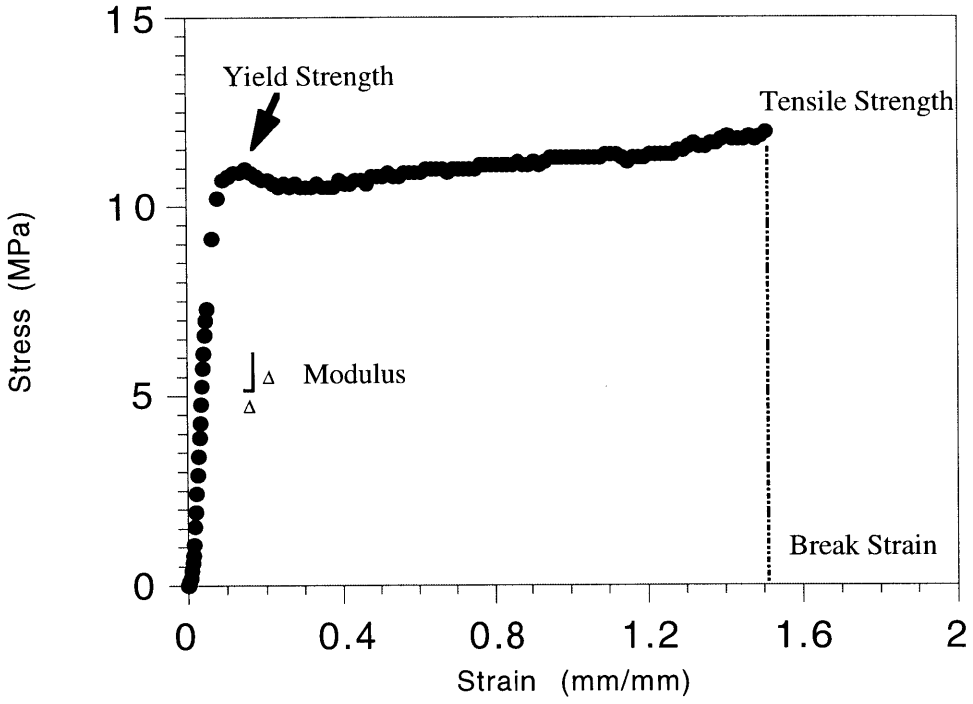

Figure 4-1: Typical stress strain curve for a styrene-butadiene block copolymer with all of the key features labeled.

4.2 Experimental

4.2.1 Polymers Chosen and Processing Conditions

The polymers chosen are the same four that were described in greater detail in Chapter 3. Two of the polymers are styrene rich, meaning that though they still microphase separate into a lamellar morphology, they contain greater than 50% by weight

polystyrene. They are sold by Phillips Petroleum Co. under the names KK31 and KR03. The other two polymers are butadiene rich and sold by DEXCO under the names DPX-555 and 4461. The static casting procedure and processing conditions are the same as those described in Chapter 3, and thus the grain sizes generated are the same as those reported in the last chapter.

In addition to the static cast samples, KK31 was provided in the form of highly oriented extruded sheets of 0.5 mm thickness, providing us with a grain-free material for upper and lower bound measurements in the mechanical tests. KK31 was deformed as a function of angle in these extruded samples as shown in Figure 4-2.

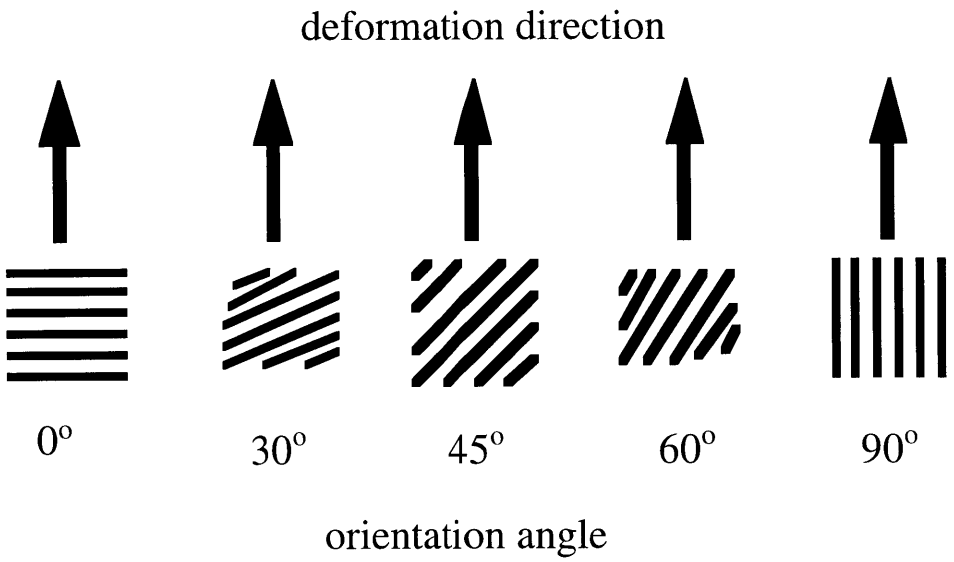

Figure 4-2: Diagram of the relationship between orientation angle and deformation direction in the extruded, grain-free KK31 polymer.

The orientation labeled as 90° represents deformation "in parallel" (mechanical upper bound) i.e. along the extrusion direction. Along the same line of thought, the 0° orientation represents perpendicular loading where the polystyrene and polybutadiene lamellar are coupled "in series" (mechanical lower bound).

In addition to these samples, a set of S12B10 low molecular weight diblock copolymer samples processed as described in Chapter 2 was tested to see the effect of grain size on material properties when annealing is the means used to influence grain growth.

4.2.2 Instron Testing

Tensile tests were performed on an Instron Model 4201. The gauge length of each specimen was 7 mm with a width of 2 mm. Prior to testing, all specimens were conditioned in the standard laboratory atmosphere of 23°C and 55-60% relative humidity for several days. The tensile tests were performed at a strain rate of 0.14 min^{-1} for the styrene rich polymers, KK31 and KR03, as well as the low molecular weight S12B10 polymer. The strain rate for the butadiene rich polymers, 4461 and DPX-555, was 0.56 min^{-1}. Yield points were determined from the peak in the stress strain curve (where applicable) or by conventional extrapolation of initial and post-yield linear regions to a point of intersection. Yield stress and modulus values reported in this chapter represent averages over repeated runs; typically 10 stress-strain curves were obtained for each prepared sample. For the S12B10 polymer, the values reported represent an average of 5 prepared samples.

The stress and strain values reported in this chapter are engineering stress and strain. Engineering stress is defined as $\sigma = \frac{L}{A_0}$ and is given in the units of MPa, where L is the applied load required to maintain the strain rate and A_0 is the initial cross sectional area. The engineering strain is reported in units of mm/mm and defined as $\varepsilon = \frac{\Delta l}{l_0}$, where Δl is the change in length of the sample and l_0 is the initial sample length.

4.3 Results

4.3.1 KK31

The stress strain curves will be reported first for the extruded, grain free sample. This will enable us to see whether any witnessed effect of grain size on material properties in the static cast, grainy samples are significant.

4.3.1.1 Extruded

Figure 4-3 shows sample stress-strain curves for the extruded, oriented, grain-free KK31 polymer as a function of an orientation angle which is defined as the angle between the tensile loading and the lamellar normals of the oriented copolymer morphology.

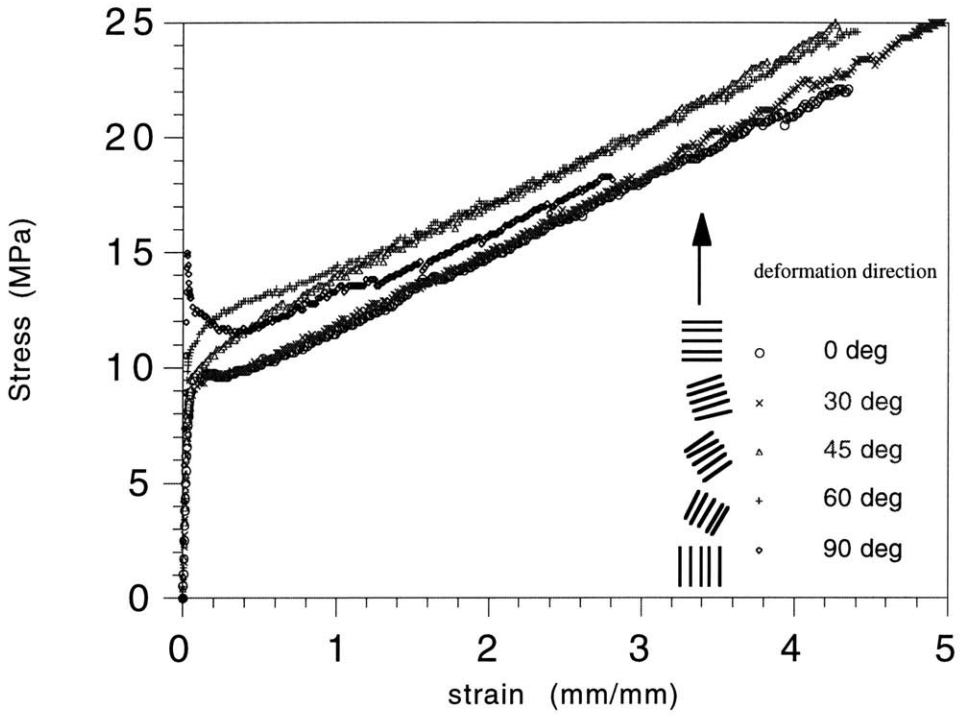

Figure 4-3: Stress (MPa) vs strain (mm/mm) curves for the extruded, grain-free KK31 polymer as a function of orientation angle.

The yield strength is highest at the parallel loading at 90° and lowest at the series loading 0°, however not much can be said about the modulus. Figure 4-4 shows the stress

at low values of the strain for the extruded, grain free KK31 as a function of orientation angle.

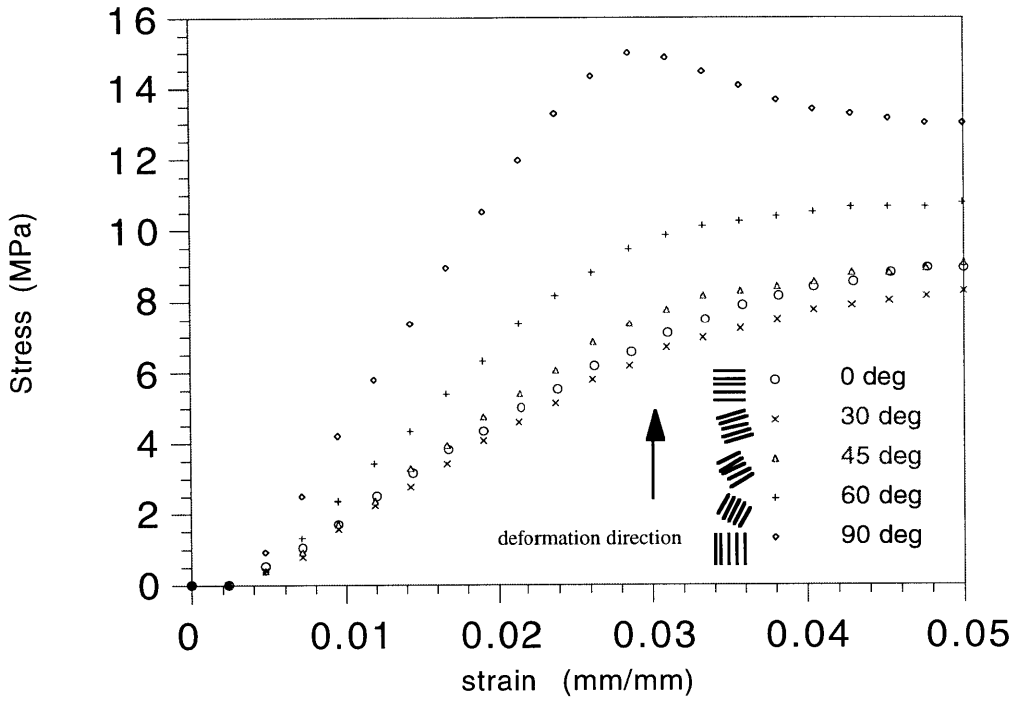

Figure 4-4: Stress (MPa) at low values of strain for the extruded, grain free KK31 as a function of orientation angle.

The modulus also increases with increasing orientation angle as does the yield strength. Figure 4-5 shows a summary of the yield strength as a function of orientation angle for the extruded, grain-free KK31. The same summary of modulus as a function of orientation angle for the extruded, grain-free KK31 are shown in Figure 4-6. The error bars are shown in the two figures, which are the standard deviation of these measured values. As expected, modulus and yield strength are lowest when deforming the lamellae in series (0°) and are highest when deforming parallel to the lamellae (90°).

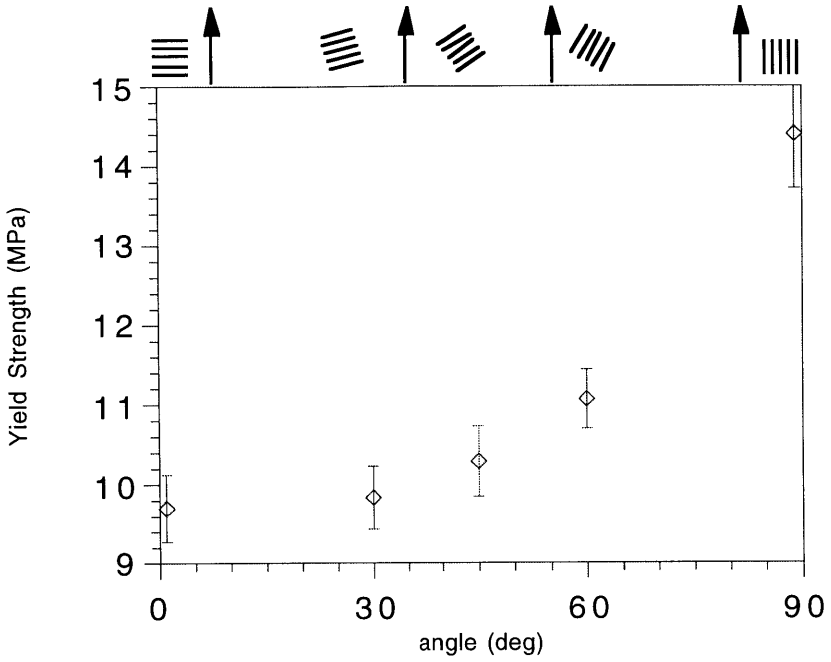

Figure 4-5: Summary of results for the yield strength vs deformation angle for the extruded, grain-free KK31 block copolymer.

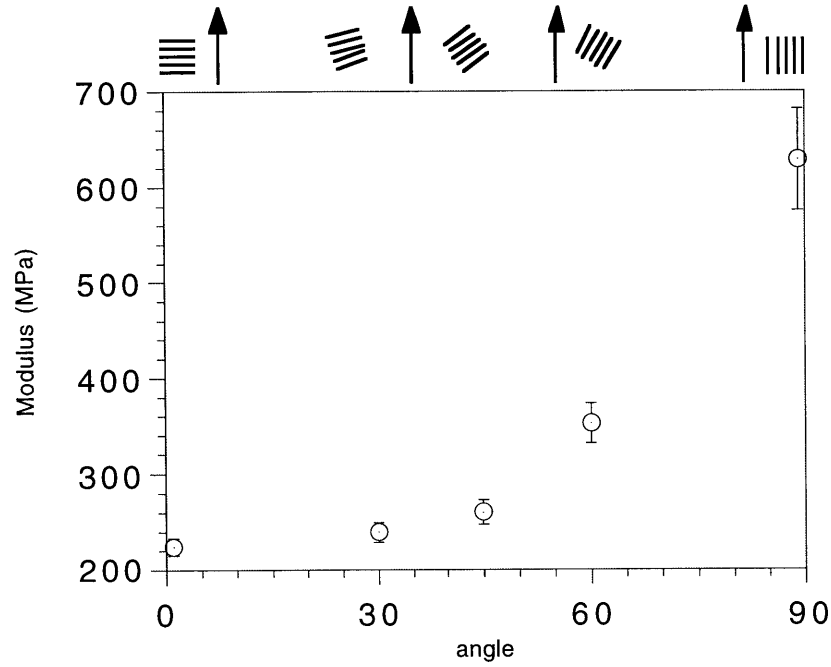

Figure 4-6: Summary of results for the modulus vs deformation angle for the extruded, grain-free KK31 block copolymer.

The yield strength ranges from about 9.5 to 14.5 MPa as a function of the orientation angle and the modulus from about 220 to 640 MPa.

4.3.1.2 Static Cast

Figure 4-7 shows sample stress-strain curves for KK31 dissolved in various solvents and cast at 22°C to generate each grain size found in Chapter 3. The legend shows both the casting solvent and the grain size measured. A change in the yield strength in these curves can definitely be witnessed.

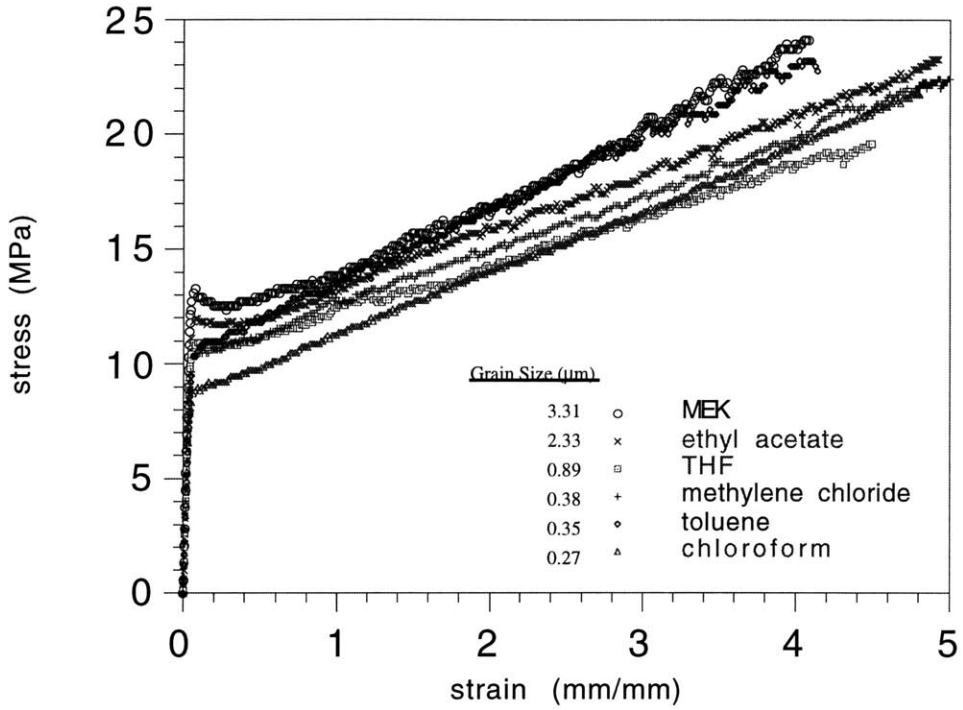

Figure 4-7: Stress (MPa) vs strain (mm/mm) curves for the static cast, grainy KK31 polymer as a function of grain size and casting solvent.

Results for the average of yield strength and modulus versus grain size from approximately ten runs are reported in Figures 4-8 and 4-9. The error bars again represent the standard deviation in the measurements.

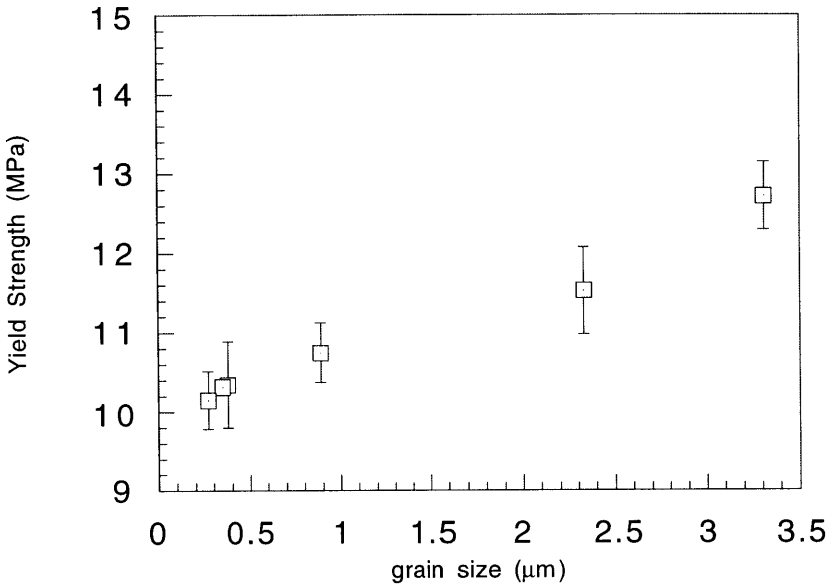

Figure 4-8: Summary of results for the yield strength and vs grain size for the static cast, grainy KK31 block copolymer.

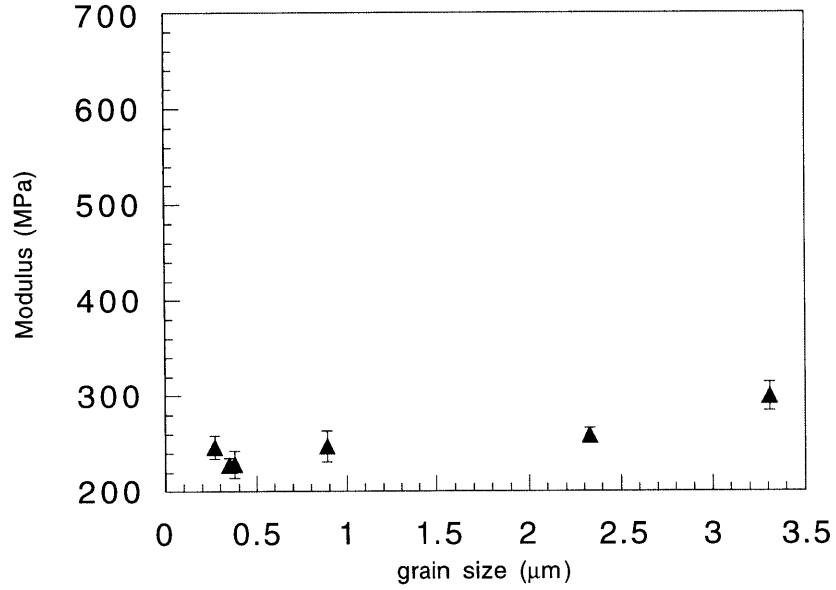

Figure 4-9: Summary of results for the modulus vs grain size for the static cast, grainy KK31 block copolymer.

The graphs for both the yield strength and modulus were put on the same scale as the results summary graphs displayed in the previous section for the oriented, grain free KK31.

Several observations may be made about the results shown on the previous page. Firstly, both the yield strength and the modulus increase with increasing grain size. This is different than what has been witnessed in grainy metals and semicrystalline polymers, where smaller grains yield at a higher stress. The span of yield strengths measured in the grainy static cast samples is over 2.5 MPa, or more than 50% of the potential span of 5 MPa that was measured in the oriented sample, which is a significant result. The span of moduli measured in the static cast and grainy KK31 specimens is only about 60 MPa, which is less than 15% of the possible span of moduli (220 to 640 MPa) measured in the oriented samples.

4.3.2 KR03

Figure 4-10 shows sample stress-strain curves for the KR03 block copolymer processed as was described in chapter 3. The legend contains the grain size, the casting solvent and the casting temperature for each specimen, since not all were cast at room temperature. Methyl ethyl ketone is abbreviated ***mek*** in the legend, ethyl acetate is abbreviated ***eac***, and cumene is abbreviated ***cum***. As was the case with the static cast KK31 samples, a distinctive difference in the yield strength can be observed in these stress-strain curves.

Approximately ten deformation experiments were performed for each grain size generated from the choice of casting solvent and evaporation temperature and a summary of the results for the yield strength and the modulus are displayed in Figures 4-11 and 4-12, respectively. Again the error bars on the figures correspond to the standard deviation from each of the runs. The legend in these two figures continue to show from which casting solvent each of these specimens was evaporated. The span of the ordinate of each graph was chosen to have the same span as the KK31 polymer. In other words, since the

previous two KK31 yield strength graphs' ordinates ranged from 9 to 15 MPa, the ordinate for the yield strength of the KR03 was chosen to range from 8 to 14 MPa, since the yield strengths were slightly lower. The graph of modulus was chosen to range from 150 to 650 MPa, the same range as the KK31 polymers, which ranged from 200 to 700 MPa.

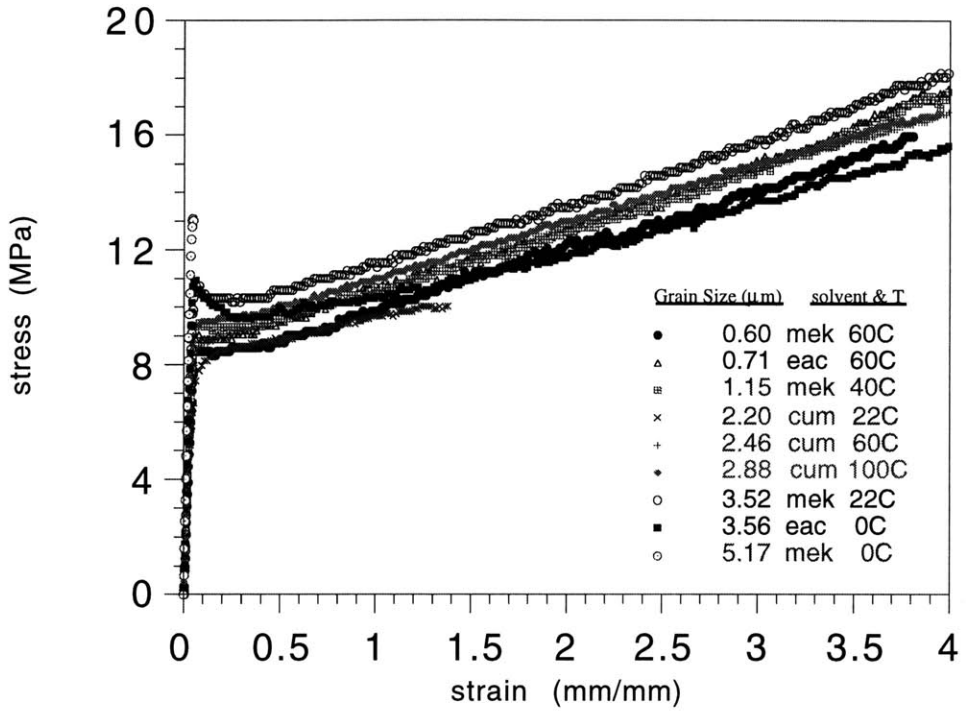

Figure 4-10: Stress (MPa) vs strain (mm/mm) curves for the static cast, grainy KR03 polymer as a function of grain size, casting solvent and evaporation temperature.

We can again make several important observations from the data presented in Figures 4-11 and 4-12. The yield strength increases with larger grains, which is the same phenomena as was observed in the KK31 polymer. Though the modulus also increases as the grains grow, the result is also less significant than the yield strength results.

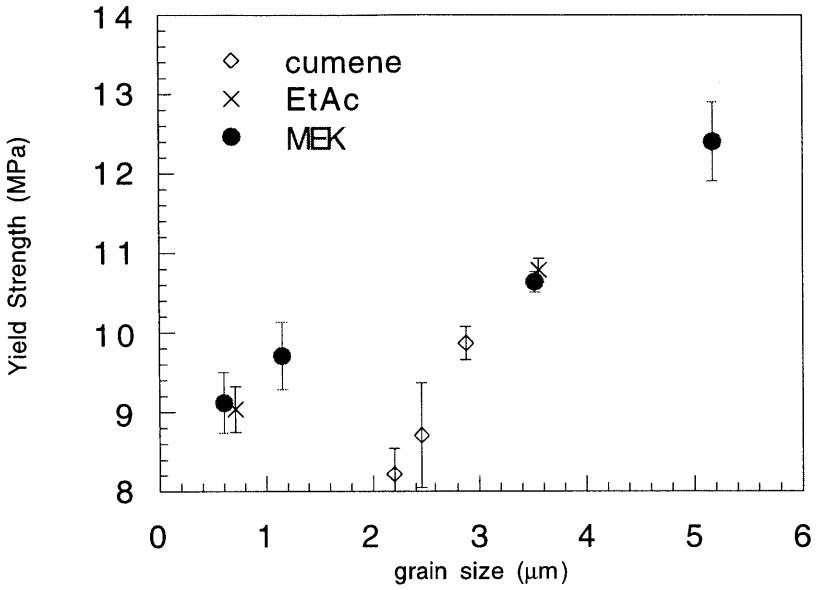

Figure 4-11: Summary of results for the yield strength vs grain size and casting solvent for the static cast, grainy KR03 block copolymer.

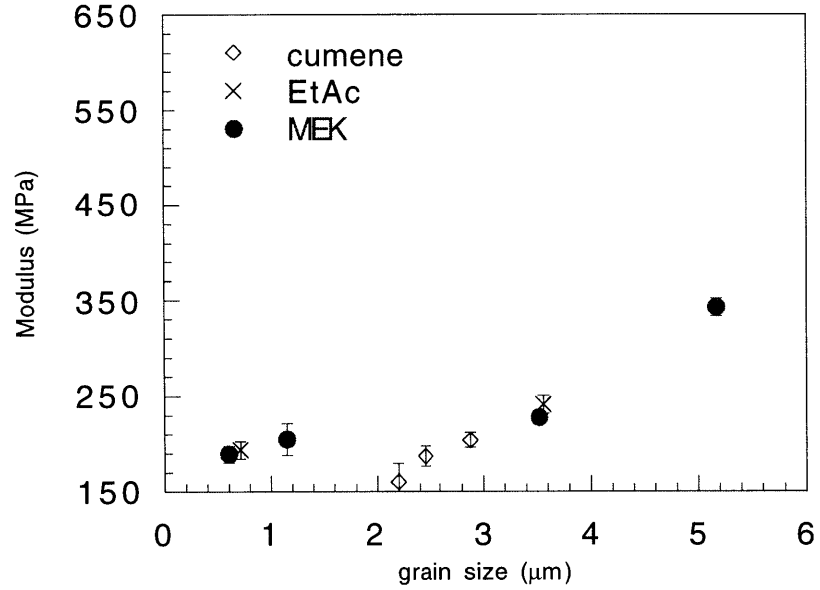

Figure 4-12: Summary of results for the modulus vs grain size and casting solvent for the static cast, grainy KR03 block copolymer.

Possibly, the most important note to make is that the two similar grain sizes generated from different processing conditions and noted in chapter 3, have similar yield strengths and moduli. This strongly hints that similar grains generated from different processing conditions have the same material properties, or that the material properties in grainy block copolymers are not processing-path dependent. The samples processed with cumene as an evaporation solvent tended to produce lower values of yield strength and modulus than what was found with the other two evaporation solvents. This is probably due to the fact that cumene has an extremely low volatility and even the exposure to vacuum for several days and the heating to 100°C cannot remove all of the residual solvent, especially at the lower evaporation temperatures. This is supported by the fact that the samples evaporated at the higher temperatures are closer to the values of yield strength and modulus that would be suspected at those particular grain sizes.

4.3.3 4461

Figure 4-13 shows a sample set of stress-strain curves as a function of casting solvent and grain size for the 4461 triblock copolymer. Unlike the KK31 and KR03 polymer, the 4461 contains more butadiene than styrene. Again, the legend of the graph contains both the casting solvent and grain size (in μm): ***chl*** corresponds to chloroform, ***tol*** is toluene, ***mcl*** is methylene chloride, ***thf*** is tetrahydrofuran, ***eac*** is ethyl acetate and ***cum*** is cumene.

Because this polymer is less rich in styrene, the yield strength of these specimens are much less than the KR03 and KK31. All of these samples had yield strengths less than 4 MPa, compared to the yield strengths ranging from above 8 to almost 14 MPa in the styrene rich block copolymers. Also, whereas the strain at break for the styrene rich block copolymers was always less than 5 mm/mm, the 4461 polymer had values of the strain at break ranging from 15 to 25 mm/mm, also attributable to the increased rubbery butadiene

content, though no connection can be made between the strain at break as well as the tensile strength and the grain size.

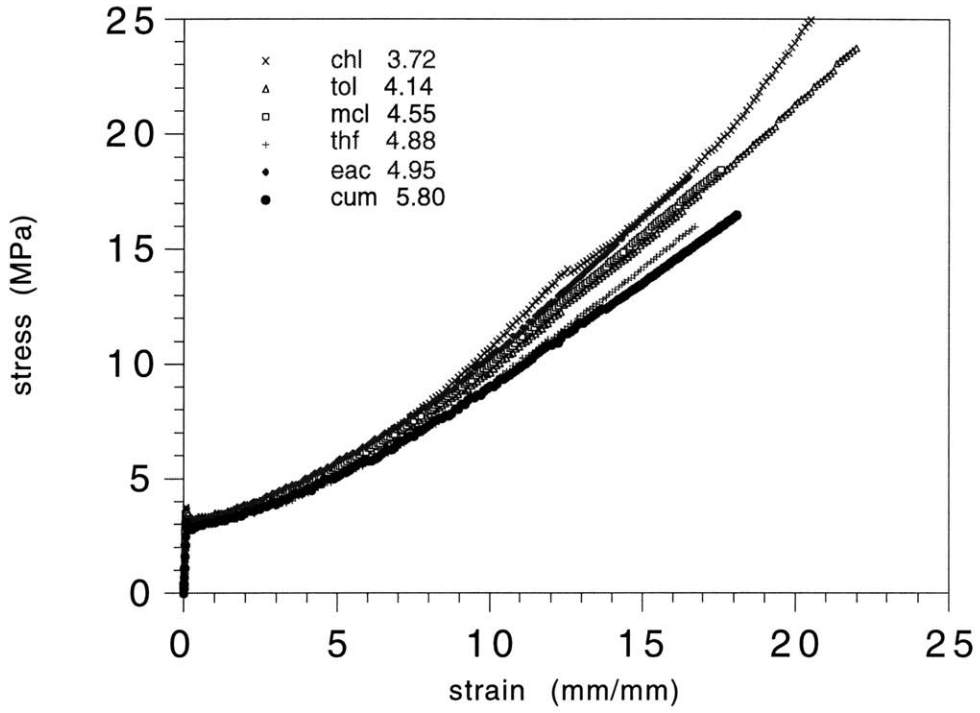

Figure 4-13: Stress (MPa) vs strain (mm/mm) curves for the static cast, grainy 4461 polymer as a function of grain size and casting solvent.

As was the case with the styrene-rich polymers, approximately 10 samples were tested for each grain size. Figure 4-14 shows a summary of results of the yield strength versus grain size and the modulus versus grain size results are displayed in Figure 4-15. The error bars reported are the standard deviation from these trials. The scale of the ordinate for the moduli and yield strength were chosen as a similar percentage of the total values as what was used for the KK31 polymer, since that was the one which we had a maximum span.

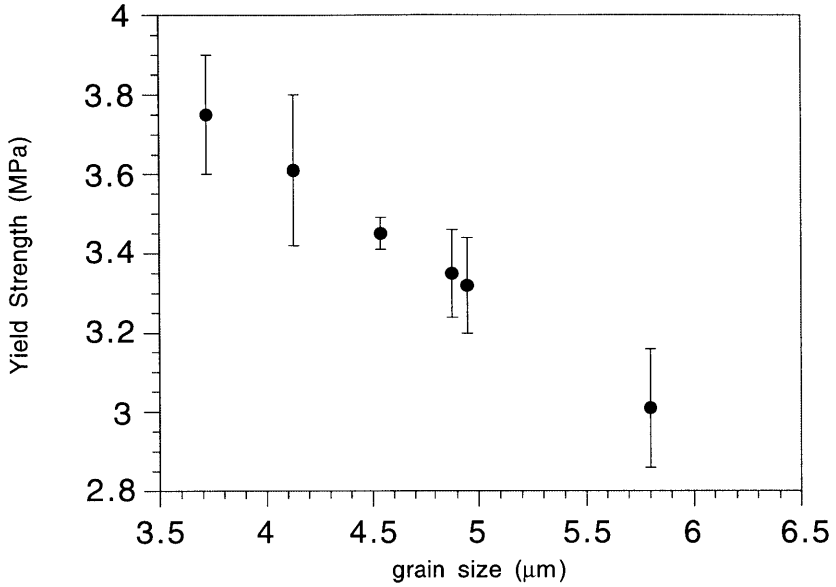

Figure 4-14: Summary of results for the yield strength and vs grain size for the static cast, grainy 4461 block copolymer.

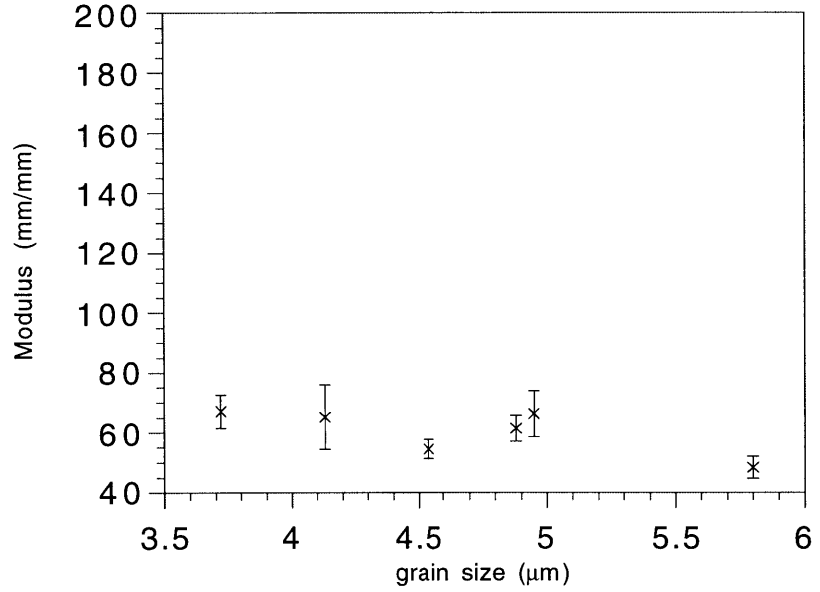

Figure 4-15: Summary of results for the modulus and vs grain size for the static cast, grainy 4461 block copolymer.

In contrast to the styrene rich block copolymers, the yield strength decreases as grain size increases. The modulus doesn't seem to decrease with grain size however, and may actually slightly increase with grain size, with the exception of the largest grain diameter. This is the sample evaporated from cumene and it is again possible that all of the low volatility solvent has been expunged from the film.

4.3.4 DPX-555

Figure 4-16 shows a sample set of stress-strain curves as a function of casting solvent and grain size for the DPX-555 radial (4-armed) copolymer. Again, the legend of the graph contains both the casting solvent and grain size (in μm). Figures 4-17 and 4-18 show a summary of results of the modulus and yield strength as a function of grain size; the scale of the ordinates of these graphs is the same as those chosen for the 4461 polymer.

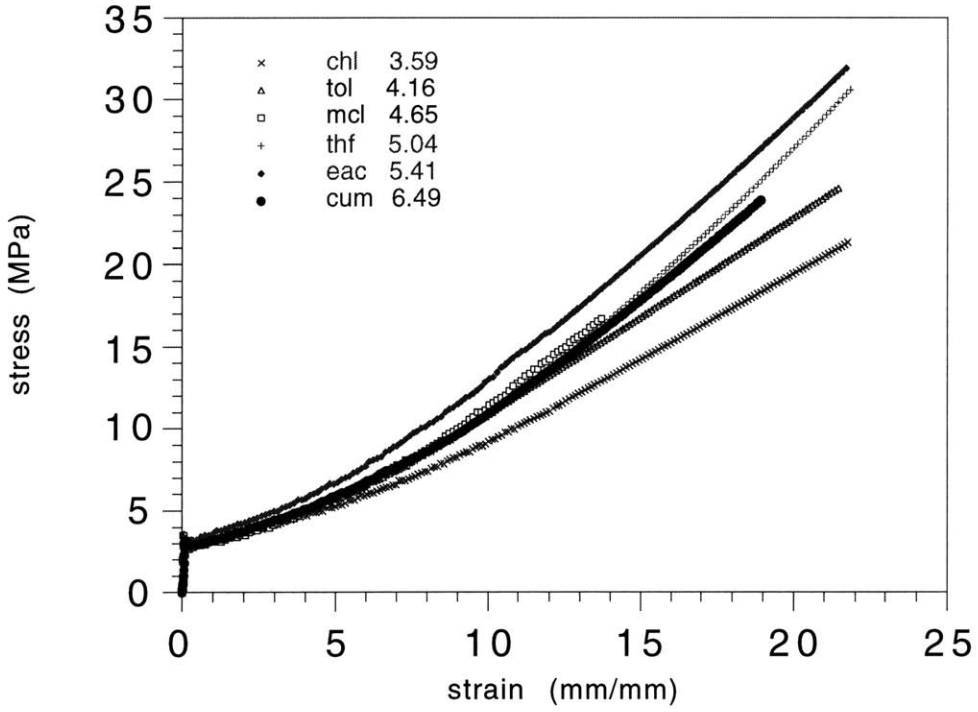

Figure 4-16: Stress (MPa) vs strain (mm/mm) curves for the static cast, grainy DPX-555 polymer as a function of casting solvent and grain size.

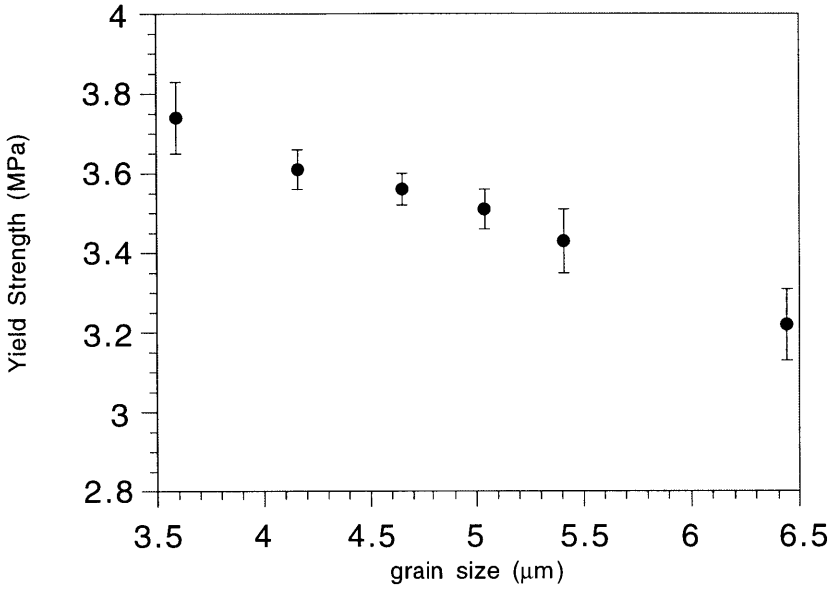

Figure 4-17: Summary of results for the yield strength vs grain size for the static cast, grainy DPX-555 block copolymer.

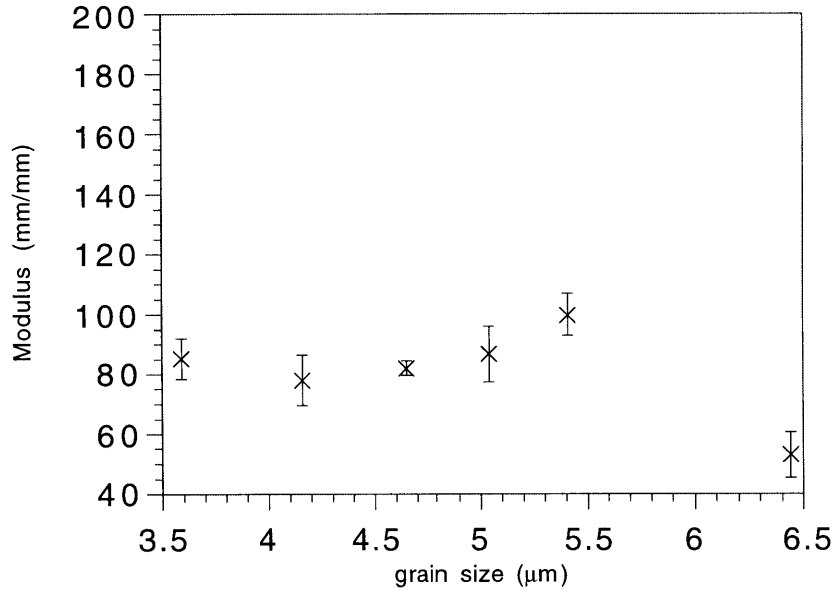

Figure 4-18: Summary of results for the modulus vs grain size for the static cast, grainy DPX-555 block copolymer.

The previous two graphs contain error bars that represent the standard deviation of the approximately ten runs for each grain size. As was the case with the other butadiene rich block copolymer, 4461, an increase in the grain size causes a decrease in the yield strength of the material. This effect wasn't as pronounced in this polymer; the drop in yield strength was only about 0.5 MPa compared to about a 0.75 drop for the 4461 polymer over a smaller range of grain sizes.

Again there doesn't seem to be a large change in the modulus over the range of grain sizes generated. There appears to even be a slight increase in the modulus over this range if you again postulate that the low modulus in the samples cast from cumene still contain trace amounts of that solvent.

4.3.5 S12B10

In addition to the commercial block copolymers shown in the previous sections, instron tests were performed on one series of the S12B10 diblock copolymer examined in Chapter 2. The polymer was dissolved in chloroform and annealed at 75°C for various amounts of time and measured using Ultra SAXS, according to the procedure outlined in Section 2.7.

A summary of the results for the yield strength as a function of grain size are presented in Figure 4-19. The results for the modulus as a function of grain size are displayed in Figure 4-20. Since this is not a commodity polymer, the amount of this material was limited, and it was not possible to complete ten tests to determine error bars. Instead the average of approximately four trials was done for all of the grain sizes generated. The error bars on both of these graphs therefore represent the standard deviation from these trials. It can be stated that the strain at break was very poor for these materials (less than 0.2 mm/mm for all trials of all processing conditions studied), because of the low molecular weight of the polymer. The fact that this is a diblock copolymer also aided in the poor strain at break in the instron test, because this minimizes potential entanglements, which would hinder fracture.

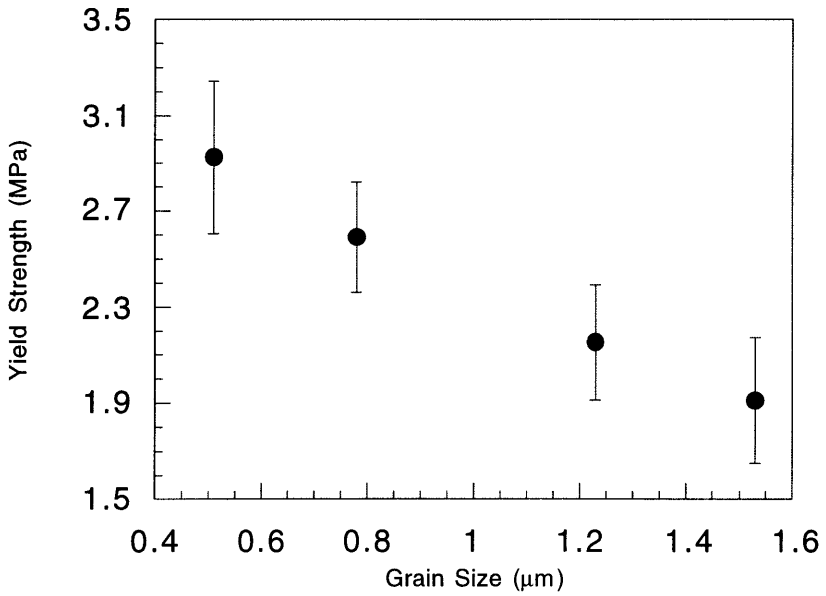

Figure 4-19: Summary of results for the yield strength vs grain size for the static cast, grainy S12B10 diblock copolymer.

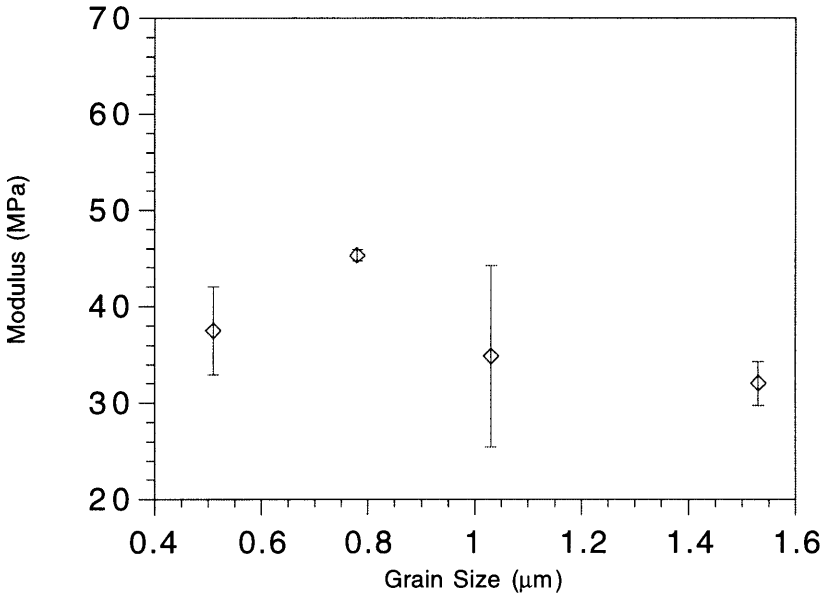

Figure 4-20: Summary of results for the modulus vs grain size for the static cast, grainy S12B10 diblock copolymer.

The yield strength apparantly decreases with increasing grain size for this series of grain sizes. No trend can be observed in the modulus as a function of grain size, it seems to be somewhat flat.

4.4 Discussion

There is no doubt that process-history-induced changes in grain size and grain boundary structure lead to significant and systematic trends in the tensile mechanical properties. The trend is most significant in the yield stress for all five block copolymers studied and to a lesser extenct modulus. However, not all five polymers exhibit the same trends in yield strength as a function of grain size. In fact, the styrene rich polymers and the butadiene rich polymers exhibit opposite trends in the yield strength, so the discussion will continue along these lines.

4.4.1 Styrene Rich Copolymers

The two commercially available styrene butadiene block copolymers: KK31 and K303, showed an increase in the yield strength as well as the modulus with increasing grain size. Because the KK31 comes in an extruded, grain-free sheet, we were able to test the as received material as a function of angle to determine upper and lower bounds for this material. Changing grain size in this polymer led to changes from about 10 to 13 MPa in the yield strength which spans over half of the complete range of values, from upper to lower bound, exhibited as a function of orientation in the extruded KK31 oriented sheet. The modulus increased only from about 240 to 300 MPa in KK31 as a function of grain size whereas the oriented KK31 showed limiting values of about 220 and 630 MPa, spanning only about 15% of the limits exhibited by the extruded, grain-free KK31 polymer. Similar results were seen for the similar material, KR03.

Taken together, these results suggest that selecting grain size as the relevant morphological parameters leads to contradictory conclusions. On the one hand, the trend of the yield stress of grain size, suggests that as grains grow in these materials there is a tendency for the lamellae to orient into the plane of the film so that the lamellar normals tend

to align with the direction perpendicular to the flat film specimen surfaces. On the other hand the relatively constant value of modulus suggests relatively little change in the in-plane orientation as a function of grain size.

To clear up this issue, we carried out edge-view SAXS experiments on KK31 and KR03 samples determine whether or not significant changes in lamellar orientation do occur with grain growth. Figures 4-21 and 4-22 show top view and edge view SAXS patterns for KK31 and KR03 respectively. The edge view patterns for both the small grained and large grained samples were prepared from stacks of pieces cut from the films and fused together using the method of Csernica[6,7]. While there is indeed evidence for a tendency of the lamellae to lie in the plane of the film, there is no clear difference in the lamellar orientation for the KK31 specimen with small grains compared to the KK31 specimen with large grains. Figure 4-22 reveals a similar result for KR03 specimens which span the full range of grain sizes for that material. Thus the trends seen in the yield strength and modulus do not arise from changes in the lamellar orientations within the grainy morphology.

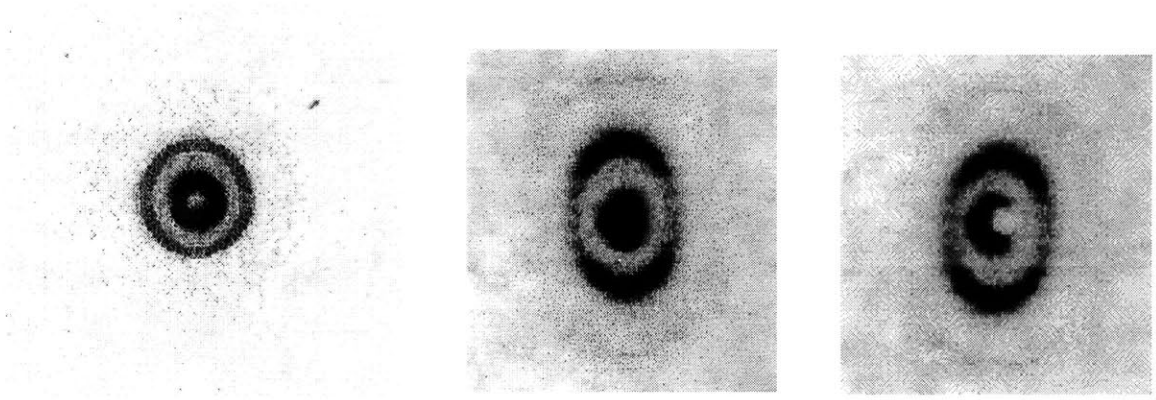

Figure 4-21: 2-dimensional SAXS patterns for the KK31 polymer from the top view (left), the edge view of a small grained sample (center), and the edge view of a large grained sample (right).

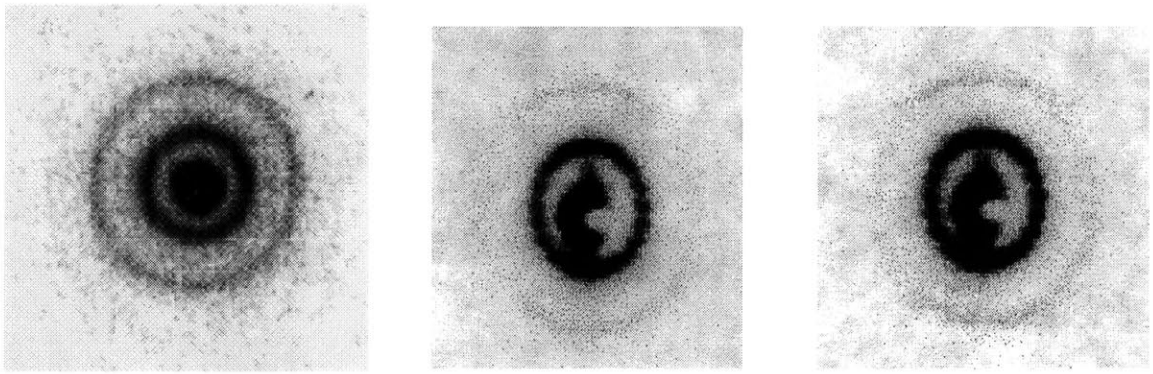

Figure 4-22: 2-dimensional SAXS patterns for the KR03 polymer from the top view (left), the edge view of a small grained sample (center), and the edge view of a large grained sample (right).

Having eliminated lamellar orientation as the primary cause for the trends seen in the grainy KK31 and KR03 polymers, we consider the grain size and grain boundary structure as possible parameters to explain the observed behavior. The trend of increasing yield strength with increasing grain size is opposite to expectation based on the behavior of polycrystalline metals[8-10] and semicrystalline, spherulitic polymers[11-14]. In those cases the smaller grains are restricted from yielding until higher stress can activate the pinned dislocations in the grain boundary material. Larger grains lead to more easily yielded materials because the soft modes of yield internal to the grains are less influenced by the more distant, more dilute grain boundary material.

From Chapter 2 and 3, we find that, when we can determine it directly from the scattering data, the volume fraction of grain boundaries remains essentially constant as grains grow; under these circumstances grain boundary thickness increases in direct proportion to grain size. As the grains grow, the contrast factor, $(\Delta\rho)^2$, also increases. Because of Babinet's principle[15], we cannot use our scattering data to determine whether the grain boundary is becoming richer in polystyrene or in polybutadiene, only that the grain boundary density is deviating more strongly from the mean density inside the grains.

We postulate, however, that because there is more styrene than butadiene present in these block copolymers, the grain boundaries for KR03 and KK31 contain an enrichment of polystyrene. Thus we believe that in the materials studied here, the grain boundaries both thicken and become more rigid as grain size increases.

Under the circumstances postulated above, it becomes clear why the yield stress increases so significantly as grain size increases. The yield process in these materials requires a break up of the styrene rich, rigid grain boundary material which percolates throughout the specimen. Because this percolating structure increases in thickness and in stiffness as the grain growth proceeds, the stress level required to elicit macroscopic yield also increases.

4.4.2 Butadiene Rich Copolymers

The two butadiene rich copolymers synthesized by DEXCO, 4461 and DPX-555, also show small increase in the modulus as the grains grow larger, but show the opposite trend with yield strength and grain size than the styrene rich copolymers previously discussed. The yield strength decreases with increasing grain size, similar to the behavior of polycrystalline metals[8-10] and semicrystalline, spherulitic polymers[11-14]. To understand this behavior, we must first observe the edge on SAXS patterns of these materials to check whether any significant changes in lamellar orientation do occur with grain growth. Figures 4-23 and 4-24 show the edge top view and edge view SAXS patterns of the 4461 and DPX-555 polymers, respectively. The procedure for generating the edge view SAXS patterns is the same as what was done in the previous section for the styrene rich block copolymers and described previously.[6,7] The edge view patterns were generated for samples containing both small grains and large grains for both polymers. It is worth noting at this time that the small grains in the butadiene rich bloch copolymers were about the same size as the large grains in the styrene rich polymers.

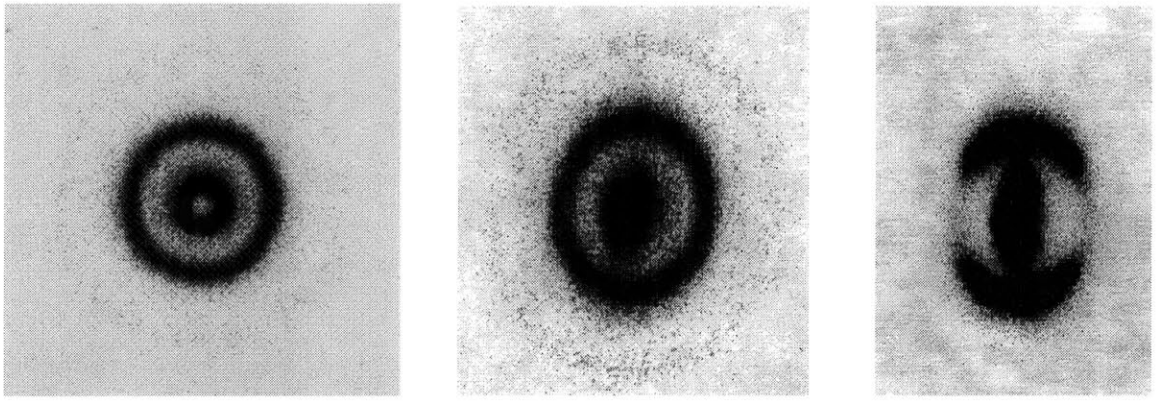

Figure 4-23: 2-dimensional SAXS patterns for the 4461 polymer from the top view (left), the edge view of a small grained sample (center), and the edge view of a large grained sample (right).

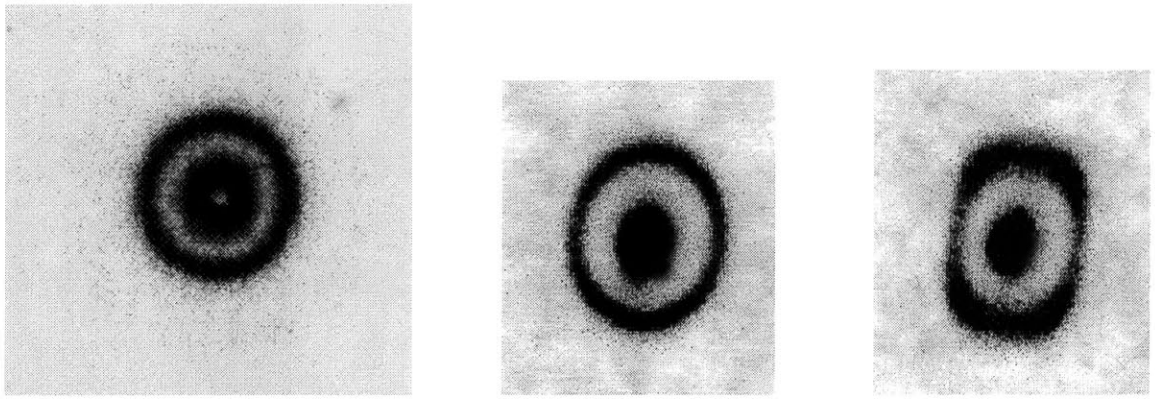

Figure 4-24: 2-dimensional SAXS patterns for the 4461 polymer from the top view (left), the edge view of a small grained sample (center), and the edge view of a large grained sample (right).

For both the 4461 and DPX-555 polymer, there appears to be a slight tendency for the grains to lie in the plane of the film at small grain sizes. At large grain sizes, a significant tendency is witnessed for grains to lie in the plane of the film. When orientation in the plane of the film occurs, deformation of this material asymptotically approaches deformation parallel to the lamellae (i.e. 90° in our nomenclature for the extruded samples).

This explains why the modulus is increasing slightly as the grains of these butadiene rich block copolymers grow.

If we look at both Figures 4-3 and 4-4, we see that more preferential orientation parallel to the deformation direction wouls also cause an increase in the yield strength. Yet, we find that the yield strength decreases as the grains grow larger *despite* this trend. In other words, if the grains weren't preferentially orienting in the plane of the film, this effect would be even more pronounced; larger grains would have an even greater decrease in the yield strength.

The next logical question to be asked is why this difference between the styrene rich and butadiene rich block copolymers. Why do the styrene rich polymers increase in yield strength as the grains grow larger, while the butadiene rich block copolymers decrease in yield strength with grain growth? In the Chapter 3, we found that with from the Ultra SAXS scattering data, the grain boundaries actually stay the same thickness and become richer in one of the two components as the grains grow larger. In the last section, we postulated that with the styrene rich polymers, the grain boundary was actually an enrichment of styrene. Because of this, the grain boundaries are actually stronger than the grains and would have to yield before the grains themselves yield, causing an increase in the overall yield strength as the grains (and thus the grain boundaries) grow.

We can use similar logic to explain the opposite trend in the butadiene rich block copolymers, 4461 and DPX-555. The richer material in these materials is the butadiene and so we postulate that the grains contain an enrichment of butadiene. Butadiene is not as strong as the grains and does not yield. Therefore, the grain boundaries would be a point where grains would be allowed to slide past each other, similar to the mechanisms given for yield strength in grainy metals and semicrystalline polymers. If we continue this line of reasoning, it is logical that smaller grains would therefore have a higher yield strength. Smaller grains would have a possess more grain boundary surface area per unit volume to impede dislocation. The grain boundaries do not yield since they are butadiene rich.

Becuase the grain boundaries don't contain excess styrene, the degree of enrichment is not important.

4.4.3 The Low Molecular Weight Diblock

The low molecular weight diblock copolymer , S12B10, has molecular weights of 9900 for the styrene block and 9700 for the butadiene block. The yield strength decreases with increasing grain size for this polymer under the processing conditions, which include casting from chloroform and annealing at 75°C. There is no noticeable change in the modulus over the range of grain sizes, implying that there is no orientation of the grains in the plane of the film. Since S12B10 contains more styrene than butadiene, yield strength should increase with grain size according to the hypothesis outlined above, which is not the case.

Two reasons exist to explain this discrepancy. Firstly, this is the only diblock copolymer which has been studied, and it is possible that there is no molecular connectivity through the grain boundaries between grains. If this is the case, even if the grain boundaries are styrene rich, they still would be the location where the slip occurs. Secondly, it has been shown that some annealing conditions cause semicrystalline polymers to become more brittle possibly because of a lack of intercrystalline links.[13] A similar phenomenon may be occuring with the annealing conditions outlined in Chapter 2 to generate the different grain sizes measured for S12B10.

4.5 References

(1) Hashimoto, T.; Nagatoshi, K.; Todo, A.; Hasegawa, H.; Kawai, H. *Macromolecules* **1974**, *7*, 364.

(2) Inoue, T.; Mroitani, M.; Hashimoto, T.; Kawai, H. *Macromolecules* **1971**, *4*, 500.

(3) Hashimoto, T.; Fujimura, M.; Saijo, K.; Kawai, H.; Diamant, T.; Shen, M. *ACS Advances in Chemistry Series: Multiphase Polymers* **1979**, 257.

(4) Hasegawa, H.; Hashimoto, T.; Kawai, H.; Lodge, T.P.; Amis, E.J.; Glinka, C.J.; Han, C.C. *Macromolecules* **1985**, *18*, 67.

(5) Pakula, T.; Saijo, K.; Kawai, H.; Hashimoto, T. *Macromolecules* **1985**, *18*, 1294.

(6) Csernica, J.; Baddour, R.F.; Cohen, R.E. *Macromolecules* **1989**, *22*, 1493.

(7) Csernica. J. *Gas Permeation in Block Copolymer Films*, PhD Thesis, M.I.T., 1989.

(8) Chen, R.W.; Argon, A.S. *Acta Metallurgica* **1979**, *27*, 749.

(9) Chen, R.W.; Argon, A.S. *Acta Metallurgica* **1979**, *27*, 785.

(10) Bao, G.; Hutchinson, J.W.; McMeeking, R.M. *Acta Metallurgica* **1991**, *39*, 1871.

(11) Halpin, J.C.; Kardos, J.L. *J. Appl. Phys.* **1972**, *43*, 2235.

(12) Andrews, E.H. *Pure and Appl. Chem.* **1972**, *31*, 91.

(13) Bassett, D.C.; Carder, D.R. *Phil. Mag.* **1973**, *28*, 535.

(14) Starkweather, H.W.; Brooks, R.E. *J. Appl. Polymer Sci.* **1959**, *1*, 236.

(15) Porod, G. in *Small Angle X-Ray Scattering*. O. Glatter and O. Kratky eds. Academic Press, London, 1982.

5. Summary and Directions for Future Investigations

5.1 Summary

Simultaneous determination of the morphological length scale, d, and the grain size, D, in a heterogeneous, lamellar styrene - butadiene block copolymer is possible through the use of Ultra SAXS measurements. The lamellar spacing, d, was revealed directly in the data by the appearance of Bragg peaks in the relevant range of scattering vector, q, traditionally above a value of 0.1 $Å^{-1}$. These values measured are the same as measured from traditional SAXS patterns. Most of the block copolymer specimens also show peaks in the Ultra SAXS range, at values of the scattering vector, 0.0004 q 0.1. An absolute length for the grain size, D, can be found from these scattering profiles through the use of the spherical form factor, $D = \frac{8}{q_{MAX}}$, where q_{MAX} is the value of the scattering vector at the grain peak. It is recognized that other methods of determining an absolute grain size exist, most notably a quasi - Bragg mechanism and a correlation function approach, but the spherical form factor is morphologically similar to Stein's spherulites, so it was continued to be the mechanism of choice for this thesis.

Plots of the Interference function, C_1-Iq^4, showed that Porod's Law was followed in the scattering tail of the Ultra SAXS peak attributed to the presence of grains. Use of this Porod Constant, C_1, and the invariant, C_2, validated the proposed mechanism via calculation of reasonable and consistent grain boundary volume fraction, ϕ, and the electron density differences $(\Delta\rho)^2$.

Through a collaboration with Dr. Alexander Karbach with Bayer A.G., we have been able to produce the appropriately uniform, large-area, ultramicrotomed sections required to produce a TEM micrograph with enough grains present to relatively accurately estimate grain size. The results compared favorably to the values determined from the Ultra SAXS scattering curves.

For scattering profiles that do not show a peak, use of the Porod region of the grain scattering mechanism and the invariant facilitated a reliable estimate of grain size D assuming the phase fraction of grain boundary, ϕ, is 0.1. Swelling KR03 resin with the low volatility solvent, cumene, addresses the contention that scattering at very low values of q is dominated by microscale voids.

Grain size can also be found from the Ultra SAXS scattering curves for commercially available, higher molecular weight, triblock, three-armed or radial block copolymers. The styrene rich block copolymers for the most part had peaks in the Ultra SAXS region and could have the grain size determined explicitly. The butadiene rich block copolymers did not have peaks in the Ultra SAXS region, so the grain sizes had to be estimated from Porod's Law, the invariant and the grain boundary volume fraction assumption, ϕ=0.1.

Grain size can be altered in these commercial block copolymers without annealing or heating above the order - disorder temperature and quenching, the two methods that had previously been established for grain growth. These two methods were deemed impractical for this thesis, since we wanted to look at deformation behavioral effects of grain size, and both of the above methods could degrade the polymer and mask any potential grain effects.

Both the choice of solvent and the evaporation temperature affected the grain size. For the reasonably volatile solvents, an increase in temperature led to significantly smaller grains. This is probably due to the decreased evaporation time required for static casting while at elevated temperatures. However, for the low-volatility solvent, cumene, an increase in temperature actually led to a small increase in the grain size. A possible reason for this is because of the significantly longer evaporation times, the elevated temperatures actually caused some annealing to occur. For all of the polymers, the solvent choice produced the same relative grain sizes. Chloroform formed the smallest grains, followed by toluene, methylene chloride, tetrahydrofuran, ethyl acetate, cumene, and methyl ethyl

ketone. The grain diameters for the styrene-rich polymers were about 3 μm smaller on average than the butadiene rich polymers: the styrene rich polymers ranged from about 0.3 to 3.5 μm, while the butadiene rich polymers ranged from about 3.5 to 6.5 μm.

This Ultra SAXS characterization of grain structure enabled us to quantify grain size in lamellar SB block copolymers and to make qualitative judgments about the variation of grain boundary thickness and composition with grain size. These characteristics of the grainy lamellar materials were used to explain the observed trends in the mechanical behavior of the materials: in particular the increase in yield stress with grain size for the styrene rich block copolymers and a similar decrease in yield strength for the butadiene rich block copolymers.

The significant increase in yield stress with grain size for the styrene rich commercial block copolymers is consistent with a mechanism of yield that requires a break-up of a rigid, polystyrene-rich structure that percolates through the material. The relatively constant modulus with changing grain size is consistent with edge-view SAXS patterns which indicated that the distribution of lamellar orientations, while not completely random, does not change significantly over the range of grain sizes (ca 0.5 to 5 μm) accessible in these polymers.

The correspondingly significant decrease in the yield strength with grain size for the butadiene rich commercial block copolymers is explained through the hypothesis that these grain boundaries contain an enrichment of butadiene. Butadiene is weaker than the grain itself and does not yield. This is consistent with a deformation mechanism similar to those proposed for grainy metals and semicrystalline block copolymers: the grain boundaries are the weakest point and when a load is applied, these boundaries are the point of slip between two grains. Smaller grains have a higher surface area to volume ratio, therefore more area to impede dislocation, and a higher yield strength than larger grains. Edge view SAXS do show a greater preference for the larger grains to lie in the plane of the film, but this

phenomena would cause an increase in the yield strength, so the decrease is in fact happening despite this occurance.

5.2 Directions for Future Investigations

5.2.1 Order - Order Transitions

Recently order-order transitions in block copolymers have been the subject of many studies.[1-4] Whereas all block copolymers have an order-disorder transition, it is not believed that all have an order-order transition. The order-disorder temperature, T_{ODT}, is defined as the temperature where the block copolymer undergoes a transition from a microphase separated, hence ordered, morphology (like cylinders or lamellae) to a homogenous and thus disordered morphology. In contrast, the order-order transition temperature, T_{OOT}, is when a block copolymer undergoes a transition from one microphase separated morphology to another; for example from spheres to bi-continuous double gyroid. The order-order transition is normally at a much lower temperature than an order-disorder transition for a given block copolymer.

It is unsure how an order-order transition affects the grain structure, but it has been recently postulated that these transitions occur within the grains.[5] Ultra SAXS can be used to explore this hypothesis, and some preliminary results follow. A sample of S/EP 7/13 was obtained from Professor Richard Register's lab at Princeton University. S/EP stands for a styrene - ethylene-propylene block copolymer (a hydrogenated styrene - isoprene block copolymer) with molecular weights of the constituent blocks at 7000 and 13000 g/mol, respectively. More details on the polymer and synthetic techniques appear elsewhere.[6]

It's known that this particular polymer undergoes an order-order transition from lamellae to cylinders when heating above 175°C for over 15 minutes, and reverts back to lamellae when quenched below 140°C for a similar amount of time. Since this polymer is saturated, it won't degrade when exposed to these elevated temperatures, as either styrene-

butadiene or styrene-isoprene would. The polymer was melt pressed into a film and then placed in a temperature cell so that the Ultra SAXS measurements could be performed while the polymer was at elevated temperatures. Figure 5-1 shows the Ultra SAXS scattering curves for this polymer at various temperatures and times.

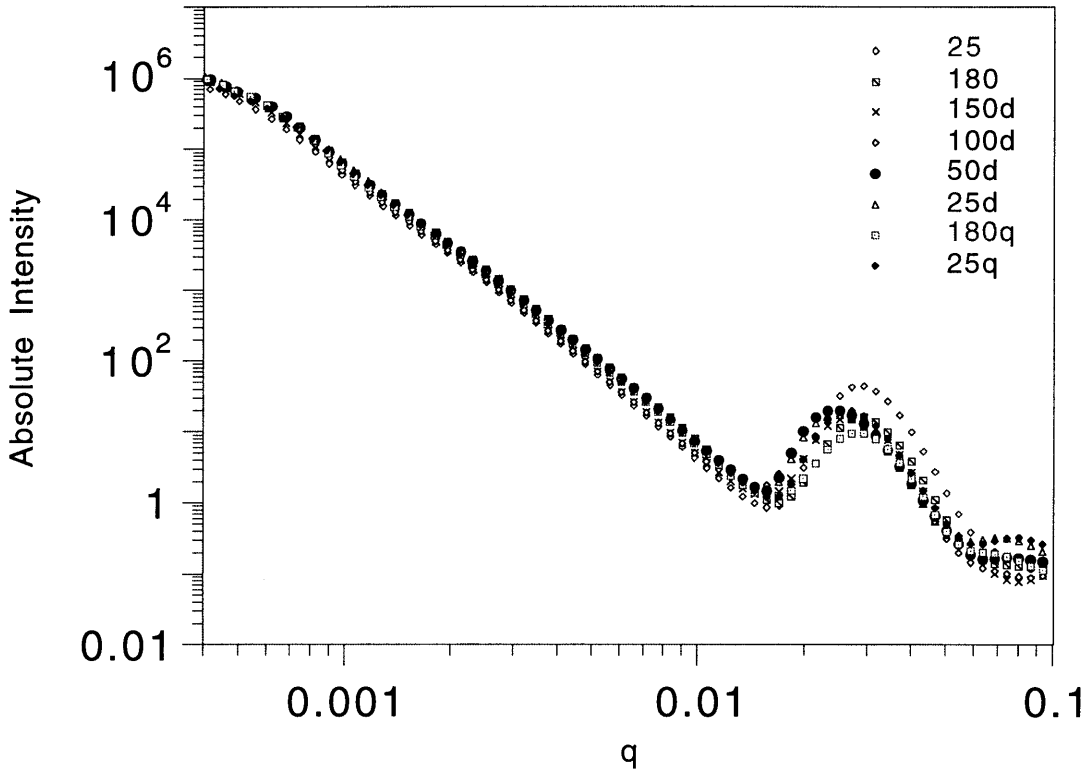

Figure 5-1: Ultra SAXS scattering profiles of the S/EP 7/13 block copolymer held at different temperatures, presumably undergoing several order-order transitions.

The polymer was first tested at 25°C, and this is called ***25*** in the legend. It was then heated to 180°C and allowed to equilibrate for over a half hour, more than enough time to undergo an order-order transition, and then more Ultra SAXS scattering

measurements were made, called ***180***. The polymer was allowed to cool to 150°C and equilibrate for 15 minutes, before the scattering curve ***150d*** was measured, though this was above the temperature that the polymer would revert back to lamellae. Similar procedures were done for ***100d***, ***50d***, and ***25d***, which all fall below the order-order transition temperature, T_{OOT}. The polymer was again heated to 180°C and allowed to equilibrate for over a half hour, and then ***180q*** was measured. The polymer was then quenched to 25°C where the final Ultra SAXS scattering profile was immediately obtained, ***25q***.

What is immediately noticed that is different from all other Ultra SAXS scattering curves in this thesis, is that the peak in the traditional SAXS region moves. This has been well documented and corresponds to the order-order transitions undergone by the polymer as caused by the temperature changes. A traditional SAXS machine is better tuned and equipped to measure this phenomena; this has been done for this polymer and published elsewhere.[6] What is added by the Ultra SAXS measurements, is the tail of the grain peak. As can be seen, the grain peak does not shift. This hints that the grain size is not changing during the series of order-order transitions, and that in fact these changes in morphology does occur within a grain, in accordance with what has been published elsewhere.[5]

Where more research should delve into this, the Ultra SAXS scattering curves hint that the grain size is constant during an order - order transition. If we make the tenuous assumption that the grain boundary volume fraction, ϕ, is equal to 0.1 for this S/EP block copolymer as it is for the SB block copolymers, we can estimate the grain size from these scattering curves and equation 2-6 at approximately 4.4 μm.

5.2.2 Grain Size and Geometry Characterization

One of the advantages of microscopy, in general, and transmission electron microscopy in particular, is that visual images are produced, eliminating any chance of

discrepancies in analyzing the data. Another advantage of microscopy specifically related to grains is images allow one to probe the exact geometrical shape the grains form. However as has been stated earlier, it is very difficult to produce samples for transmission electron microscopy that show enough area to get a statistically significant grain size measurement or a hint on all the grain shapes present. One solution might be high resolution scanning electron microscopy (SEM). SEM images are able to probe larger images, as the preparation method is easier. Figure 5-2 shows a high-resolution SEM image of the same KR03 sample shown in Figure 1-7. Unfortunately, unlike TEM, SEM does not possess the fine resolution required to show the lamellar morphology. Therefore, the first task required when using SEM as a grain measurement tool is to prove that the contrast seen is due to the presence of grains and not from surface imperfections. These objects to appear to be on the same length scale as grains, but more studies need to be done. If the contrast in the SEM image is in fact due to grains, the same methods proposed by Underwood and outlined in chapter 2 for TEM can be applied to these images to determine a grain size.[7]

Other methods of image quantification may be used on these SEM micrographs. Since these images are digitized, it may also be possible to use computerized image analysis software to quantify grain size and more exactly determine size distributions and shapes. Techniques like this could potentially lead to a greater understanding of grains and why they are formed.

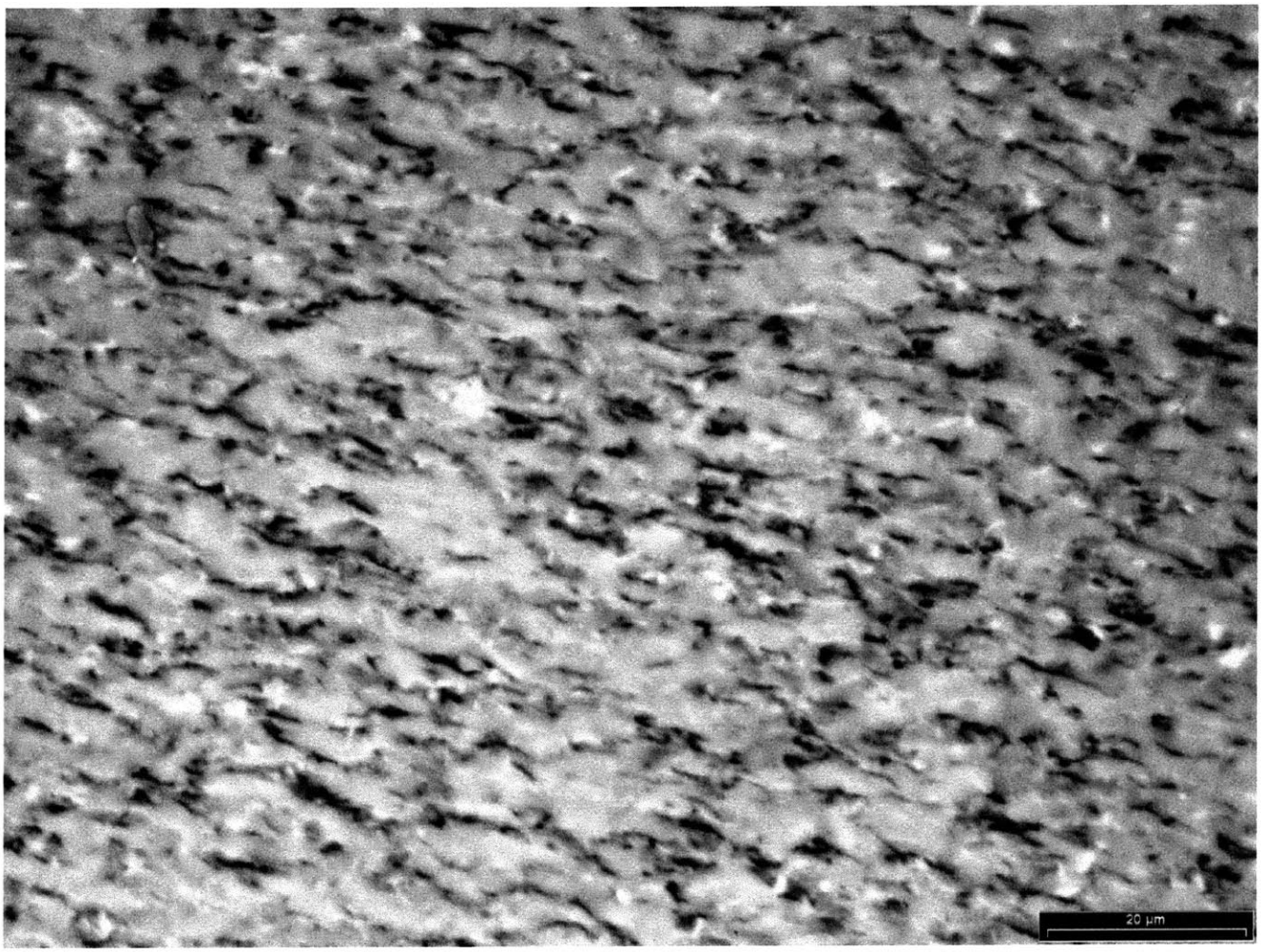

Figure 5-2: High resolution SEM image of KR03 resin, depicted by TEM in Figure 1-7. Micrograph courtesy of Dr. A. Karbach, Bayer A.G.

Another unexplored method for grain size determination is Ultra Small Angle Neutron Scattering (Ultra SANS). Small angle neutron scattering data are reported in the similar intensity versus scattering vector, q, form. However, the source of contrast is different than the electron densities, which is the case in X-ray scattering. The coherent scattering lengths vary as a function of the atomic number isotope and nuclear spin state in an apparently irregular way, as neutrons are scattered by nuclei. Table 5.1 shows the coherent scattering lengths, a, of some of the most common atoms and isotopes as viewed by SANS.

atom or isotope	*a (fermes $=10^{-15}m$)*
hydrogen	-3.74
deuterium	6.67
carbon	6.65
oxygen	5.8
nitrogen	9.4

Table 5.1: Coherent scattering lengths, a, for selected important atoms and isotopes as viewed by SANS

A scattering length for a polymer, b, is the source of contrast as viewed by SANS (units are cm/cm^3) and is defined as:

$$b = \frac{\rho N_A}{M_0} \sum n_i a_i \qquad (5\text{-}1)$$

where: ρ is the mass density

N_A is Avogadro's number

M_0 is the molecular weight of the monomer

n_i is the number of atoms/isotopes of *i* in the monomer

a_i scattering length of atom/isotope *i*

Preliminary studies have been done with a traditional SANS beamline at the headquarters of the National Institute of Standards and Technology in Gaithersburg, MD, to see if there is a significant enough contrast to induce scattering on the grain length scale. Figure 5-3 shows an absolute intensity versus scattering vector, q, for S12B10 cast from chloroform and annealed for certain lengths of time.

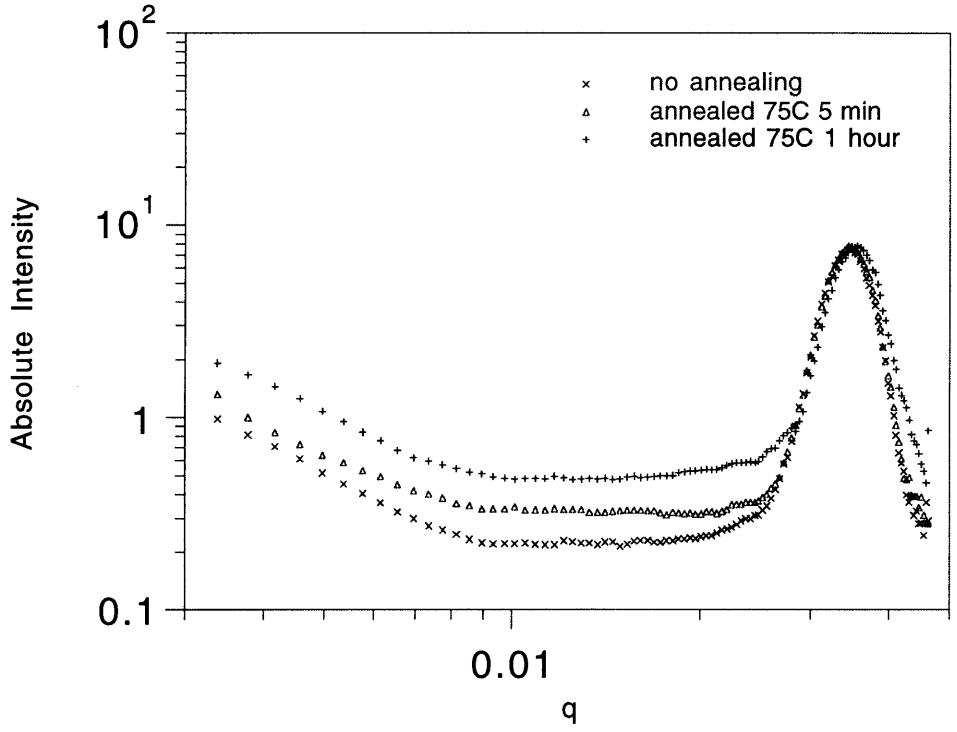

Figure 5-3: Small Angle Neutron Scattering graph of absolute intensity versus scattering vector, q, for S12B10 polymer cast from chloroform, as a function of annealing time at 75°C.

As was the case for the SAXS and Ultra SAXS graphs, the peak due to lamellar spacing at a length of approximately 170 Å is unchanged by the annealing protocol. The limit of the SANS instrument is q=0.0038, approximately an order of magnitude less precise than the Ultra SAXS machine, but a small upturn in the scattering curves is witnessed at values of q less than 0.1, which quite possibly is due to the presence of grains in the samples. Also, there seems to be a systematic increase in the scattering intensity of these tails, corresponding to the previously understood grain growth with annealing phenomenon,[8] and what was witnessed with Ultra SAXS for these samples. This hints that the scattering is due to grains. Figure 5-4 shows SANS scattering curves for the KK31 polymer processed as described in Chapter 3.

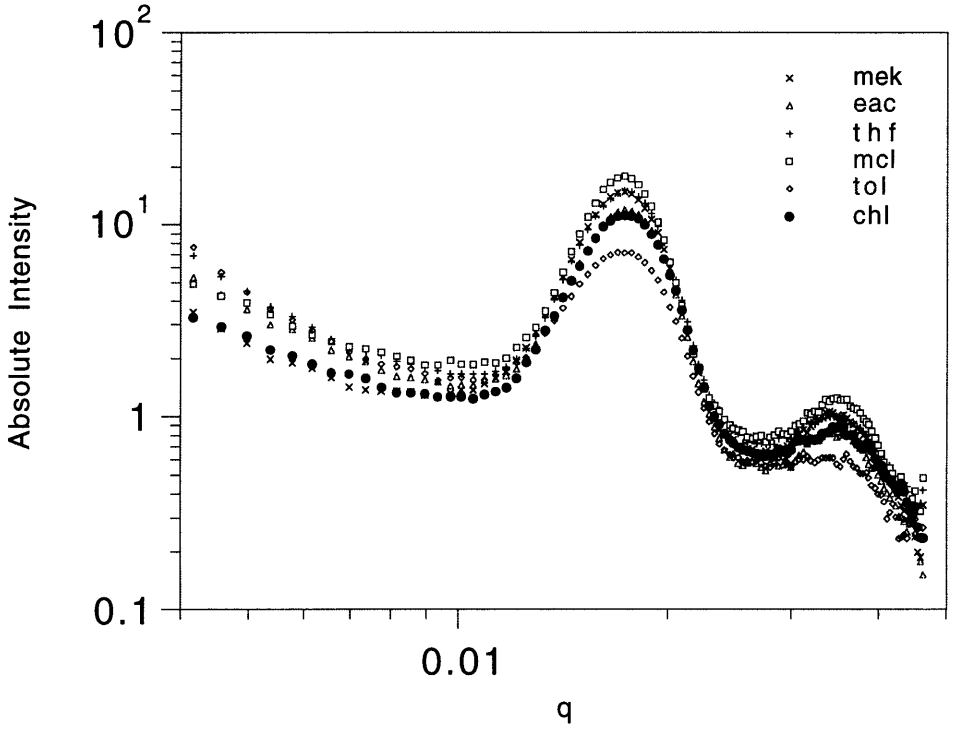

Figure 5-4: SANS absolute intensity versus q scattering curves for the KK31 polymer cast from various solvents.

The legend corresponds to the solvent from which KK31 was cast: ***mek*** means methyl ethyl ketone, ***eac*** is ethyl acetate, ***thf*** is tetrahydrofuran, ***mcl*** is methylene chloride, ***tol*** is toluene and ***chl*** is chloroform. What is first noted from this curve is that again the lamellar spacing is unchanged and the upturn at small scattering angles is probably due to the presence of grains. However, the trend does not exactly correspond to what was witnessed in Chapter 3 for this polymer, so this should be examined in future studies.

The reason these studies were performed was that a new Ultra SANS machine is now operational that can probe sizes up to 20 μm, two orders of magnitude greater than traditional SANS and a full order of magnitude greater than the Ultra SAXS machine used extensively in this thesis for grain size determination. If Ultra SANS turns out to be a feasible tool for grain size measurement, much larger grains can be measured, without the need to estimate potentially larger grain sizes from Porod's Law and the invariant calculations.

5.2.3 Grain Boundary Explorations

In this thesis, we have posed the theory that there is an enrichment of one of the two component blocks in the homogenous grain boundary. It has been further postulated that this enrichment leads to the change in physical properties witnessed when grain size is altered. It is therefore desirable to further explore the grain boundary, not with TEM as this has been done extensively, but through other means. SANS and Ultra SANS may be ways to indirectly determine the richer component at the grain boundary.

As has been stated in the previous section, the atomic number isotope and nuclear spin states are important for SANS to determine coherent scattering lengths, and therefore the presence of deuterated solvents should greatly alter the scattering curves, and allow us to probe the grain boundary composition. Some preliminary studies have done just that and will be reported here, though future studies should explore this in much more detail. A sample of KK31 cast from chloroform was exposed to vapors of deuterated toluene, and the SANS curves of both the unexposed and exposed films are shown in Figure 5-5. The

amount of vapors present were small relative to the size of the film, and therefore this exposure didn't affect the size of the film or cause any macroscopic swelling, and presumably no swelling of the lamellae.

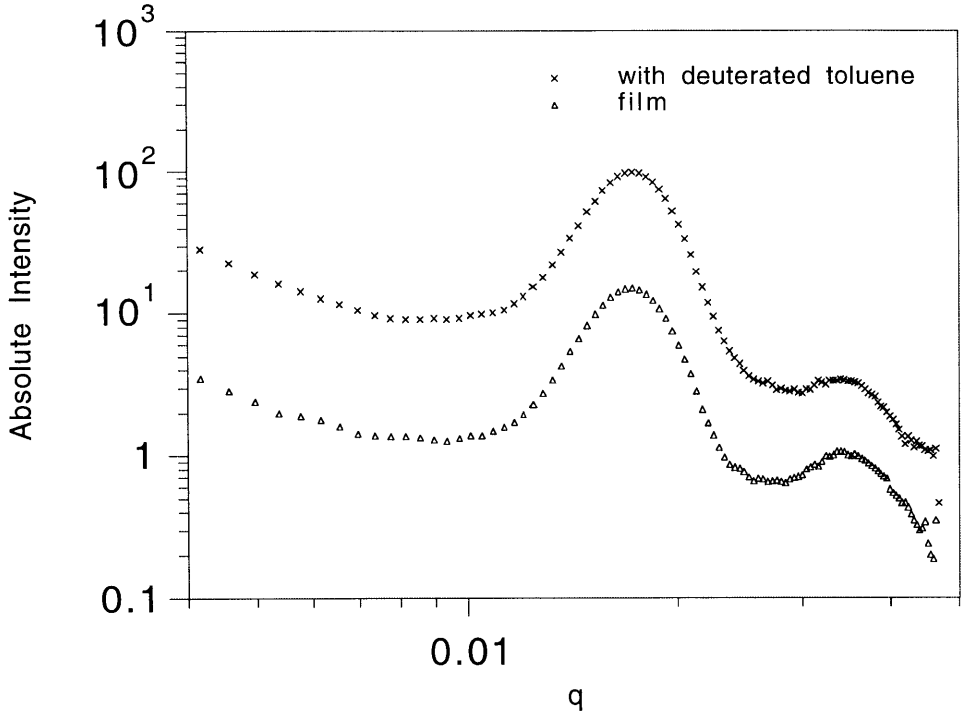

Figure 5-5: SANS scattering profiles of KK31 film cast from chloroform and the same film exposed to deuterated toluene vapors.

Toluene (and presumably deuterated toluene) is a neutral solvent, meaning that no preference is given to either styrene or butadiene. That being the case, it is believed that the deuterated toluene would partition itself equally in the styrene lamellae, butadiene lamellae and the grain boundaries, since this is a homogenous mixture of styrene and butadiene. We see that this is the case when we look at Figure 5-5. The peak that corresponds to the lamellar spacing is at the same value of q, and the shape of the peak is exactly the same. The slope of the tail in the low-q region of the SANS curves also show the same slope, presumably corresponding to an equal partition of the deuterated toluene in both the grains

and grain boundaries. Actually, the only difference in the two scattering curves is that the fact that the film exposed to deuterated toluene curve is about a decade higher than the regular film. This is probably due to the fact that the SANS machine at NIST measures absolute intensity and the uniform presence of deuterium uniformly raises the intensity at all values of q.

Now that it has been established how the SANS pattern of a grainy, styrene - butadiene block copolymer reacts to exposure to vapors of a deuterated neutral solvent, more interesting information can be found from exposure to a selective solvent. A selective solvent is one which preferentially dissolves one of the component blocks over the other one. For styrene - butadiene block copolymers, long chain alkanes such as heptane and hexane are selective for the polybutadiene block. Also, styrene is slightly selective for the polystyrene block. Figure 5-6 shows a SANS pattern of the S12B10 diblock copolymer dissolved in chloroform , evaporated, and annealed at 75°C for 1 hour. Figure 5-6 also shows the SANS pattern of this film exposed to deuterated styrene vapors. In order to prevent the deuterated styrene from polymerizing, BHT was added as an inhibitor. As with the sample exposed to deuterated toluene, the S12B10 sample wasn't exposed to enough deuterated styrene to affect the size of the film or cause any macroscopic swelling. Presumably no swelling of the lamellae occurred just due to the fact that solvent is present.

Looking at Figure 5-6, an escalation of the absolute intensity is witnessed, as was the case with the deuterated toluene film. However, the intensity isn't uniformly raised at all values of q. Two different changes in the scattering curves can be seen. A shift in the lamellar spacing peak is seen, from a value of 170 Å for the unexposed film to about 210 Å for the film exposed to deuterated styrene. This may be due to preferential settling of the deuterated styrene in these films. The second, and perhaps more subtle, difference in the shape of the SANS curve can be seen in the tail of the peak associated with grains, at a value of q less than 0.1 $Å^{-1}$. Not only does the increase in intensity start closer to the lamellar peak, but the intensity increases with a sharper slope. From this data, it can be

seen that the deuterated styrene preferentially resides in either the grains or grain boundaries, but more studies with SANS and hopefully Ultra SANS will be necessary to make any significant conclusions from these observations.

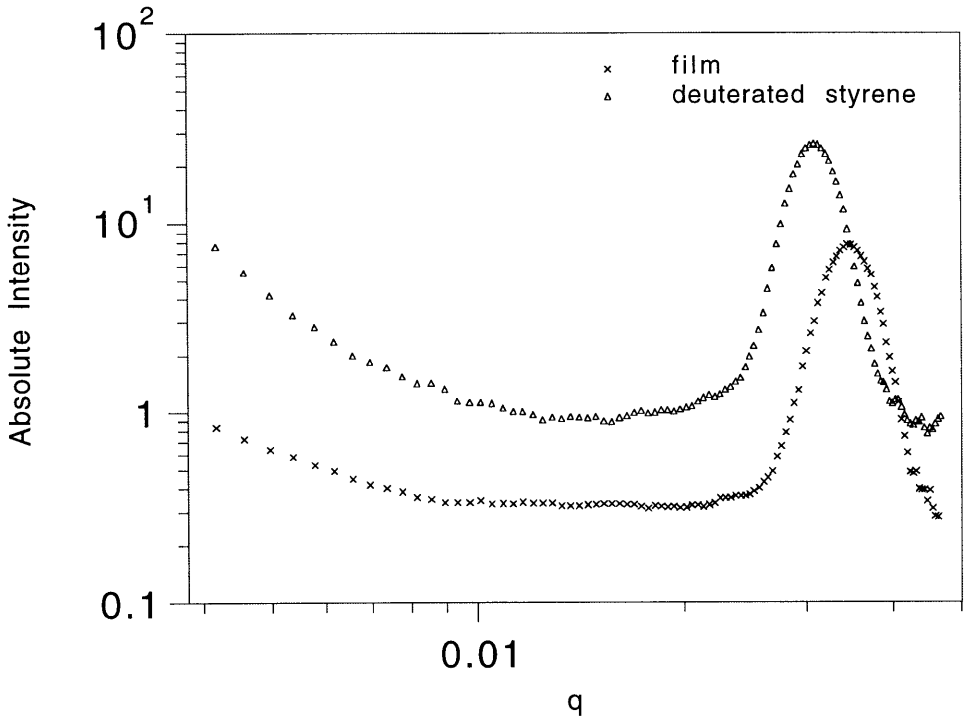

Figure 5-6: SANS scattering profiles of S12B10 film cast from chloroform and annealed at 75°C for 1 hour and the same film exposed to deuterated styrene vapors.

There are immediate future directions that can be pursued from this preliminary research, using traditional SANS or hopefully Ultra SANS. A static cast film can be divided into four different quadrants: the first one exposed to no solvent vapors, the second fourth exposed to small quantities of deuterated toluene vapors (or some other suitable neutral solvent), the third exposed to small quantities of deuterated and inhibited styrene vapors (or another selective solvent for the polystyrene block), and the fourth exposed to small quantities of deuterated hexane vapors (or another selective solvent for the

polybutadiene block). SANS data can then be taken for all four quadrants for three different polymers: a polystyrene rich K-resin (i.e. KR03 or KK31), a butadiene - rich polymer like 4461 (or DPX-555), and a low molecular weight diblock copolymer like S12B10 (or SB15). This information should help explain what is going on at the grain boundaries, and if, in fact, the enrichment at the grain boundaries is different for the styrene - rich and butadiene - rich block copolymers.

A long range goal of grain boundary exploration with Ultra SANS involves synthesizing styrene - partially deuterated butadiene block copolymers. As can be seen from the introduction to SANS in section 5.2.2, replacing hydrogen with deuterium will vastly change the scattering length, b, of a polymer, and therefore it is entirely possible to synthesize a block copolymer of styrene - partially deuterated butadiene where the coherent scattering length of butadiene is equal to that of the styrene. This is called "contrast matching," and has been done before.[9-10] In other words, a contrast matched styrene butadiene block copolymer will not show the lamellar peak. What is interesting is that with Ultra SANS, this knowledge can be used to explore the composition of the grain boundaries. A series of matched styrene - butadiene block copolymers can be synthesized similar to what had been done before,[11] except that two each of a styrene - rich, equal proportions and butadiene - rich lamellar block copolymers. For each type, two types of matched block copolymers should be made: one with a styrene block and a block consisting of a random copolymer of butadiene and deuterated butadiene and one with a styrene block, a butadiene block and a deuterated butadiene block, such that the overall butadiene scattering length is contrast matched. Even more future studies could probe into radial and tri-block contrast matched block copolymers.

5.2.4 Physical Properties

Dynamic mechanical analysis (DMA) is a technique similar to dielectric relaxation, except instead of an applied electric field being applied, an oscillatory mechanical stress is

applied at various frequencies as a function of temperature. The complex dielectric function:

$$\varepsilon = \varepsilon' + i\varepsilon'' \tag{5-2}$$

and the loss tangent:

$$\tan(\delta) = \frac{\varepsilon'}{\varepsilon''} \tag{5-3}$$

are important parameters in both dielectric and dynamic mechanical analysis.[12] The real and imaginary portions, ε' and ε", and the loss tangent, tan(δ), are all parameters that can be directly measured by dynamic mechanical analysis. For polymers, the most important variable is the loss tangent, as the peaks in the loss tangent versus temperature graph corresponds to the glass transition temperature, Tg, and the area under these peaks correspond to the relative amounts of each component in the blocks. Figure 5-7 shows tan(δ) vs T (°C) data for the KR03 block copolymer, with the styrene and butadiene peaks identified.

From Figure 5-7 it can be seen that the glass transition temperature is approximately 100°C for the polystyrene block and -70°C for the butadiene block of the KR03 resin. Also, the polystyrene peak is much larger than the polystyrene peak, due to the fact that KR03 is 79% polystyrene. If there was any effects of the grains or grain boundaries, it would probably be in between the two peaks, as the grain boundaries are a homogenous combination of both components. Figures 5-8 and 5-9 show a close-up of this region of the loss tangent versus temperature graph for the KR03 polymer having undergone two separate processing conditions.

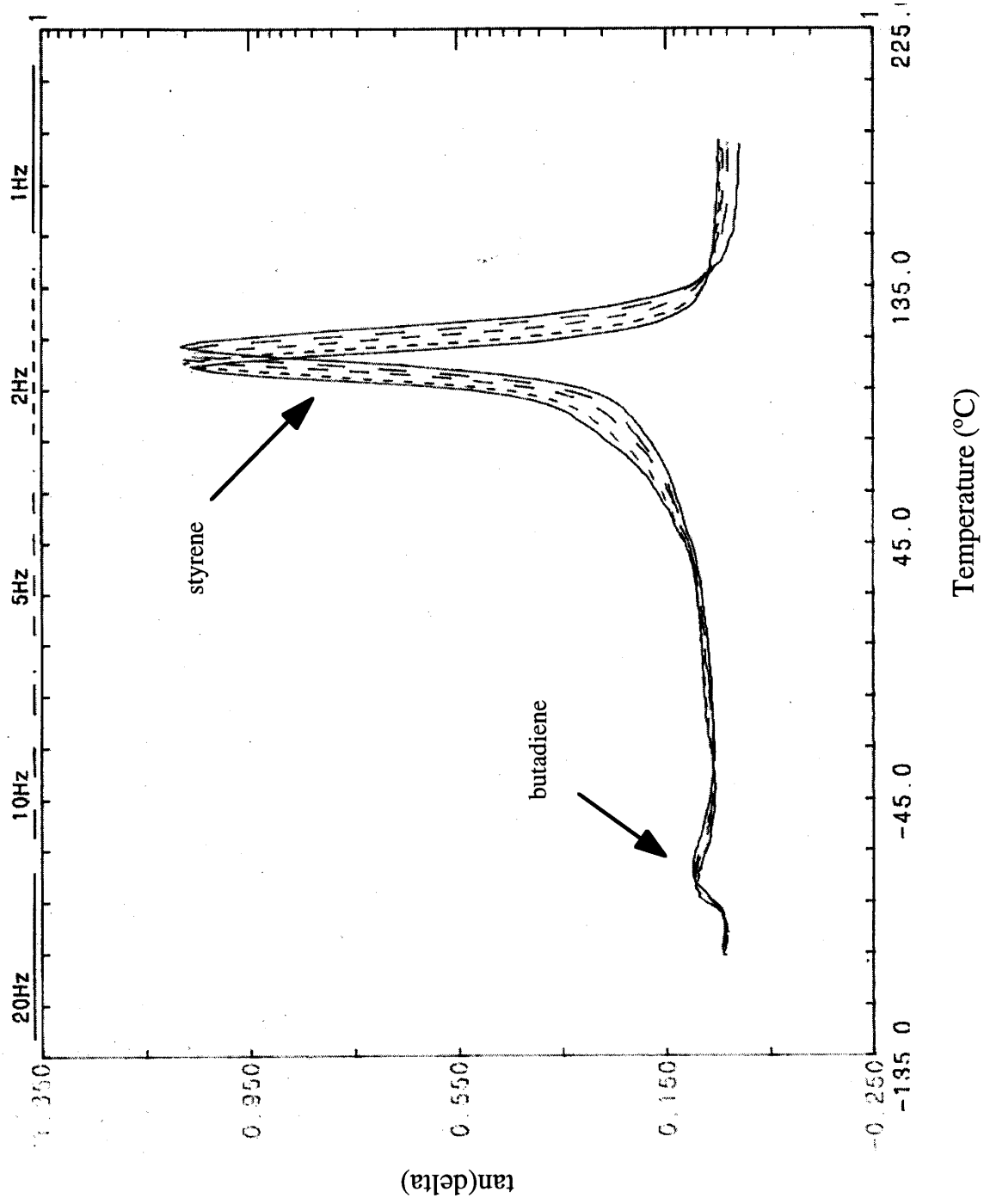

Figure 5-7: Dynamic mechanical analysis graph of loss tangent, tan(δ), versus temperature at various frequencies for KR03.

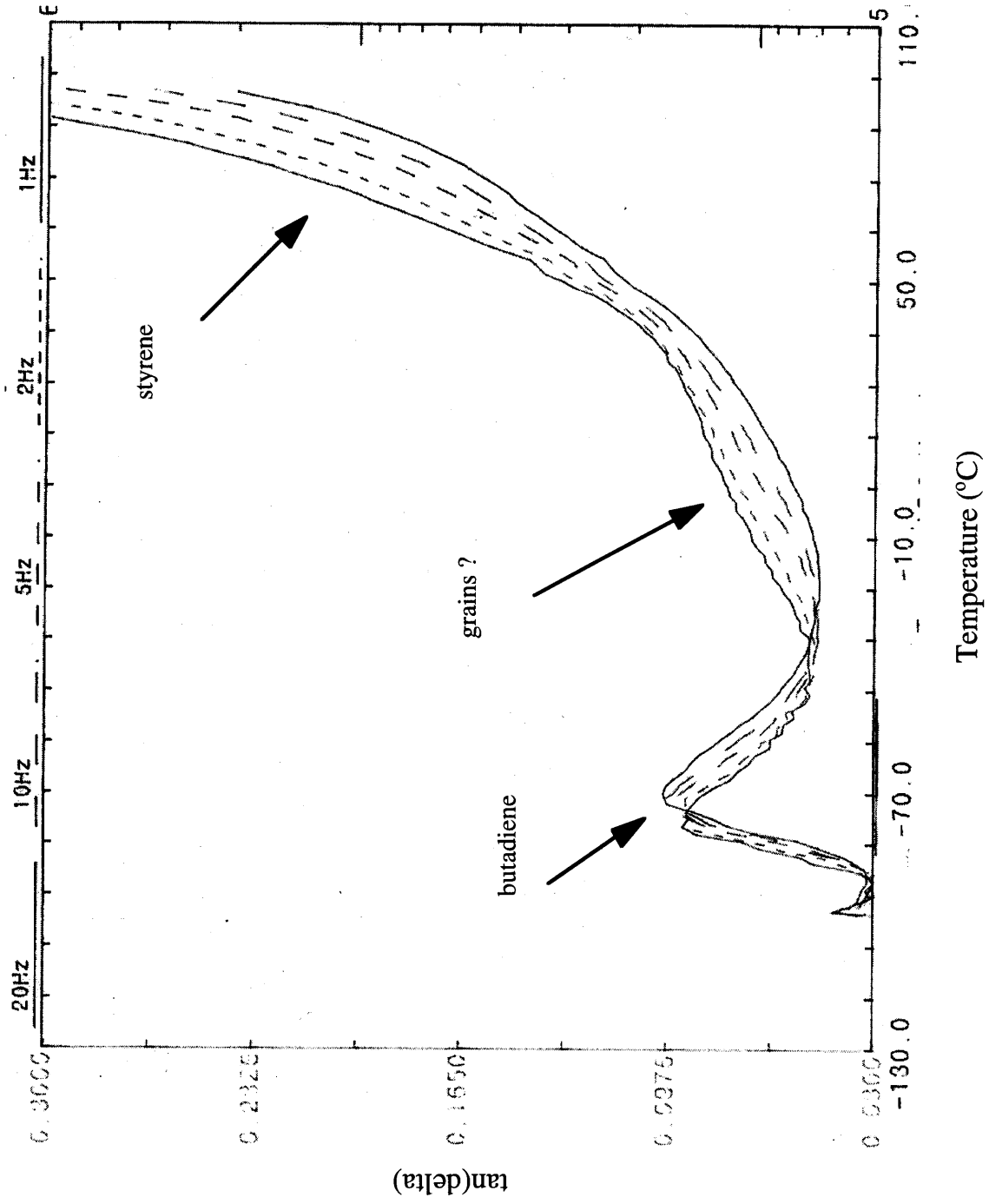

Figure 5-8: DMA graph of loss tangent, tan(δ), versus temperature in between the two glass transitions at various frequencies for KR03.

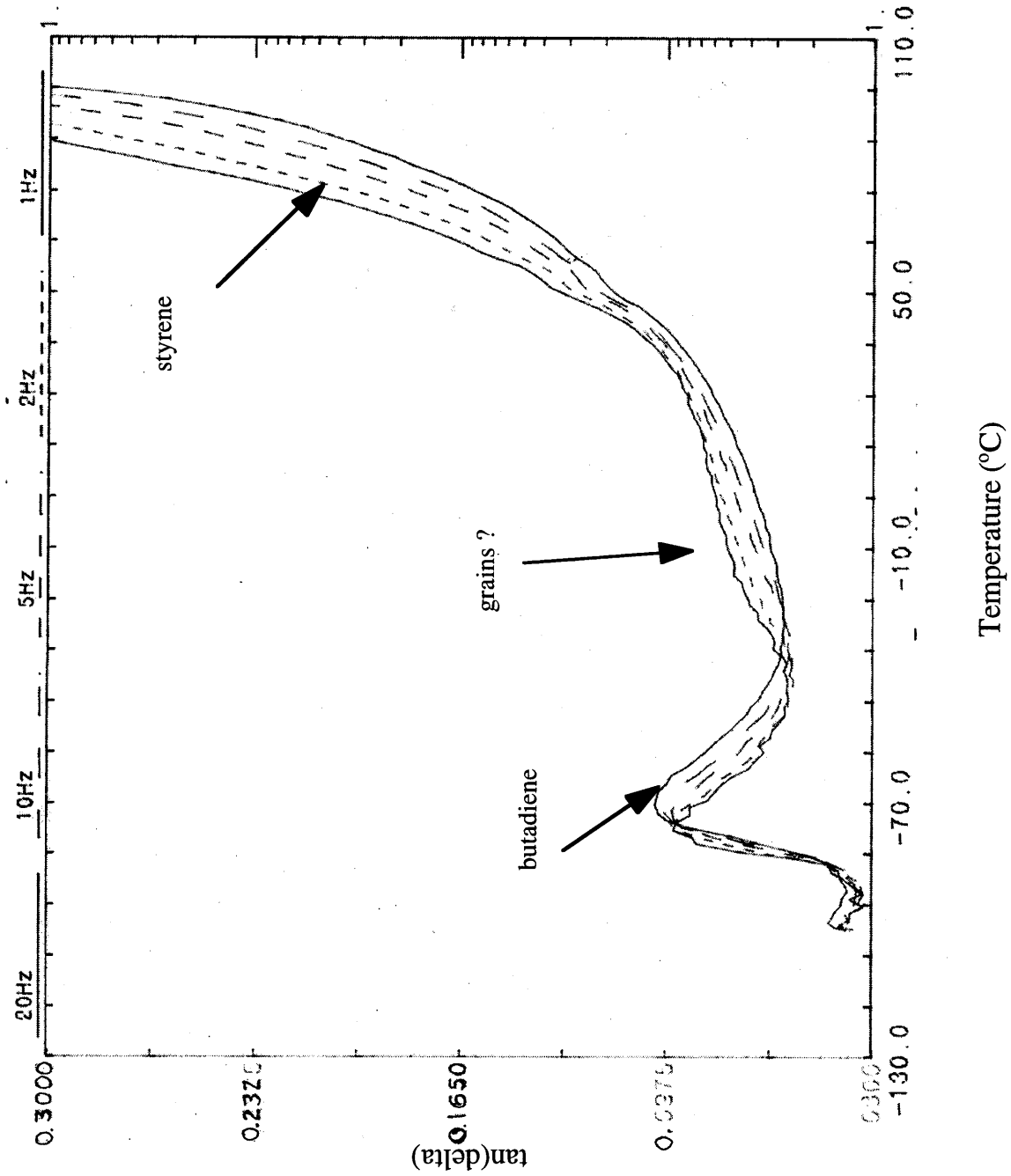

Figure 5-9: DMA graph of loss tangent, tan(δ), versus temperature in between the two glass transitions at various frequencies for KR03, having undergone different processing conditions.

Unfortunately, the grain sizes for the polymer in Figures 5-8 and 5-9 isn't known. What can be seen from these graphs is that there is in fact a small peak, possibly attributable to the presence of grain boundaries, in both samples. Also the peak location and size are slightly different. Further studies could show link these effects to grain size; the results could tell us something about the relative fraction of grain boundaries as the grains grow, based on the area under the peak, and relative composition of the grain boundary based on the temperature of the peak. Other mechanical tests that might show grain and grain boundary effects include, notched izod tests, compressive stress strain behavior, and dielectric measurements.

5.3 References

(1) Hajduk, D.A.; Grunner, S.M.; Rangarajan, P.; Register, R.A.; Fetters, L.J.; Honeker, C.; Albalak, R.J.; Thomas, E.L. *Macromolecules* **1994**, *27*, 490.

(2) Sakurai, S.; Momii, T.; Taie, K.; Shibayama, M.; Nomura, S.; Hashimoto, T. *Macromolecules* **1993**, *26*, 485.

(3) Khandpar, A.K.; Forester, S.; Bates, F.S.; Hamley, I.W.; Ryan, A.J.; Bras, W.; Almdal, K.; Mortenson, K. *Macromolecules* **1995**, *28*, 8796.

(4) Sakuri, S.; Hashimoto, T.; Fetters, L.J. *Macromolecules* **1996**, *29*, 740.

(5) Kimishima, K.; Koga, T.; Kanazawa, Y.; Hashimoto, T. *Fall Proceedings of the ACS, PMSE Division* **1998**, *79*, 371.

(6) Lai, C.; Russel, W.B.; Register, R.A.; Adamson, D.H. *Fall Proceedings of the ACS, PMSE Division* **1998**, *79*, 380.

(7) Underwood, E.E. *Quantitative Stereology*, Addison Wesley, Reading MA: **1970**. 80-95.

(8) Garetz, B.A.; Balsara, N.P.; Dai, H.J.; Wang, Z.; Newstein, M.C. *Macromolecules* **1996**, 29, 4675.

(9) Quan, X.; Koberstein, J.T. *J. Polym. Sci. Polym. Phys. Ed.* **1987**, *25*, 1381.

(10) Koberstein, J.T. *J. Polym. Sci. Polym. Phys. Ed.* **1982**, *20*, 593.

(11) Cheng, P.L.; Berney, C.V.; Cohen, R.E. *Macromolecules* **1988**, *21*, 3442.

(12) McCrum, N.G.; Read, B.E.; Williams, G.E. *Analestic and Dielectric Effects in Polymeric Solids*. Dover Publications, NY, **1991**.

Appendix A: Two Dimensional Point Collimated SAXS Profiles

As mentioned in this thesis, in order to both measure grain size and determine the effect of grain size, it is important to have an isotropic material. The upper half of Figures A-1 through A-8 show the two - dimensional, point - collimated SAXS profiles for the static cast films studied in this thesis. As can be seen by the solid, uniformly intense rings, all materials are in fact isotropic when static cast. The other important determination to be made from the SAXS patterns is whether the materials microphase separate into a lamellar morphology. The bottom graphs in Figures A-1 to A-8 show arbritrary intensity versus scattering vector, q, for all of the polymers, and since the peak locations are in the ratio of 1,2,3... it can be stated that all of these polymers do possess a lamellar morphology. Lamellar spacing can be found using Bragg's Law, $d = \frac{2\pi}{q_{MAX}}$. Table A.1 shows the lamellar spacing, d, for all of the static cast polymers studied in this thesis.

Polymer	*d (Å)*
S12B10	170
SB15	230
SB9	290
SB5	100
4461	280
DPX-555	280
KR03	320
KK31	350

Table A.1: Lamellar spacing, d, determined by SAXS for all the static cast polymers studied.

In addition to the static cast samples, Figure A-9 shows the two dimensional SAXS pattern of the extruded KK31 sample and the 1,2,3,4... ratio of the peak locations shows that the morphology is still alternating lamallae. However the lack of a complete ring shows that the material is in fact oriented. From Bragg's Law, we can also see that the lamellar spacing is different from the static cast sample, and this is displayed in Table 2.2.

Processing	*d (Å)*
static cast	350
extruded	380

Table A.2 Lamellar spacing for KK31, extruded and static cast.

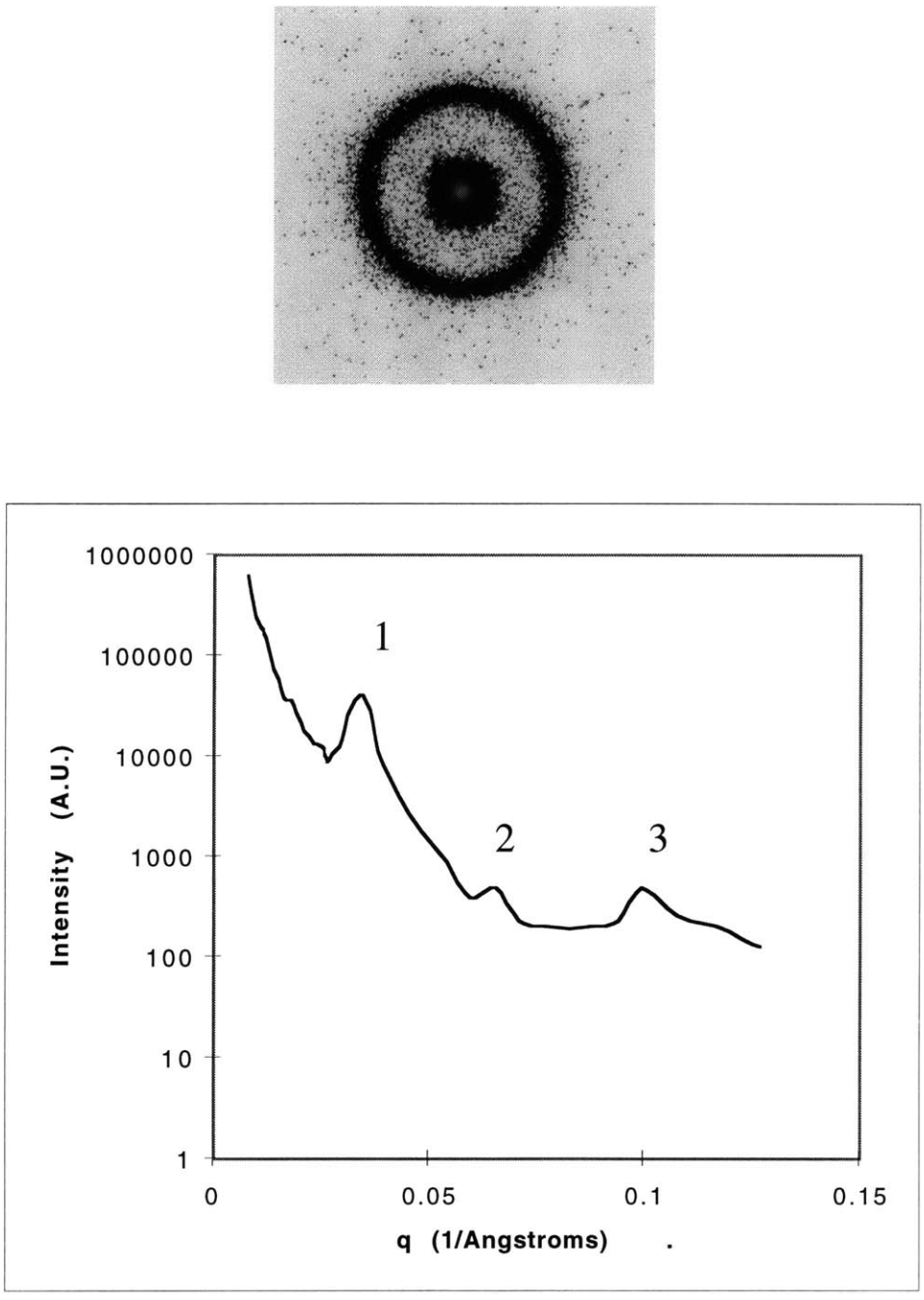

Figure A-1: Two Dimensional Point Collimated SAXS profile (above) and integrated Intensity versus q profile (below) for the S12B10 polymer. The solid ring indicate the presence of grains, and the peaks in the ratio of 1,2,3... indicate a lamellar morphology.

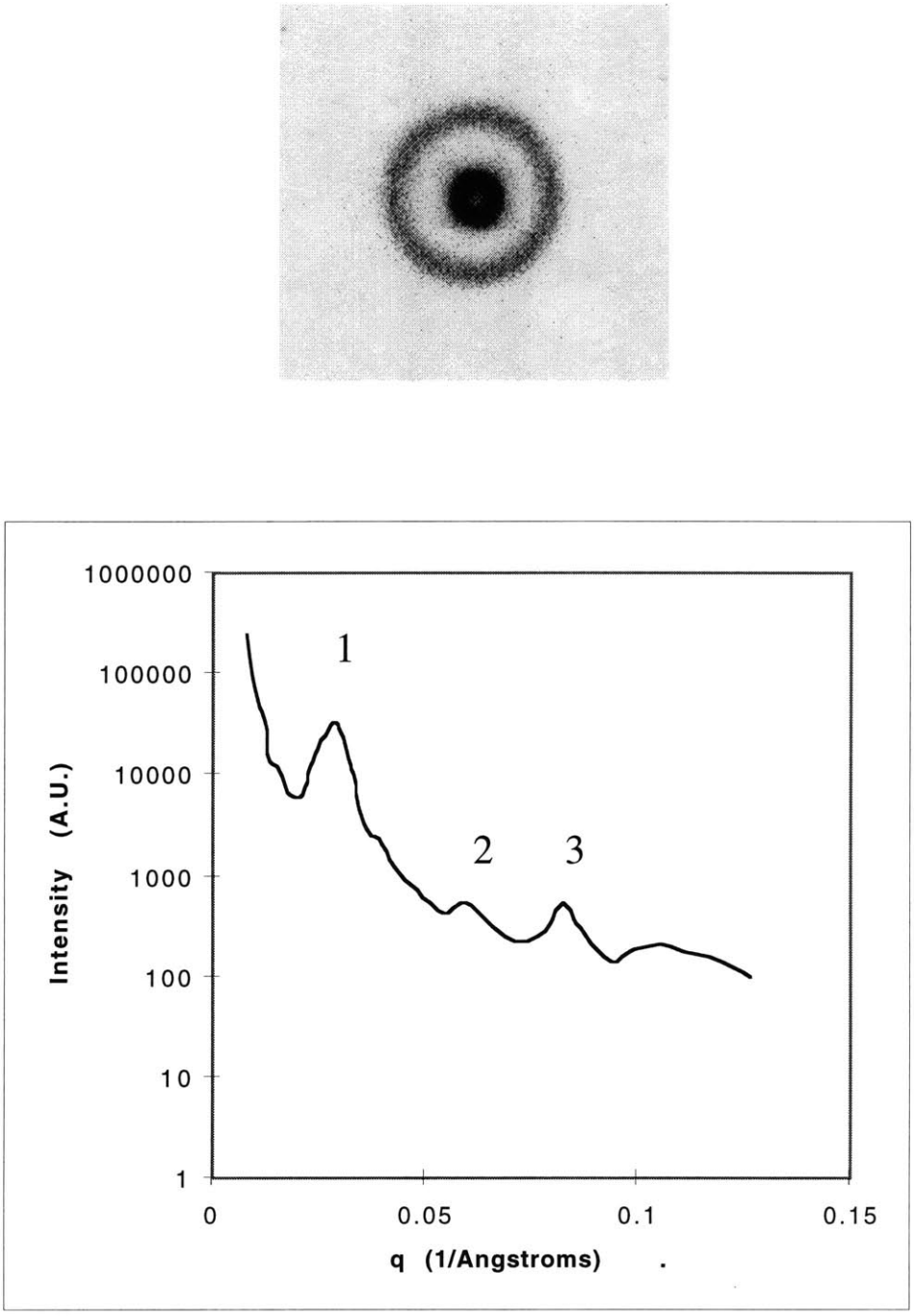

Figure A-2: Two Dimensional Point Collimated SAXS profile (above) and integrated Intensity versus q profile (below) for the SB15 polymer. The solid ring indicate the presence of grains, and the peaks in the ratio of 1,2,3... indicate a lamellar morphology.

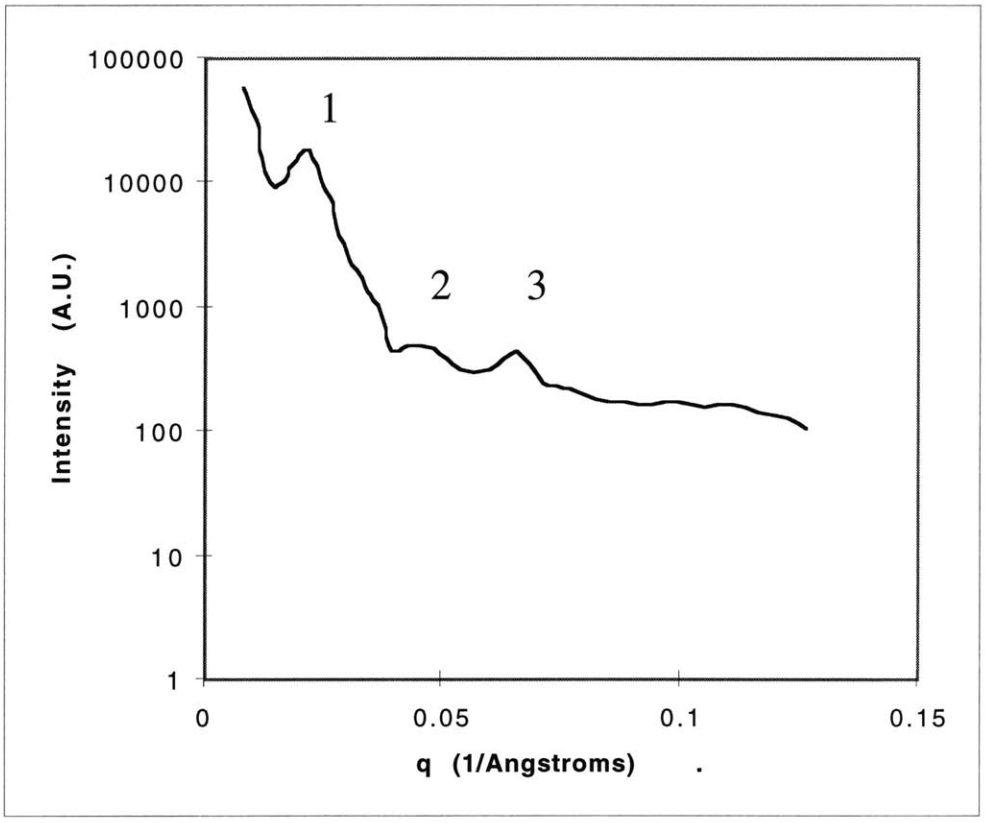

Figure A-3: Two Dimensional Point Collimated SAXS profile (above) and integrated Intensity versus q profile (below) for the SB9 polymer. The solid ring indicate the presence of grains, and the peaks in the ratio of 1,2,3... indicate a lamellar morphology.

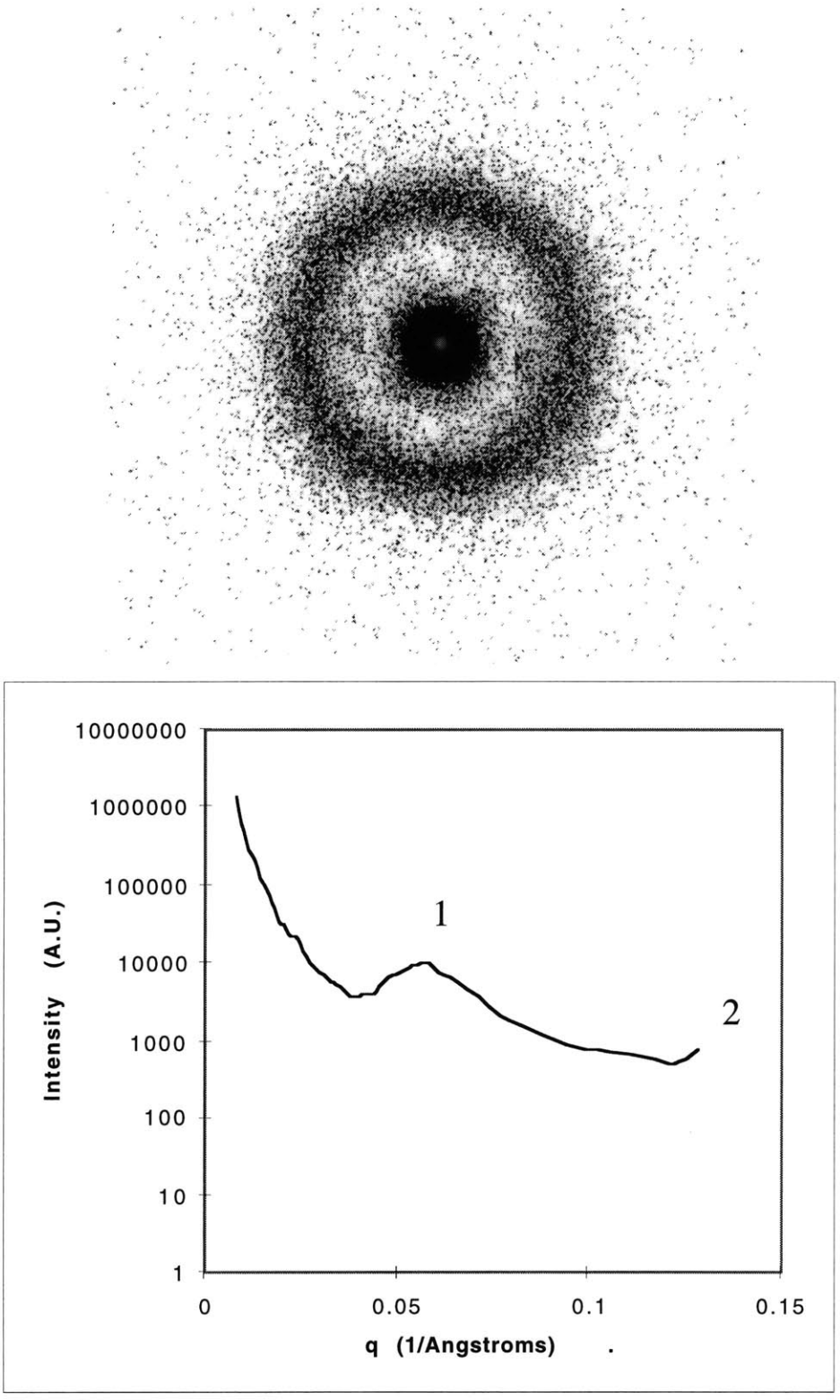

Figure A-4: Two Dimensional Point Collimated SAXS profile (above) and integrated Intensity versus q profile (below) for the SB5 polymer. The solid ring indicate the presence of grains, and the peaks in the ratio of 1,2... indicate a lamellar morphology.

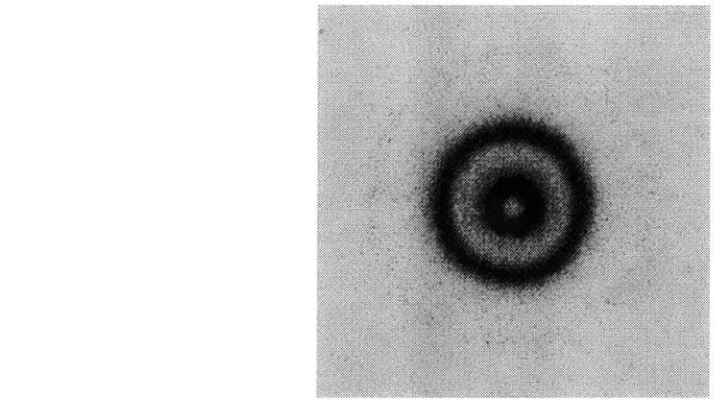

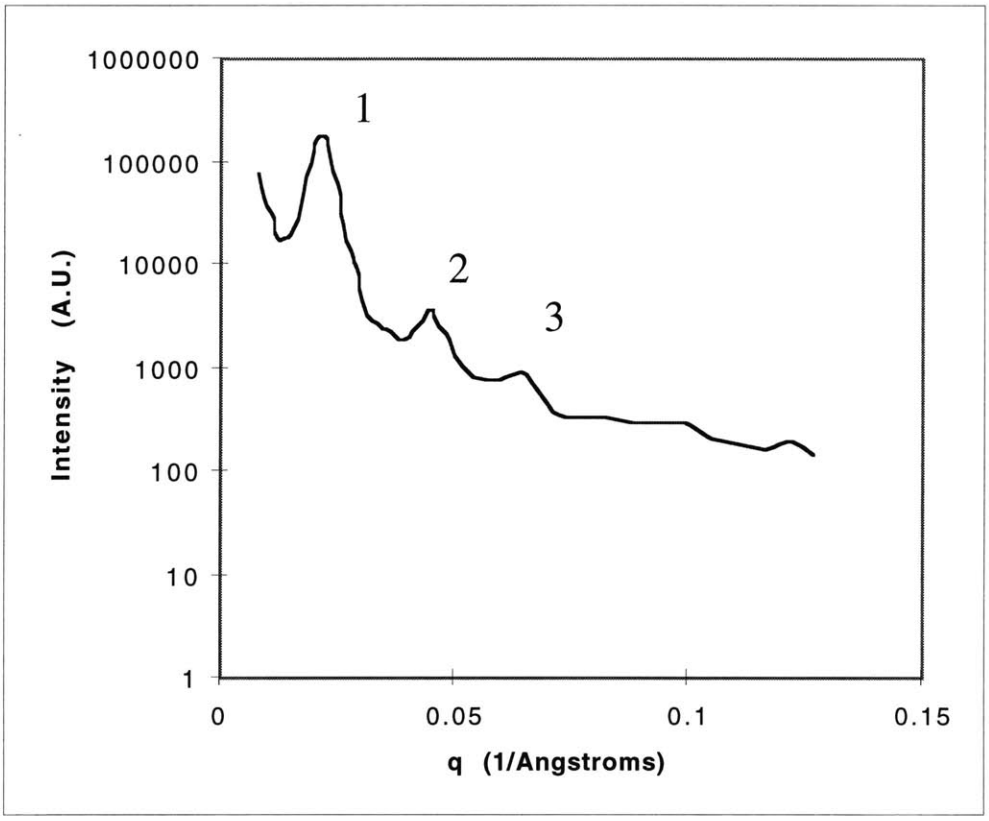

Figure A-5: Two Dimensional Point Collimated SAXS profile (above) and integrated Intensity versus q profile (below) for the 4461 polymer. The solid ring indicate the presence of grains, and the peaks in the ratio of 1,2,3... indicate a lamellar morphology.

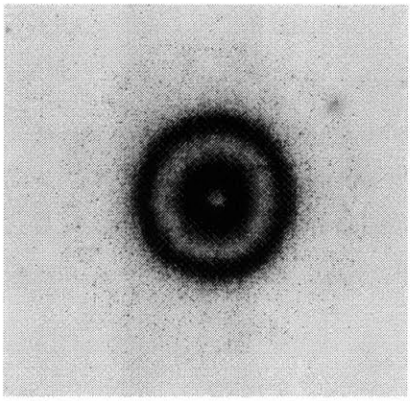

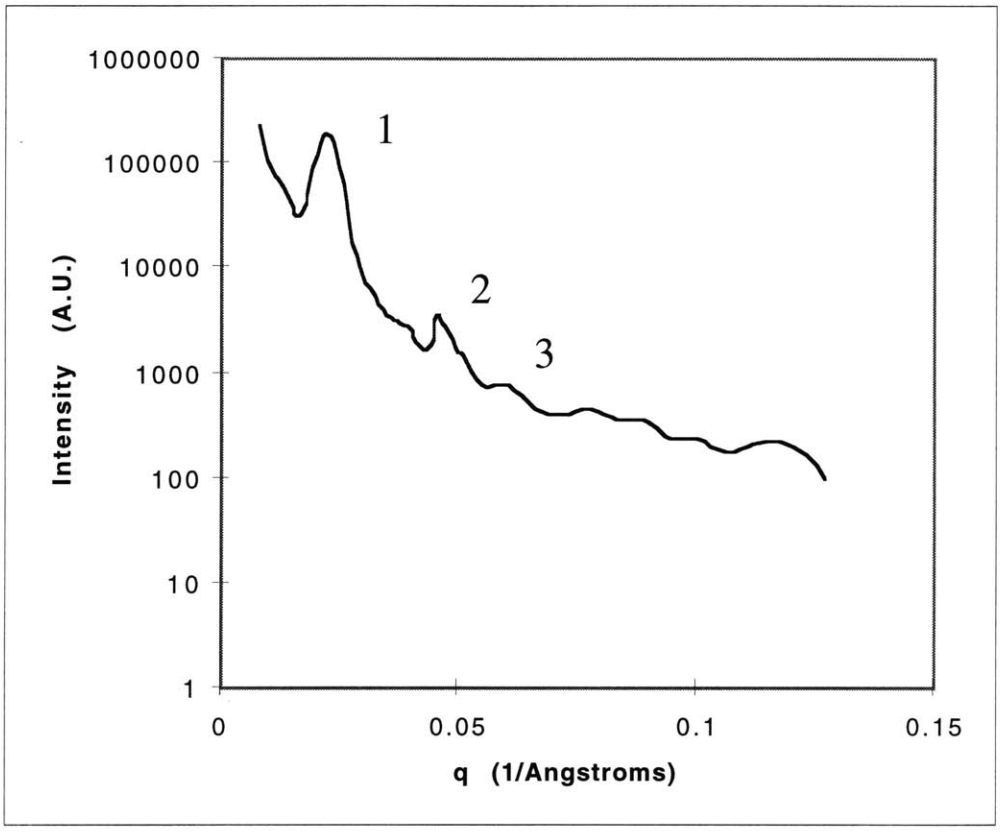

Figure A-6: Two Dimensional Point Collimated SAXS profile (above) and integrated Intensity versus q profile (below) for the DPX-555 polymer. The solid ring indicate the presence of grains, and the peaks in the ratio of 1,2,3... indicate a lamellar morphology.

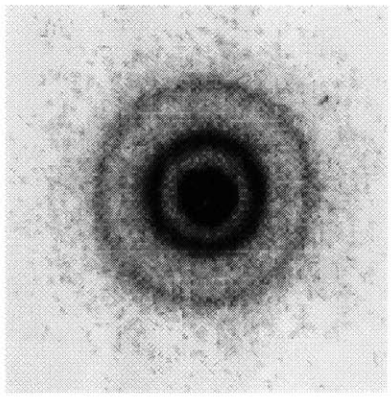

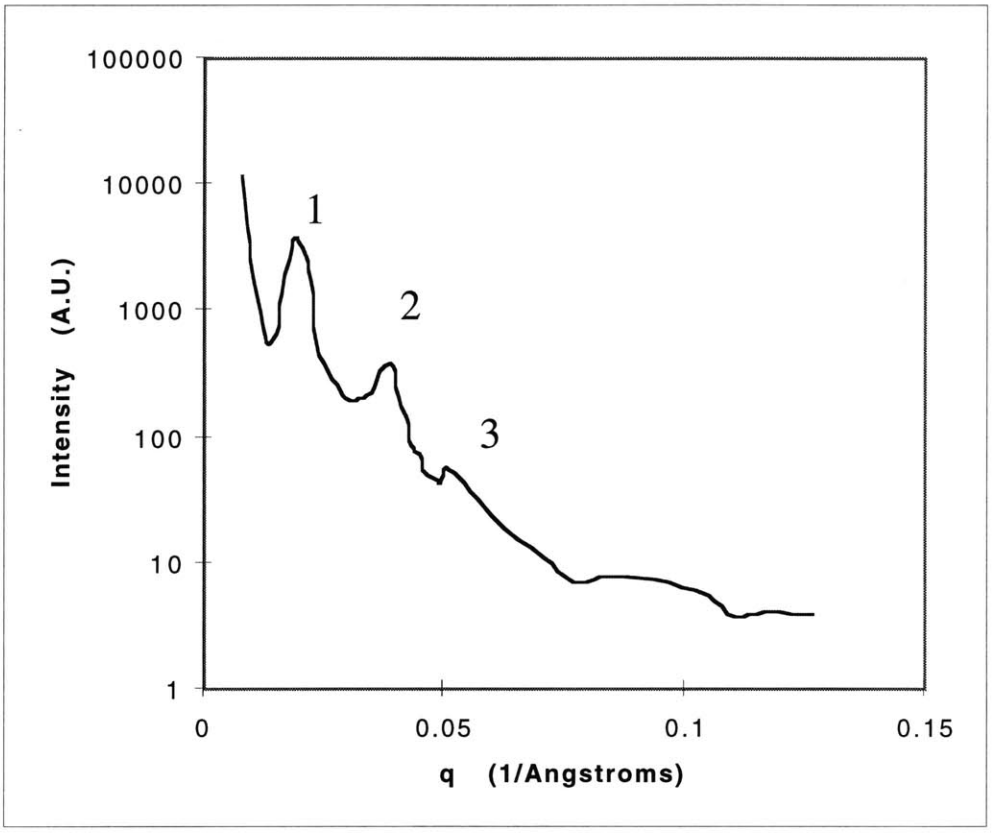

Figure A-7: Two Dimensional Point Collimated SAXS profile (above) and integrated Intensity versus q profile (below) for the KR03 polymer. The solid ring indicate the presence of grains, and the peaks in the ratio of 1,2,3... indicate a lamellar morphology.

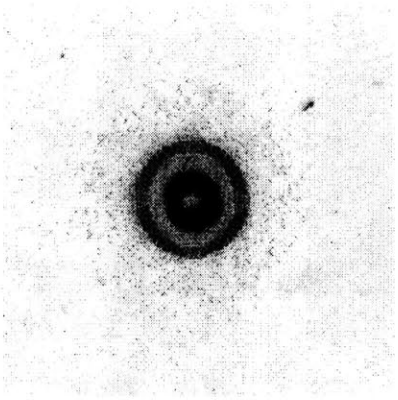

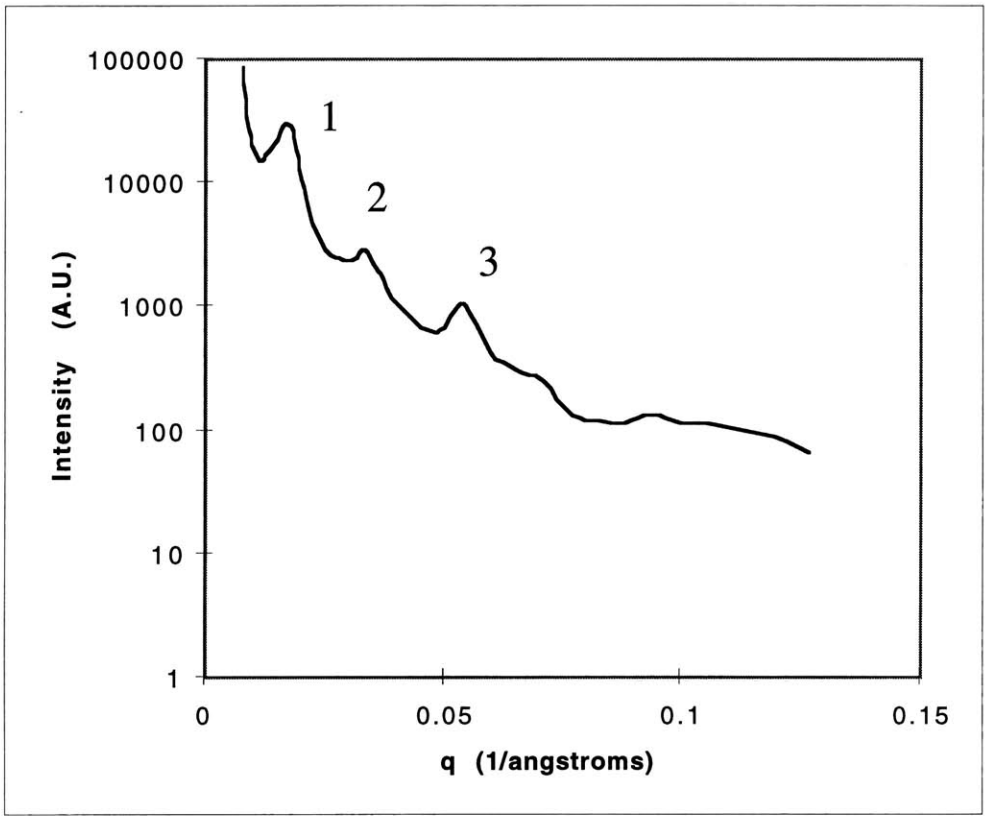

Figure A-8: Two Dimensional Point Collimated SAXS profile (above) and integrated Intensity versus q profile (below) for the static cast KK31 polymer. The solid ring indicate the presence of grains, and the peaks in the ratio of 1,2,3... indicate a lamellar morphology.

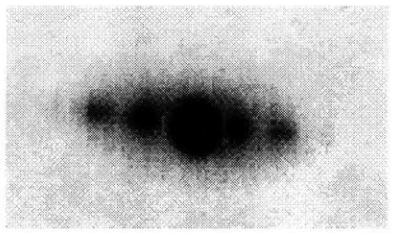

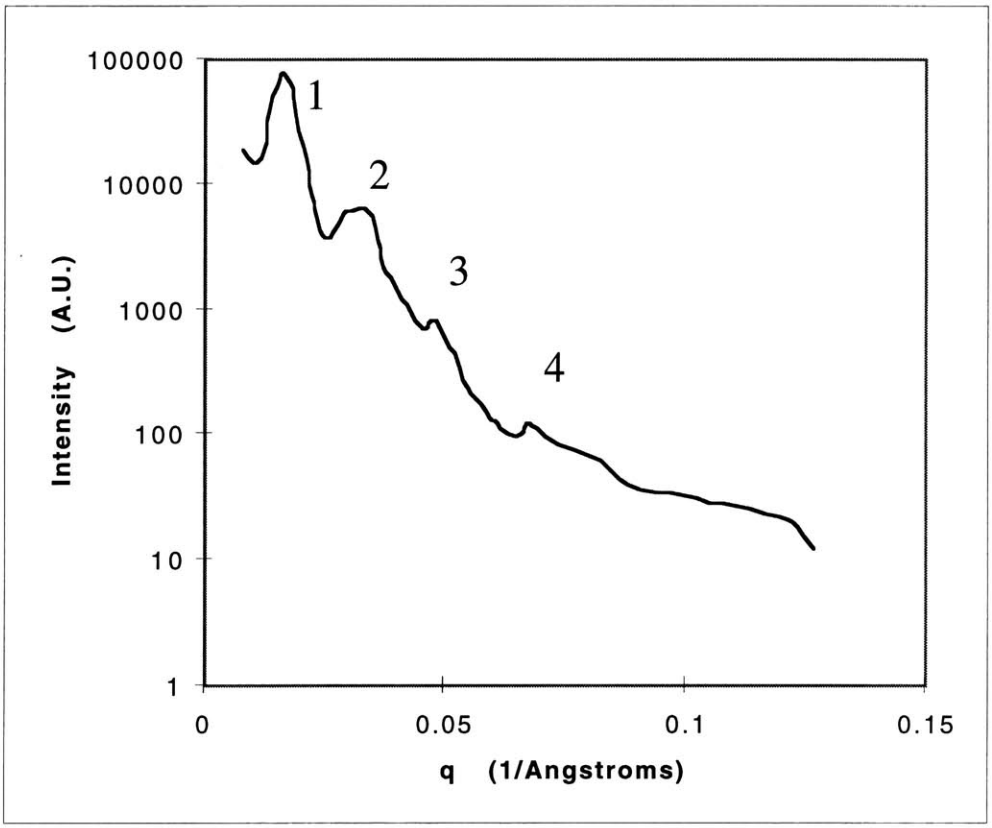

Figure A-9: Two Dimensional Point Collimated SAXS profile (above) and integrated Intensity versus q profile (below) for the extruded KK31 polymer. The lack of a solid ring indicate preferential orientation, and the peaks in the ratio of 1,2,3,4... indicate a lamellar morphology.

Appendix B: NMR Analysis

High resolution NMR is a method that can be used to determine the presence and amounts of polystyrene, 1,2-polybutadiene, and 1,4-polybutadiene in a given block copolymer. The block copolymers were dissolved to a 5 wt% solution in deuterated chloroform, and a proton NMR spectrum (250 Mhz) was generated. These proton NMR spectrums as well as identification of key peaks appear in Figures B-1 to B-3 for three of the polymers studied: KR03 is an industrial, three armed block copolymer containg over 50 wt% styrene and the polybutadiene is 1,4 rich; 4461 is an industrial triblock containing less than 50 wt % styrene with a 1,4-rich polybutadiene; and S12B10 is a low molecular weight polymer containing more 1,2-polybutadiene than 1,4-polybutadiene.

Determination of relative amounts of polystyrene and polybutadiene was first resolved by Senn (Senn Jr., W.J. *Anal. Chim. Acta* **1963**, *29*, 505). Table B.1 shows the mass fractions of styrene, 1,2-butadiene and 1,4-butadiene in KR03, 4461, and S12B10.

Polymer	**Weight Percents**		
	Styrene	***1,2-butadiene***	***1,4-butadiene***
KR03	79 %	3 %	18 %
4461	42 %	6 %	52 %
S12B10	50 %	44 %	6 %

Table B.1: Mass fractions of constituent blocks obtained by NMR spectroscopy for three selected block copolymers.

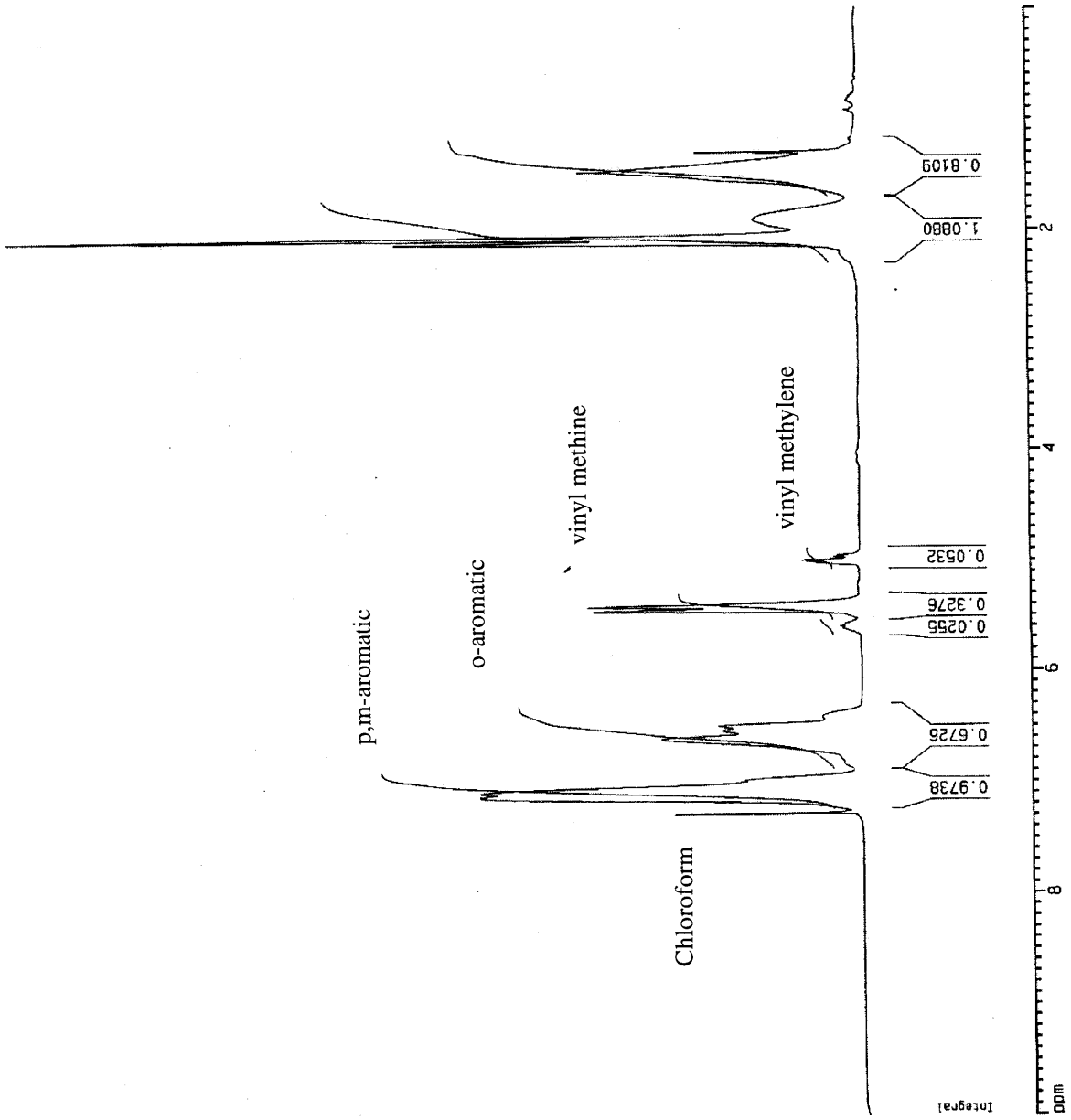

Figure B-1: Proton NMR spectra of KR03 dissolved in deuterated chloroform. Key peaks are identified.

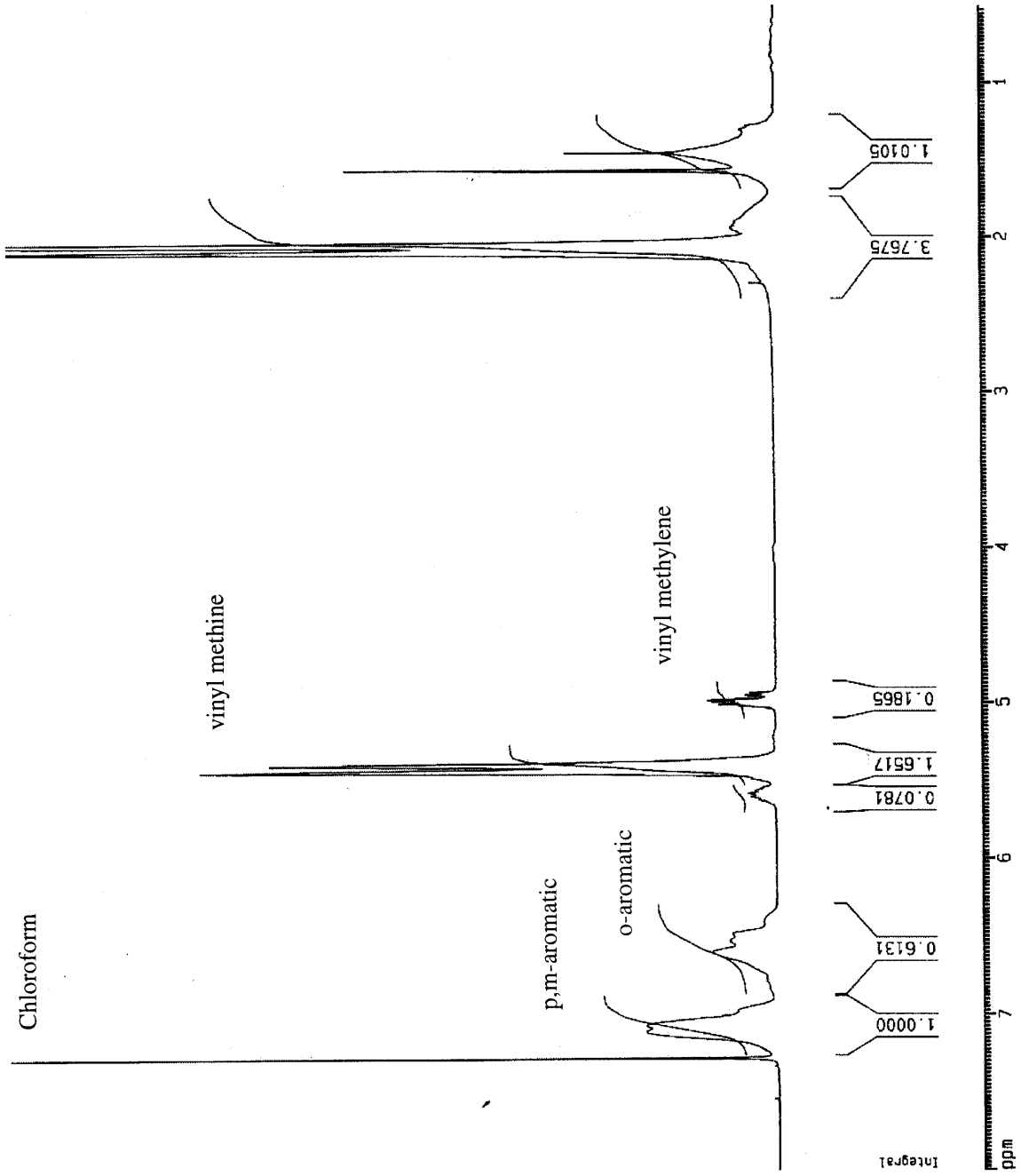

Figure B-2: Proton NMR spectra of 4461 dissolved in deuterated chloroform. Key peaks are identified.

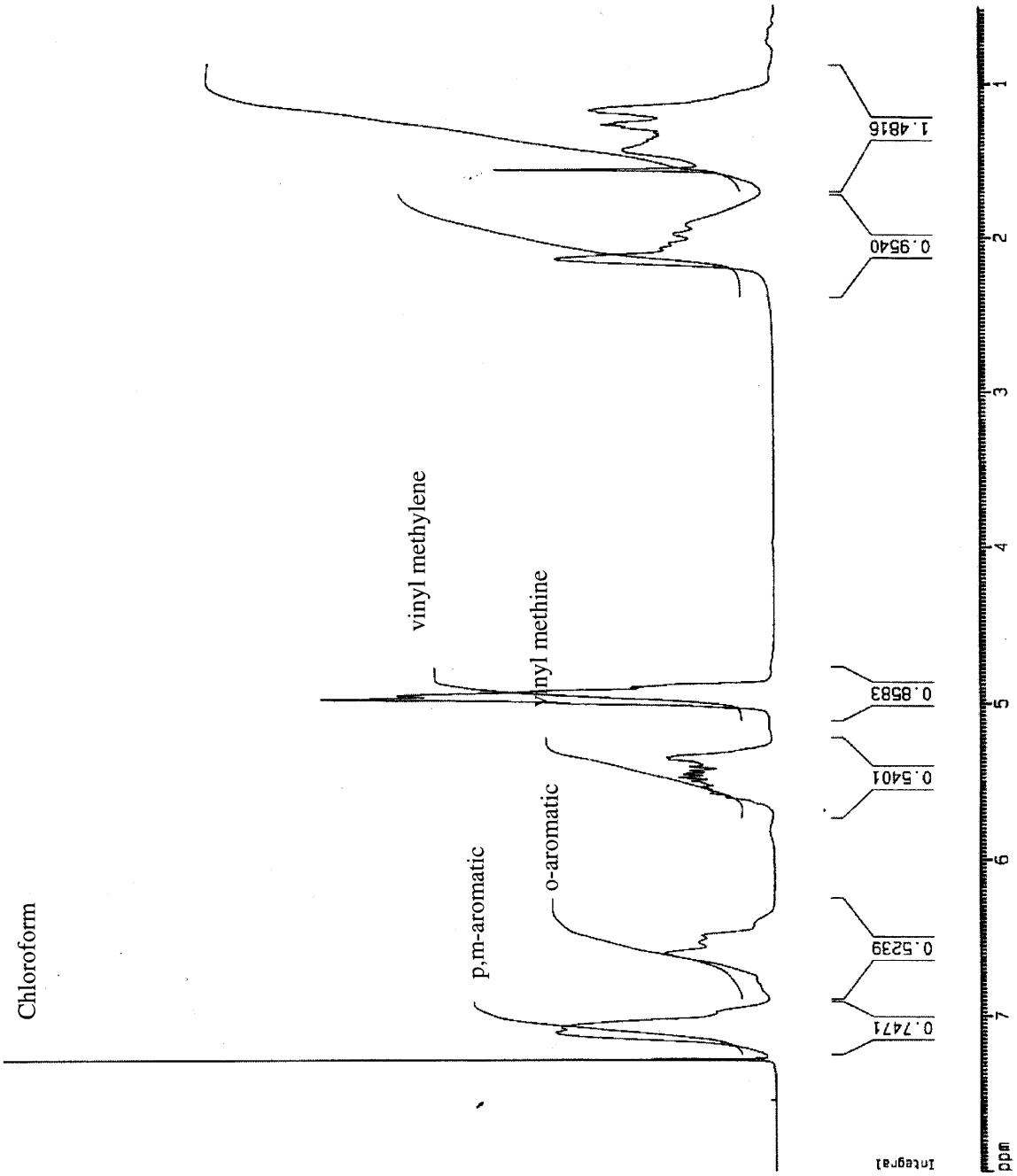

Figure B-3: Proton NMR spectra of S12B10 dissolved in deuterated chloroform. Key peaks are identified.